Functional Characterization of the TRP-Type Channel PKD2L1

by

Shaimaa Abdelrazik Hussein

A thesis submitted in partial fulfillment of the requirements for the degree of

Doctor of Philosophy

Department of Physiology
University of Alberta

ABSTRACT

Polycystic kidney disease (PKD) protein 2 Like 1 (PKD2L1), also called transient receptor potential polycystin-3 (TRPP3), regulates Ca^{2+}-dependent hedgehog signalling in primary cilia, intestinal development and sour tasting but with an unclear mechanism. PKD2L1 is a Ca^{2+}-permeable cation channel that is activated by extracellular Ca^{2+} (on-response) in *Xenopus* oocytes. PKD2L1, co-expressed with PKD protein 1 Like 3 (PKD1L3) receptor protein, exhibits acid-induced off-response activation (i.e., activation occurs only after the removal of an acidic solution).

Whether PKD1L3 participates in acid sensing and what is the exact mechanism of PKD2L1 channel function remain unclear. In Chapter 2, we provided an answer for the first question. By using the two-microelectrode voltage-clamp, site directed mutagenesis, Western blotting, reverse transcriptase-polymerase chain reaction (RT-PCR) and immunofluorescence, we showed that PKD2L1 expressed alone in oocytes exhibits sustained off-response currents in the absence of PKD1L3. PKD1L3 co-expression augmented the PKD2L1 plasma membrane localization but did not alter the observed properties of the off-response. PKD2L1 off-response was inhibited by an increase in intracellular Ca^{2+}. We also identified two intra-membrane residues aspartic acid 349 (D349) and glutamic acid 356 (E356) in the third transmembrane domain that are critical for PKD2L1 channel function. Our study suggests that PKD2L1 may itself sense acids and defines off-response properties in the absence of PKD1L3.

It was previously reported that PKD2L1 and PKD1L3 form heterotetramers with 3:1 stoichiometry. C-terminal coiled-coil-2 (CC2) domain (G699-W743) of PKD2L1 was reported to be important for its trimerization but independent studies

showed that CC2 does not affect PKD2L1 channel function. Thus, it remains unclear how PKD2L1 proteins oligomerize into a functional channel. In Chapter 3, by use of SDS-PAGE, blue native PAGE and mutagenesis we identified a novel C-terminal domain called C1 (K575-T622) involved in stronger homotrimerization than the non-overlapping CC2, and found that the PKD2L1 N-terminus is critical for dimerization. By electrophysiology and *Xenopus* oocyte expression, we found that C1, but not CC2, is critical for PKD2L1 channel function. Our co-immunoprecipitation and dynamic light scattering experiments further supported involvement of C1 in trimerization. Further, C1 acted as a blocking peptide that inhibits PKD2L1 trimerization and the channel function of PKD2L1 and PKD2L1/PKD1L3. Thus, our study identified C1 as the first PKD2L1 domain essential for both PKD2L1 trimerization and channel function, and suggests that PKD2L1 and PKD2L1/PKD1L3 channels share the PKD2L1 trimerization process.

In Chapter 4, we studied roles of phospholipase C (PLC), lipid messengers and phosphorylation in PKD2L1 channel function. As PKD2L1 is expressed in type III taste receptor cells (TRCs) which are known to have a phospholipase C-dependent Ca^{2+} signalling, we wondered whether PKD2L1 function is downstream of a PLC pathway or is affected by different lipid messengers. Using *Xenopus* oocyte expression system, two-microelectrode voltage-clamp (TMVC) and immunofluorescence (IF), we found that PKD2L1 function is indeed downstream of a PLC pathway. PLC activator m-3M3FBS opens the channel in a Ca^{2+}-dependent manner, while the PLC inhibitor U73122 inhibits the Ca^{2+}-induced channel function. Moreover, we found that phorbol 12-myristate 13-acetate (PMA), a commonly used PKC activator, but not its

biologically non-active analogue, 4α-phorbol 12,13-didecanoate (4αPDD), inhibits PKD2L1 channel function and reduces its plasma membrane localization. Consistently, when we used a PKC blocker GF109203x the channel activity was increased. Further, we tested a number of potential phosphorylation sites and found that PKD2L1 mutant T338A has a substantially reduced response to the PMA treatment. Our results indicate that 1) PLC regulates PKD2L1 channel function and that PKD2L1 inactivation is PKC-dependent, and 2) PKC regulates PKD2L1 channel function through phosphorylating threonine 338 and affecting its surface membrane density. This study will constitute an important step towards understanding the molecular mechanism underling the biological functions of PKD2L1 such as its role in sour tasting.

In summary, our studies constitute valuable contributions to understanding the function and regulation of PKD2L1.

PREFACE

Chapter 2 of this thesis is accepted for publication in the Scientific Reports journal as 'Acid-induced off-response of PKD2L1 channel in *Xenopus* oocytes and its regulation by Ca^{2+}'

Shaimaa Hussein, Wang Zheng, Chris Dyte, Qian Wang, JungWoo Yang, Fan Zhang, Jingfeng Tang, Ying Cao, and Xing-Zhen Chen

SH designed and performed the major parts of the experiments, analyzed the data and wrote the first version of the manuscript and revisions. WZ performed RT-PCR experiments, analyzed the data and revised the manuscript. CD performed some of the electrophysiology experiments. QW and JY performed parts of the experiments and analyzed data. FZ analyzed part of the data and participated in paper revision. JT and YC participated in design of experiments and paper revision. XZC conceived or designed the experiments, helped analyzing the data and revised the manuscript.

Chapter 3 of this thesis has been published as 'A novel PKD2L1 C-terminal domain critical for trimerization and channel function.'

Zheng W, Hussein S, Yang J, Huang J, Zhang F, Hernandez-Anzaldo S, Fernandez-Patron C, Cao Y, Zeng H, Tang J, Chen XZ. Sci Rep. 2015 Mar 30;5:9460.

Wang Zheng and I contributed equally to this paper;
In this paper, I performed all immunofluorescence experiments, most mRNA preparations and microinjections, all electrophysiology experiments for figures 3-2 A-E, 3-4 A-E, 3-6 A-F. I also participated in manuscript revisions and initially got the

idea of the importance of this domain and initiated the struction/function characterization studies.

Conceived and designed the experiment: WZ, CFP, YC, HBZ, JFT and XZC. Performed the experiments: WZ, SH, JWY, JH, FZ and SHA. Analyzed the data: WZ, CFP, YC, HBZ, JFT and XZC. Wrote the paper: WZ and XZC.

Chapter 4 of this thesis is going to be submitted as 'PKD2L1 is downstream a phospholipase C pathway with a PKC-dependent inactivation mechanism'

Shaimaa Hussein, Qiaolin Hu, JungWoo Yang and Xing-Zhen Chen

Experimental design: SH and XZC. Performed experiments, analyzed the data and revised the manuscript: SH, QH, and JY. Wrote the manuscript: SH and XZC.

.

DEDICATIONS

For my husband who was always loving and caring.

For my parents who always provided care, love and support. They are also the main reason I am here now and doing research.

For my kids who tolerated their mom while doing a PhD.

For my friends who were always there for me to share my successful and faulty experiments.

My deepest gratitude goes to all my family and friends for their unflagging love and support throughout my life; this thesis is simply impossible without you.

Last but not least, praise Allah, from before and after. Thanks to God for my life through all tests in the past years. You have made my life more bountiful. May Your name be exalted, honoured, and glorified

ACKNOWLEDGMENTS

I would like to thank all people who have helped and inspired me during my PhD studies.

I especially want to thank my supervisor, Dr. Xing-Zhen Chen, for his guidance during my research and study at the University of Alberta. Without his support, my ambition to do a PhD could hardly be realized. He offers advice and suggestions whenever I need them. In addition, he was always accessible and willing to always help and support me. As a result, research life became smooth and rewarding for me.

Special thanks to Dr. Todd Alexander and Dr. Warren Gallin my thesis committee members and advisors, Dr. Elaine Leslie for her continuous support throughout my PhD program and Dr. Jonathan Lytton, my external examiner.

All my lab buddies made it a convivial place to work. In particular, I would like to thank JungWoo Yang, Wang Zheng, Qian Wang, Carlos Lara, Qiaolin Hu and Fan Shen for their help and valuable discussions over the past years. All other folks who had helped me, special thanks to Deb O'Neill, Ensaf Almomani and Vanessa Marensi, who had inspired me in research and life through our interactions during the long hours in the lab.

Thanks to everyone in the Physiology, with special thanks to Sharon Orescan who was always there for help and advice. Thanks to everyone in the membrane protein research group (MPDRG); I have learned a lot from you and I was very grateful to be part of the group for the past years.

.

TABLE OF CONTENTS

LISTOF FIGURES

Chapter 1

Chapter 2

Chapter 3

Chapter 4

LIST OF ABBREVIATIONS

2-ME	2-mercaptoethanol
4EBP1	Human eukaryotic initiation factor 4E binding protein
4αPDD	4α-phorbol 12,13-didecanoate
aa	Amino acid
ADP	Adenosine diphosphate
ADPKD	Autosomal dominant polycystic kidney disease
AFM	Atomic force microscopy
BN- PAGE	blue native PAGE
BSA	Bovine serum albumin
CaM	Calmodulin
CCD	Coiled-coil domain
Co-IP	Co-immunoprecipitation
CRD	C-terminus regulatory domain
CSF-cN	Cerebrospinal fluid contacting neurons
CT	Carboxyl-terminus
DAG	Diacylglycerol
D_H	Hydrodynamic diameter
DLS	Dynamic light scattering
DMEM	Dulbecco's modified Eagle's medium
dTRP	*Drosophila* TRP
DTT	Dithiothreitol
FBS	Fetal bovine serum

FSGS	Familial focal segmental glomerulosclerosis
GFP	Green fluorescence protein
HEK	Human embryonic kidney cells
hPKD2L1	Human PKD2L1
hr	Hour
hRPE	Human RPE
IMCD	Inner medullary collecting ducts
IP3	Inositol (1,4,5) triphosphate
IP3R	IP3 receptor
KO	Knockout
$K_v7.1$	Voltage-gated K^+ channels
MEF	Mouse embryonic fibroblasts
MOT	Mean open time
mPKD2L1	Mouse PKD2L1
mRPE	Mouse RPE
MS	Multiple sclerosis
NEM	N-Ethylmaleimide
NMDG	N-methyl-D-glucamine
NOMPC	No mechanoreceptor potential C
NP	Niemann-Pick syndrome
NP_o	Open probability
NT	Amino-terminus
PAGE	Polyacrylamide gel electrophoresis

pBPB	4-bromophenacyl bromide
PBS	Phosphate buffered saline
PFA	Paraformaldehyde
PH	Plextrin homology
PIP2	Phosphatidylinositol (4,5)biphosphate
PIs	Phosphoinositides
PKA	Protein kinase A
PKC	Protein kinase C
PKD1	Polycystic kidney disease protein 1
PKD1L1	Polycystic kidney disease protein 1 like 1
PKD1L3	Polycystic kidney disease protein 1 like 3
PKD2	Polycystic kidney disease protein 2
PKD2L1	Polycystic kidney disease 1protein 2 like
PLA_2	Phospholipase A 2
PLC	Phospholipase C
PMA	Phorbol 12-myristate 13-acetate
RACK1	Receptor for activated C kinase 1
RPE	Retina pigmented epithelium
SHH	Sonic hedgehog signalling pathway
SK_{Ca}	small conductance voltage-gated Ca^{2+}-activated K^+ channel
SNP	Single nucleotide polymorphysim
TBA	Tetrabutylammonium

TBST	Tris Buffered Saline, 1% Tween 20
TEA	Tetraethylammonium
TM	Transmembrane domain
TMVC	Two-microelectrode voltage clamp
TnI	Troponin-I
TPA	Tetrapropylammonium
TPeA	Tetrapentylammonium
TRP	Transient receptor potential
TRPA	Transient receptor potential ankyrin
TRPC	Transient receptor potential canonical
TRPL	Transient receptor potential like protein
TRPM	Transient receptor potential melastatin
TRPML	Transient receptor potential mucolipin
TRPN	Transient receptor potential NOMPC
TRPP	Transient receptor potential polycystin
TRPV	Transient receptor potential vanilloid
UPR	Unfolded protein response
WB	Western blot
ZO-1	Zonula occludens 1

CHAPTER 1

1. INTRODUCTION

1.1 TRP superfamily

The founding member of the TRP superfamily of ion channels was the *Drosophila* TRP (dTRP) gene. *Drosophila* trp gene mutant exhibited a 'transient receptor potential' response to light resulting in visually impaired flies. TRPs, mostly non-selective cation channels, are involved in various sensory functions and cation homeostasis; including detection of changes in light, pH, osmolarity, temperature, tastants, pheromones and mechanical stimuli. These integral membrane proteins are now known to underlie various abnormalities and diseases if disrupted (*1-4*). Such disruption can range from fatal neonatal effect as in the case of the loss of TRP polycystin-2 (TRPP2) to stationary night blindness and decreased visual acuity in the case of mutated TRP melastatin-1 (TRPM1) (*5*). Other diseases have been linked to other TRP members, with neurodegenerative, kidney, cardiac and chronic pain diseases are examples (*1;4;5*).

Members of TRP superfamily comprise seven subfamilies with similar membrane topology; TRPN (no mechanoreceptor potential C-like), TRPC (canonical), TRPM (melastatin), TRPML (mucolipin), TRPP (polycystin), TRPV (vanilloid) and TRPA (ankyrin). Each TRP member has six transmembrane domains with intracellular amino and carboxyl termini. Each subfamily has distinct channel domains and properties, with closely related members can share up to 80% protein homology (*5*). A phylogenetic tree, from Nilius B. et al. (*6*), illustrates the homology between mammalian TRP superfamily members (Figure 1-1)

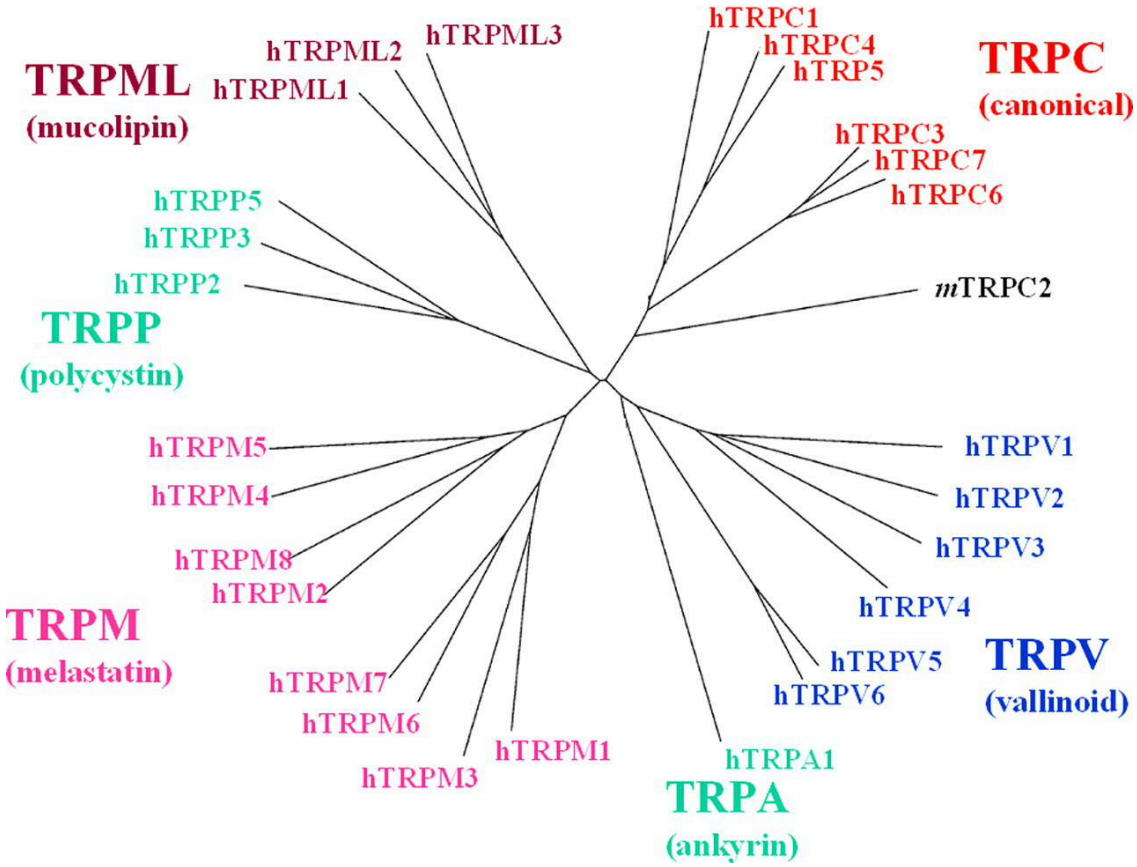

Figure 1-1 Phylogenetic tree of the mammalian transient receptor potential (TRP) channel superfamily *(6)*. Permission was not required for this figure to be reused in a thesis.

1.1.1 TRP superfamily structure/function relationship

A number of conserved structural domains have been reported in TRP subfamilies, with either a determined or an undetermined functional effect (*7*). Ankyrin repeats, TRP box, C-terminal coiled coil domain, EF hand, PDZ-binding domain, calmodulin binding domain, enzyme domain and phosphorylation sites are some examples of these regulatory structural domains (*7*). Below is a short summary of the most recent available knowledge about each domain and how it affects the TRP channel function.

Ankyrin repeats

Ankyrin repeats, the 33 amino acid (aa) long motifs, are present in the intracellular N-terminal domain of members of the TRPA, TRPN, TRPV and TRPC subfamilies (*8*). These protein-interacting domains are composed of multiple ankyrin repeats in human homologues, ranging from 2 repeats in TRPC5, 15 in TRPA1 (*7*), to 29 in TRPN members (*8*). Such repeats are proposed to serve as scaffold structures allowing ligand binding. This protein-protein interaction mediates and regulates the channel function (*8*). The longer repeats are proposed to sense mechanical stimuli in humans as well as in lower animal classes (*8;9*).

TRP box

A TRP box is a short (about 25 aa) conserved amino acid sequence found in the C-terminal domain of the TRP subfamilies: TRPN, TRPV, TRPC and TRPM (*10*). The function of TRP boxes was elusive until in 2005 when Rohacs and colleagues found

that the TRPM8 TRP box binds phosphatidylinositol (4,5)-bisphosphate (PI(4,5)P(2)) (*11*). The TRP box of TRPV1 was found to bind PIPs thereby regulating the channel gating and desensitization (*12*). Other studies revealed the role of conserved residues in the TRP box of TRPV1 and TRPV4, and highlighted the role of the tryptophan (W) residue within the box (*13;14*). For example, W733 in the TRPV4 TRP box interacts with L596 in the linker between the transmembrane domain 4 (TM4) and TM5 (*13*). Such interaction was reported to affect the channel open probability and gating (*13*). This, however, does not exclude the important role of other residues in the domain that mediates binding to lipid messengers and modulates channel functions (*12*).

Coiled coil domain

Coiled-coil domain (CCD) is a regulatory motif, composed of α-helices, that keeps the protein in a particularly stable state. CCD is a common C-terminal structure that serves as an oligomerization domain for several TRP members as well as for other ion channels, structural proteins and transcription factors (*15*). A number of determinants govern the function of the CCD, including: amino acid composition, length and how distal from TM6. Accordingly, CCDs have different roles in different TRP members; it is important for oligomerization and trafficking in some melastatin (TRPM) (1, 3, 6, 7) and vanilloid (TRPV) (1) TRP members but not essential for other members (*15;16*). Previous and recent studies highlight the interesting role of a CCD in channel gating (*17;18*), with a proposed mechanism where a CCD is involved in maintaining a closed channel state (*15;17;18*).

EF hands

EF hands are putative Ca^{2+} binding motifs. Their function can be either stimulatory or inhibitory. TRPA1 has a controversial N-terminal structure which has similar characteristics to known EF hands (*8*). This TRPA1 motif resembles EF hand motifs in binding Ca^{2+} and is capable of activating the TRPA1 channel (*19*). In contrast, when the EF hand domain in the C-terminus of the polycystin subfamily member TRPP3 (i.e. PKD2L1) was deleted, an increase in channel activity and a decrease in channel inactivation were observed (*18*).

Calmodulin binding domain

Calmodulin (CaM) binding domain is another Ca^{2+}-dependant regulatory motif found in TRP channels. While CaM binding sites were found in the N- and C- termini of TRPV1, it is usually detected in the C-terminal domain as in other TRPV members (*20-22*). CaM binding has been largely accepted for its inhibitory and desensitization role in the TRP superfamily (*15;20;21;23*).

PDZ-binding domain

PDZ-domain is a protein sequence of about 90 amino acids. It was initially identified in three proteins from which the acronym PDZ was derived. P is the first letter from the post-synaptic density-95 protein, D from the *Drosophila* discs large protein, and Z from the zonula occludens-1 (ZO-1) protein. TRP channels are known to have PDZ-binding sequences that facilitate the association of different scaffolding

proteins containing PDZ domains (*1;24;25*). Such association is critical for the proper arrangement of the signalling molecules along with the cytoskeletal components and TRP channels. Montell in 2005 called this macromolecular arrangement a signalplex (*26*), which was reported as a required assembly for the most efficient signalling retrieval and channel function.

Enzyme domain

A number of TRPM members are known to have an enzymatic domain and activity. While TRPM6 and TRPM7 have an α-kinase domain that is capable of serine/threonine kinase activity (*27*) and autophosphorylation (*28*), TRPM2 contains a NUDIX domain with adenosine diphosphate (ADP) ribose phosphohydrolase activity (*7;15*). In the case of the α-kinase of TRPM7, kinase activity is not a determinant of channel function (*29*); however, the NUDIX domain enzymatic activity in TRPM2 is essential for channel gating (*30*).

Post-translational modifications (PTMs)

TRP channels, as other cellular proteins, are regulated by post-translational modifications (PTMs). N-linked glycosylation, lipidation and phosphorylation are some of these cellular processes (*31*). All PTM modifications need a specific consensus region and structural site to accommodate them. Their roles are diverse, ranging from a reversible regulatory effect that can turn the channel function on/off to a modification that targets the channel to degradation (*31*). Here, the major focus will be on regulation by phosphorylation of different TRPs (*31-33*) for its relevance to the work performed

in the fourth chapter of this thesis. Phosphorylation has been reported to change the function of a number of TRP channels. A well-studied example is TRPV1 channel. TRPV1 sensitization/desensitization processes are affected by protein kinase C- (PKC) and protein kinase A- (PKA) dependent phosphorylation (*31*) and has a number of important serine residues identified (*34*).

Owsianik and colleagues summarized the major TRP structural domains and phosphorylation sites (Fig. 1-2) discussed above, with the phylogenetically related members illustrated beside each other at the same level (*7*).

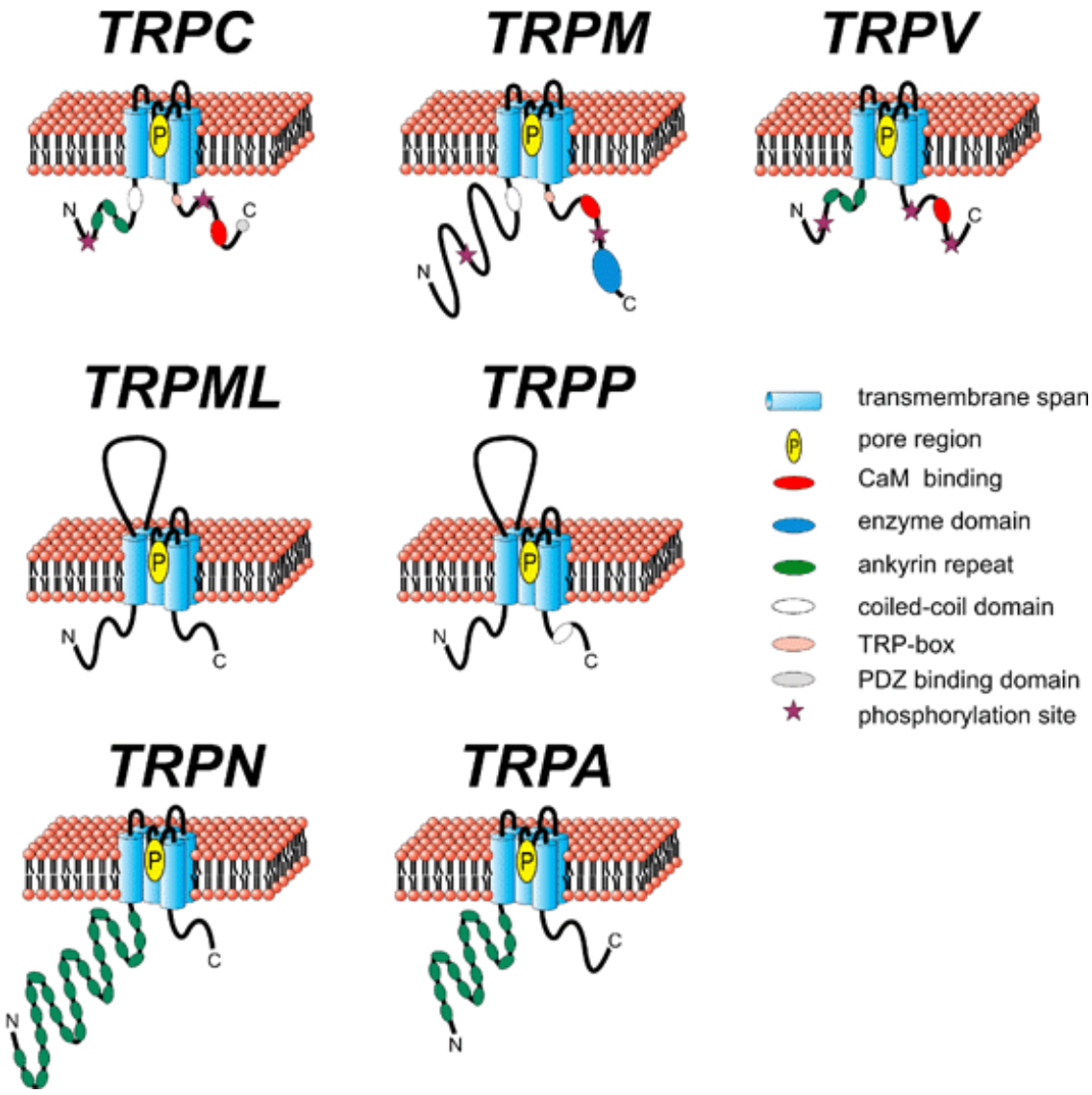

Figure 1-2 Schematic representation of the structural topology of TRP channels. The transmembrane segments are similar in all TRP channels. The putative pore region is localized between TM5 and TM6 and its length and amino acid composition are variable in different subfamily members. Only the most representative domains are annotated and lengths of the N- and C-termini are approximated. Reprinted, with permission, from Owsianik and others (2006) *(7)*.

1.1.2 TRP superfamily main functional regulation mechanisms

For their importance and relevance to the research described in this thesis, functional regulation of TRP channels by forming proper oligomers as well as the role of phosphoinositides in this regulation are discussed here.

Oligomerization

The tetrameric structure of functional TRP channels is evident (*35-37*). Although TRP channels can form homotetramers, they are still capable of heterotetramerization. For example, TRPC1 can form homotetramers as revealed by the atomic force microscopy (AFM) (*35*), and it can still form heterotetramer with TRPP2 (i.e. PKD2) in a unique alternating subunit assembly and 2:2 stoichiometry (*38*). Functional homo- and heterotetrameric channels were reported for many TRPs e.g.; TRPC1 (*35;38*), TRPP2 (*38-40*), TRPV5 and 6 (*41*) and TRPP3 (i.e. PKD2L1) (*23;42*). Domains for TRP channel tetramer formation and proper channel assembly were identified in the N-terminal (*43*), C-terminal (*39;44*), as well as the transmembrane domains (*45*)

Dimerization and trimerization domains were identified in many TRPs with some proved as non essential for channel function while others are prerequisite for proper channel tetramerization and function. One model of a functionally critical dimerization domain, that regulates tetramerization, is in the TRPP2 (i.e. PKD2) protein. Cysteine 632 (C632) was found important for dimerization along with residues in the N- and C-termini (*43*). Another model is in the TRPM subfamily where TRPM6 and 7 form a functional homo- and heterodimers with kinase activity (*46*). On the other

hand, although TRPP3 (i.e. PKD2L1) CCD crystal structure and chromatography experiments showed that it constitutes a trimerization domain (*47;48*), it was reported as a non essential domain for channel function (*18;45*).

Phosphoinositides

Phosphoinositides (PIs) constitute a small population of the cellular phospholipids but they represent powerful signalling messengers with pivotal roles in all aspects of cell regulation (*49*). Their phosphorylated heads provide enough charge to interact with various cellular proteins allowing a dynamic functional modulation of different proteins including ion channels (*49*). Functional regulation of TRP channels by phosphoinositides is evident and previously reviewed (*50-54*).

One of the most controversial regulatory phospholipids is PI(4,5)P2 (i.e. PIP2). PIP2 is the substrate for one of the major enzyme classes in cell signalling, phospholipase C (PLC). It is also the precursor of the key lipid messengers, inositol (1,4,5) trisphosphate (IP3) and diacylglycerol (DAG), upon hydrolysis by PLC. IP3 has its role in releasing Ca^{2+} from the intracellular stores through binding to IP3 receptors (IP3R), while DAG can activate many forms of PKC (*55*). PIP2 effects on TRP channels, even within the same subfamily, can differ substantially. Within the TRPC subfamily, one recent study reported the direct role of PIP2-mediated inhibition and DAG-mediated activation on TRPC6 and 7 channel function, independent of the downstream signalling molecules (*56*), yet other previous studies showed that DAG induces TRPC subtype inhibition by activating the downstream PKC (*57*). TRPP2 (i.e.

PKD2) also shows PIP2-dependent inhibition and its epidermal growth factor-mediated activity is phospholipase C-gamma dependent (*58*).

Figure 1-3 from Rohacs T. review (*59*) summarizes an interesting gating/desensitization mechanism that involves phosphoinositides and the activation of PLC pathway.

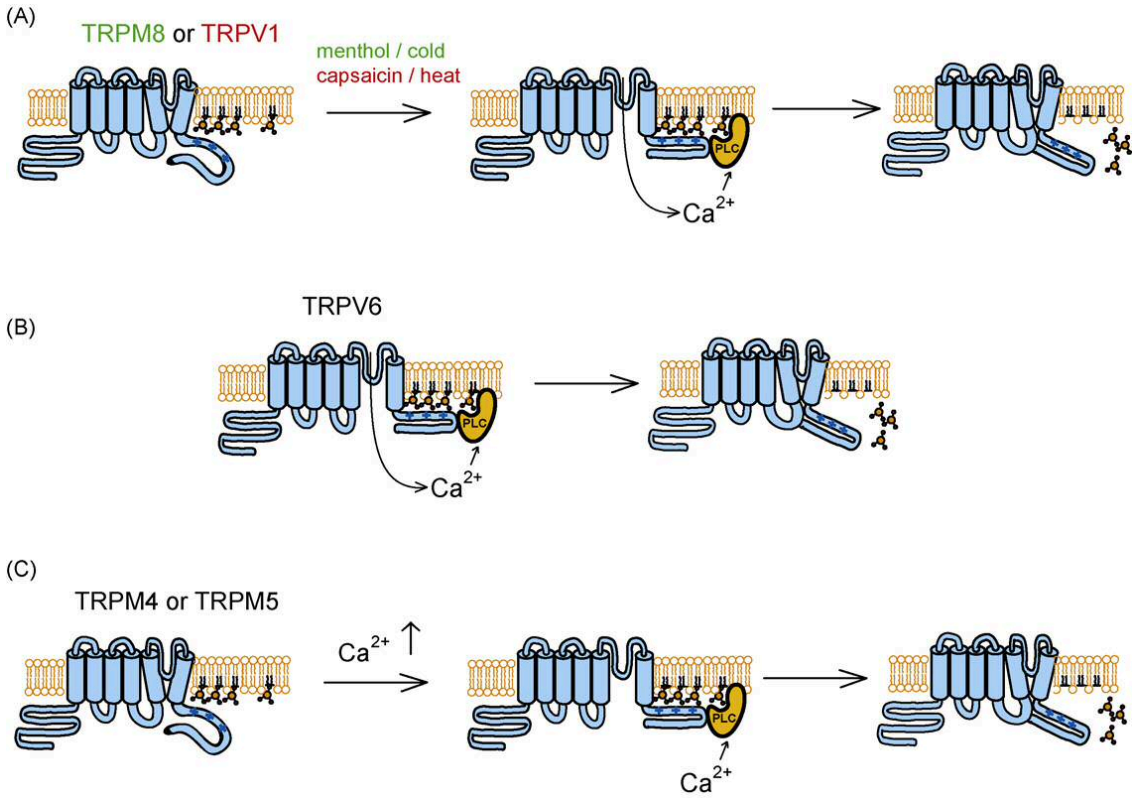

Figure 1-3 Calcium-induced activation of PLC leads to channel inactivation. (**A**) Menthol or cold opens TRPM8, capsaicin or heat opens TRPV1. Calcium flowing through the channels activates a Ca^{2+} sensitive PLC, probably a PLCδ isoform. This leads to the depletion of PIP2 (and PIP) and diminished channel activity (desensitization or adaptation). (**B**) TRPV6 is constitutively active; Ca^{2+} flowing through the channel activates PLC and the ensuing PIP2 depletion inactivates the channel, i.e., it stabilizes its activity at a lower steady state. (**C**) TRPM4 and 5 are impermeable to Ca^{2+}. Increased cytoplasmic Ca^{2+} activates these channels (fast effect), but it also activates PLC leading to the depletion of PIP2 (slower effect). This

sequence of events leads to a transient activation of these channels. Reprinted, with permission, from Rohacs review (2009) *(59)*.

1.1.3 TRP channelopathy

TRPs are known for their role in Ca^{2+} homeostasis, maintenance of other cation levels (like Mg^{2+}), as well as their role in maintaining the proper cell cytoskeletal structure. Many TRP mutations have been linked to the progression of human cardiovascular, metabolic, nephropathic, neurological and neoplastic disorders (*1;4;60*). Here, the focus will be on the main pathologic structural and functional mutations within members of each TRP subfamily. Channelopathies are ordered according to the phylogenetic relationship between subfamilies as arranged in Figure 1-1; starting with the classical TRPC channelopathies.

Although TRPN members are not expressed in mammals; its mutations and subsequent physiological defects will be mentioned as well for their importance in the general understanding of malfunctioned TRP channels and their being widely studied in *Drosophila melanogaster* and *Caenorhabditis elegans* models.

TRPC channelopathies

TRP superfamily founding members, the dTRP and TRPL, belong to the TRPC subfamily, with their mutations resulted in visually impaired flies (*61*). TRP mutant flies were not able to adapt to prolonged exposure to intense light and behaved as blind flies, with a reversible blindness. Flies with double *null* mutation of both TRP and TRPL lost their light-activated conductance (*61;62*). Cytoskeletal connections of dTRP and TRPL are of considerable importance in channel gating and signal termination (*1*), with any mutation that disrupt the proper assembly of the signalplex or Ca^{2+} homeostasis, such as the gain-of-function mutations in dTRP, is a factor contributing to retinal degeneration (*63*). TRPC1 is the first human TRP member to be cloned (*64*).

Although it is not directly linked to any genetic disease (*65*), its polymorphisms and low mRNA copies have been associated with diabetic nephropathy in humans and animal models (*65-67*). Through their role in Ca^{2+} homeostasis, TRPCs expression levels affected the progression of a number of human diseases; including, cancer (*68;69*), neurodegenerative and neuropsychiatric disorders (*65;70*). Familial focal segmental glomerulosclerosis (FSGS) and childhood nephrotic syndrome are two nephropathologic disorders linked to some mutations in TRPC6, mainly gain-of-function mutations (*71-75*). Interestingly, some TRPC6 genetic variants were not identified as pathogenic but rather affected the FSGS patients' therapeutic responses (*76*). Moreover, TRPC1, 3, and 6 are involved in the progression of cardiac hypertrophy, with their targeting representing a promising therapeutic manipulation (*77*).

TRPV channelopathies

A number of TRPV channels are associated with kidney and sensory defects. TRPV1 and TRPV4 are connected to a number of disorders including overactive bladder, chronic cough, diabetes and pain disorders (*77;78*). Inhibition of TRPV1 represents a good pharmacological intervention for its analgesic effect. In addition, TRPV4 inhibition was proven to improve bladder function in overactive bladder disorder (*77*). While the role of TRPV1 and 4 in obesity is controversial, recent studies point to their involvement in obesity in both human subjects and mouse model (*79;80*). Structural and/ or functional disruption in either TRPV5 or TRPV6 was linked to idiopathic hypercalciuria and vitamin D-dependent rickets, due to their role in renal

Ca^{2+} reabsorption. Additionally, some TRPV6 gain-of-function polymorphisms detected in patients forming kidney stones (*4*). TRPV3 is widely expressed TRP channel in the skin, with a critical role in skin and hair health and disease (*81;82*).

TRPM channelopathies

TRPMs, akin to other TRPs, are involved in many diseases. Their name is referred to, by some authors, as melanoma-related TRPs for their first member, TRPM1, presence in benign nevi and absence in malignant metastatic melanoma (*83*). TRPM1 expression level was inversely proportional to the aggressiveness of the disease. Beside their unique kinase and ADP binding domains, two TRPMs (4 and 5) are selective to monovalent cations only (*84*). TRPM4 may be involved in bladder and neurological disorders as well as cardiovascular disease (*84*), while TRPM5 single nucleotide polymorphisms (SNPs) are associated with increased risk of Type-2 diabetes (*85*). Moreover, TRPM2, 5 and 8 are involved in metabolic disorders and obesity (*80*). TRPM6, on the other hand, has a role in magnesium absorption and its non functional mutations are causing a hypomagnesaemia/hypocalcaemia hereditary syndrome (*86-88*). While the role of SNPs in TRPM7 in a number of neurodegenerative disorders and stroke are still controversial (*89;90*), the inhibition of TRPM7 was associated with reduced neuronal cell loss (*91;92*). Such an observation highlights its role in Ca^{2+}-overload mediated neuronal cell death (*93*).

TRPP channelopathies

The growth of numerous fluid filled cysts in the kidney in what is known as the Autosomal dominant polycystic kidney disease (ADPKD) is one of the most common genetic renal diseases, affecting 7-10% of patients in need of renal replacement (*94*). TRP polycystin 2 (TRPP2) or polycystic kidney disease 2 protein (PKD2) is the protein from the TRP superfamily responsible for 15-20% of the disease. PKD2 interacts with polycystic kidney disease 1 protein (PKD1), the other ADPKD protein responsible for 80-85% of the disease. Few ADPKD cases were not linked to either gene. The exact mechanism of the disease is not clearly delineated yet, with interrupted intracellular Ca^{2+} levels are pointed out by several studies (*94;95*). A reported unfolded protein response (UPR), increased ER stress and disrupted cytoskeletal structural connections of the channels were also highlighted as potential mediators of the disease (*96-100*). PKD2 is involved in cell proliferation and also has a profound role in placenta (*101*). PKD2 knockout mice fail to survive and die *in utero* (*101*). On the other hand, the physiological roles of the other two TRPP members TRPP3 (also called polycystic kidney disease 2 like 1 protein (PKD2L1)) and TRPP5 (i.e. PKD2L2) are even less studied. PKD2L1 absence is not lethal as shown in PKD2L1 knockout studies, with a mild signalling and developmental defect (*102*). Absence of PKD2L1 as well as other genes from the tongue was associated with loss of sour taste in two patients in one study (*103*), with retinal detachment in another one (*103;104*) and linked to circulating phospholipid levels in others (*105;106*). On the other hand, nothing is known about a pathological role for PKD2L2.

TRPML channelopathies

Interestingly, TRPML1 is not only responsible for Ca^{2+} permeability, but it is also permeable to iron (as Fe^{2+}, ferrous ion) and Manganese (Mn^{2+}) (*107*). It has an important role in controlling cation concentrations in the late endosomes and lysosomes and its loss-of-function mutations results in mucolipidosis type IV (*108*). Mucolipidosis type IV is an autosomal recessive lysosomal storage disorder characterized by delayed development, visual abnormalities and anaemia (*109*). Pathological mechanisms underlying the disease are still unclear. The roles of TRPML1 in other lysosomal disorders have been proven and the use of TRPML1 agonist has shown improvement of Niemann-Pick (NP) syndrome type C, another lysosomal storage disorder (*110*). Other studies had shown that TRPML2 and 3 have similar function to TRPML1 and may potentially heterooligomerize (*108*). These studies highlight the pivotal role of TRP channels in maintaining the proper ion homeostasis in different subcellular organelles.

TRPA channelopathies

The only member of the TRPA subfamily, TRPA1, is known to be activated by a wide range of irritants; for example, allyl isothiocyanate found in mustard oil and cinnamaldehyde found in cinnamon activates the channel (*111*). It is known also as a pain sensor and implicated in the pathogenesis of migraine, dental pain as well as other types of pain (*112*). For this, two TRPA1 antagonists have been identified for their pharmaceutical potential as pain killers (*113*). Moreover, TRPA1 may be a molecular determinant in many human disorders; including, asthma, respiratory distress and inflammation, skin irritation, diabetes, cancer and bladder disorders (*77;112*).

TRPN channelopathies

The no mechanoreceptor potential-C (NOMPC) channels in *Drosophila* were identified in 2000 by Walker *et al.* and form the TRPN subfamily, which was considered the first member of the TRP superfamily phylogenetically distal from the mammalian members (*114*). It was discovered for its profound effect in mechanosensory transduction. NOMPC loss-of-function mutant flies loses their mechanosensory responses, and several point mutations altered the flies mechanosensory signalling transduction (*114*). *Caenorhabditis elegans* TRPN members have been the focus for further recent studies that revealed the role of TRPN gain-of-function mutations in neurodegenerative disorders (*115*).

Figure 1-4 summarizes the distribution pattern of the major human pathogenic TRP channels members and their main associated disorders as illustrated by Kaneko and Szallasi (*77*).

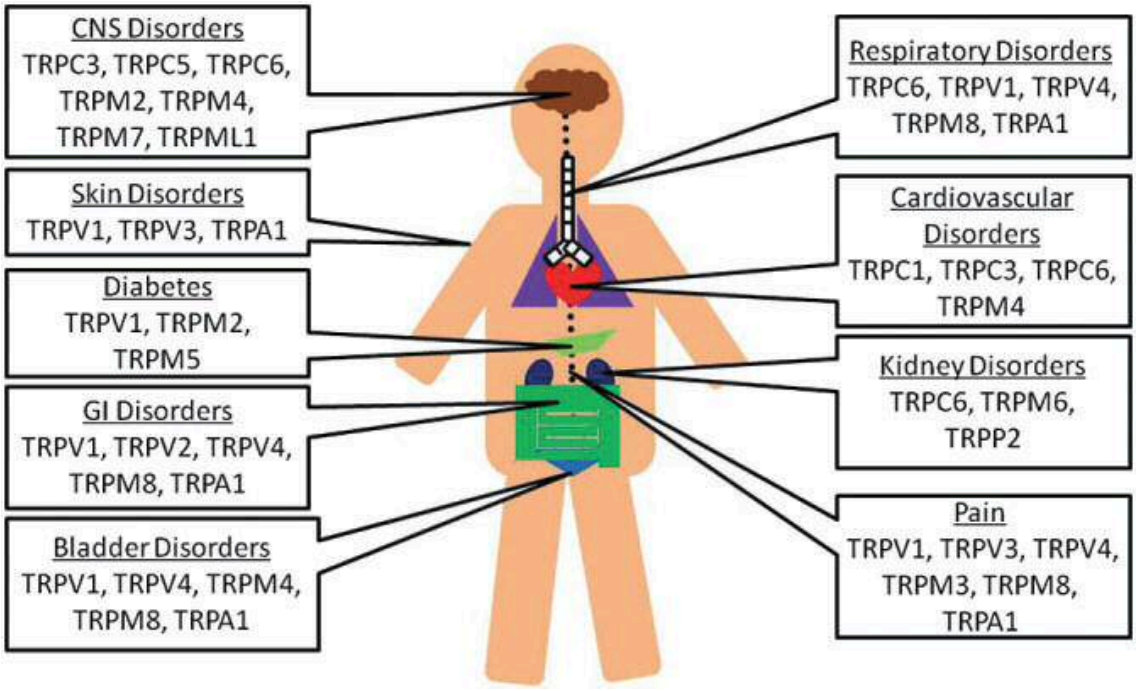

Figure 1-4 Schematic illustration of the tissue-distribution of TRP channels and their putative roles in the pathogenesis of human disease. Reprinted, with permission, from Kaneko and Szallasi (2014) *(77)*.

1.2 PKD2L1 structure and main biophysical characteristics

PKD2L1 belongs to the TRPP subfamily and possesses a membrane topology similar to all TRPs with six transmembrane domains, intracellular N- and C-termini and a pore domain between TM5 and TM6. Figure 1-5 shows PKD2L1 membrane topology and highlights the major domains and posttranslational modifications as described previously (*116;117*). It shares about 50% sequence identity and 71% similarity to PKD2 protein (*116*). It also shows an overall ≈ 21% identity and ≈ 47% similarity to many other cation channels and more specifically to the α subunits of the pore-forming Ca^{2+} channels (*116*). A major difference between PKD2L1 and the α subunit of voltage-gated cation channels is the absence of an adequate number of positively charged residues in its predicted TM4, while the presence of 5 to 8 positively charged arginine (R) and lysine (K) residues in TM4 of these channels act as voltage sensors (*118*).

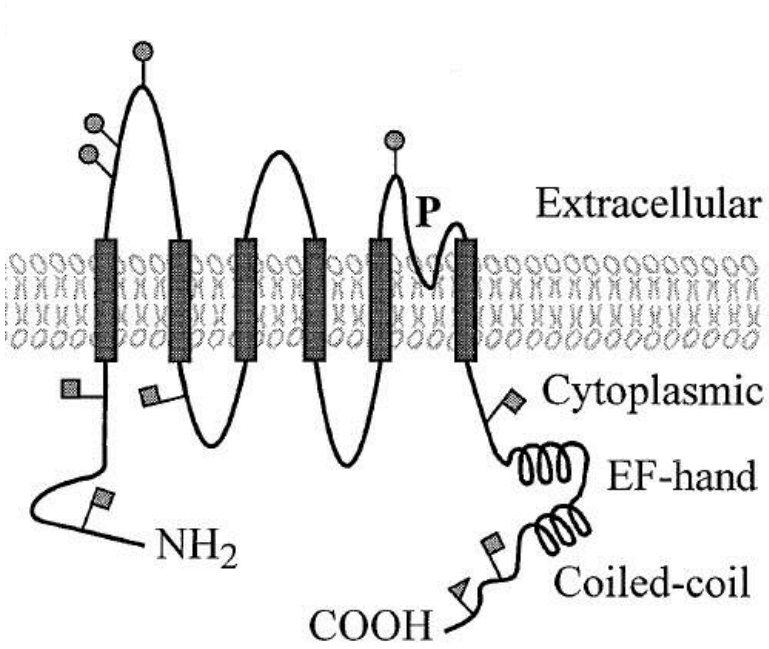

Figure 1-5 Proposed membrane topology for PKD2L1. `P' and circular, triangular and square flags indicate, respectively, the pore region, N-glycosylation, PKA- and PKC-phosphorylation sites. Reprinted, with permission, from Chen *et al.* (1999) *(117)*.

Both TRPP and TRPML subfamily members are recognized by their long putative first extracellular loop, which is predicted to be the longest among other TRPs reaching around 200 aa (*119*). PKD2L1 predicted first extracellular loop, according to Uniprot online data base, is 189 aa in length while the pore domain is 42 aa. Two aspartic acid residues in the pore domain have been reported to be important for channel Ca^{2+} permeability. These are the D523 and D525 (*42;120*).

The PKD2L1 N-terminus is where the main difference between PKD2 and PKD2L1 lies, as it lacks a 100 aa sequence present in PKD2. Part of PKD2L1 N-terminus was reported to include a sequence essential for docking the receptor for activated protein C kinase 1 (RACK1), a scaffolding protein that regulates cellular functions and found to regulate PKD2L1 channel expression and function (*121*).

PKD2L1 C-terminus contains an EF hand and a coiled coil domain. Both are not involved in the initiation of the channel activity but rather share in the inactivation process (*18*). The coiled coil domain was found to contribute to the oligomerization process (*47;48*), but is not a determinant of the channel function (*45*). Proximal to the TM6, the C-terminus has two ER retention signals (*122*) and a plextrin homology (PH) domain (*52*), with the first ER retention signal (starting at K575) has a primary function over the second one (*122*). In addition, amino acid residues starting at T622 are not essential for channel function (*18*).

Akin to other TRP channels, functional PKD2L1 channel is found in homo-or heterotetramers, with an estimated pore size of ≈7 Å (*123*). With this pore size, the channel is reported permeable to small mono- and divalent cations like, Ca^{2+}, Ba^{2+}, Sr^{2+}, K^{+}, Rb^{+}, Li^{+} and Na^{+} (*117*). PKD2L1 is also permeable to small organic cations

like methylamine, dimethylamine, triethylamine and tetramethylammonium (*123*) but impermeable to protons and larger ones like N-methyl-D-glucamine (NMDG) and choline. Large cations have an inhibitory effect on cation permeation through PKD2L1, which may be due to blocking the pore region, or competing at a binding site through the permeation pathway. The inhibition potency of large organic cations is inversely correlated with their sizes (*117;124*). PKD2L1 channel is also reported to have higher permeability to NH_4^+ and Cs^+ than Na^+ (*124*).

Noteworthy, the channel's mono- and divalent cation permeability is not additive and cations may compete to bind to the same site if present in the same solution or they may interact with each other in what is called the anomalous mole fraction effect (*123*). The anomalous mole fraction effect can be described when an ion channel conduct less current of two permeant ions when mixed than in their pure solution (*125*). Moreover, PKD2L1 have a relatively high single channel conductance of ≈ 137 ± 7 pS (*117*). While the channel is not voltage-gated, it showed some modulation by voltage. An increase in the open probability (NP_o) and mean open time (MOT) at negative voltages compared to positive ones is evident (*124*).

1.3 PKD2L1 tissue-distribution and expression

1.3.1 Taxonomic overview

PKD2L1 gene was assigned to the long arm of the human tenth chromosome in band q24 (*116*). Murine PKD2L1 was translated from 15 exons that spread over 29 kb. In contrast to the other homologous ion channels in which each transmembrane domain was coded by one exon, coding of four PKD2L1 transmembrane domains was divided between two exons (*122*).

Considering the importance of the sense of taste in animals and its role in detecting harmful food and control of the animal's feeding behaviour, recent evolutionary studies have an interesting addition. Surprisingly, different whale and dolphin species have various pseudogenes that include *PKD2L1* among others (with premature stop codon after exon 4 or 5 depending on species) and lack the functional gene, to make them very unique mammals that lack four out of the five basic taste qualities with only one putatively functional taste modality (*126*).

The sagittal organ is another sensory system where PKD2L1 is an essential component and widely accepted as a marker for its main constituents, the cerebrospinal fluid contacting neurons (CSF-cNs) (*127-129*). CSF-cNs are GABAergic neurons that line the central canal along the entire length of the mice spinal cord (*128;130*) as well as other bony vertebrate species (*127*). This sensory system is hypothesized to modulate the sense of locomotion, body movement and position. Recently, it was determined that this sensory system is marked by the expression of PKD2L1 and is conserved from bony fish to primates (*127*).

1.3.2 Endogenous PKD2L1 expression in experimental animals

In adult mice, PKD2L1 expression was detected in the apical membrane of the principal cells of the inner medullary collecting ducts (IMCDs) (*131*). Basora *et al.* (*131*) also detected PKD2L1 expressed in adult mice in ganglion cells in the retina, biliary ducts in the liver, epithelial cells in the pancreatic ducts, spermatocytes in the testis, reticular cells in the spleen, endothelial cells of the major blood vessels and the epicardium in the heart. Later studies by Huang *et al.* (*130*) documented the presence of PKD2L1 in the brain stem and CSF-cNs in P1-P4 mice. It is reported also that PKD2L1 expression is abundant in adult mouse brain (*132*). Another study confirmed the presence of PKD2L1 in stria vascularis, spiral ganglion cells, vestibular sensory cells, dark cells, and ganglion cells of the mouse inner ear (*133*).

PKD2L1 was detected early during the embryonic development. Similar to adult mice, PKD2L1 localization was evident in mouse embryonic IMCDs starting at the 16th day of gestation (E16) (*131*). As just mentioned, PKD2L1 is reported in perinatal mice (P1-P4) CSF-cNs (*130*), it was recently also detected in CSF-cNs starting at E14.5 in mice and somite-18 stage in zebrafish (*127*).

In 2006, PKD2L1 was the first protein to be identified as a good candidate for sour taste perception (*130;134;135*). PKD2L1 has a distinct expression to the taste bud pore in all mouse taste bud papillae and areas. These studies along with others (*136;137*) confirmed the labelled line mode of taste coding and further proved the segregated perception of different taste modalities at the periphery; which means each taste quality is mediated by a special type of taste receptor cells (TRCs), independent of

the other taste modalities. Of note, PKD2L1 is now a widely accepted marker for sour tasting TRCs (*130*) and CSF-cNs (*127-129*).

Interestingly, the Basora lab (*138*) found that PKD2L1 was having a distinct localization pattern in proliferative and non proliferative rat and mouse IMCDs as well as in Madin–Darby canine kidney (MDCK) cells. For subconfluent cultures, PKD2L1 was localized mostly in the endoplasmic reticulum (ER) with a little plasma membrane portion. In confluent cultures, some PKD2L1 was still in the ER with a good PM targeting and this report was the first to demonstrate the presence of PKD2L1 in the primary cilia and centrosomes of the above mentioned cell types (*138*). Subsequent studies confirmed the abundance of PKD2L1 in primary cilia using the mouse embryonic fibroblasts (MEF) and mouse retina pigmented epithelium (mRPE) (*23*).

1.3.3 Expression in Humans

Human tissue samples subjected to RNA dot blot and Northern hybridyzation analysis revealed the presence of PKD2L1 in adult and fetal tissues, with more abundance in fetal tissue when compared to the adult state (*116*). This pattern of expression is in contrast to the expression in mice described in the previous section (*131*). Three human PKD2L1 splice variants were isolated from kidney (805 aa), liver (lack the EF-hand) and testis (lack 45 aa from the C-terminus). PKD2L1 was detected in human heart as well, but with no splicing information available (*139*). All variants kept the basic channels properties (*18*). PKD2L1 was found at high densities in the primary cilia of two human cell types where it interacts with PKD1L1 (*23*).

SNPs in PKD2L1 sequence are evident as well. PKD2L1 has two SNPs. One reported in nucleotide 2147, where there is an A in the first reported sequence (*116*) and a C in a later report (*18*), but it did not result in a change in the aa residue. Another SNP at nucleotide 2203 (from C to T) resulted in a change in the 716 aa residue from glycine to proline (*18*).

1.4 PKD2L1 Function; what is already known

1.4.1 pH sensing

PKD2L1 was proposed as a pH sensing channel by three independent studies in 2006 (*130;134;135*). While low extracellular pH inhibits the channel and decreases its basal conductance (*117;140*), the channel was proposed to have a 'delayed response to acids' (*134*). Two years later, Inada *et al.* (*141*) proposed that this 'delayed response' is an off-response, where the stimulus (in this case the acid) has to be replaced by a less acidic solution for the channel to elicit its activity. In human embryonic kidney (HEK) cells, TRCs but not CSF-cNs, off-response activity was determined to require two main factors: the expression of a polycystic kidney disease protein 1 like 3 (PKD1L3) and a specific H^+ ion concentration (threshold pH). The latter is dependent on the biological or heterologous expression system used.

PKD2L1/PKD1L3 complex off-response current amplitude was proportional to the difference between the stimulating pH and the wash pH (*141*). PKD2L1/PKD1L3 channel off-response has some fundamental properties; PKD2L1/PKD1L3 channel activity is dependent on the stimulating pH (*130;134;141;142*) and type of acid but independent of the duration of acid application time. The type of acid is further explained and comparable to the degree of the dissociation of the acid (*134;143*). In addition, PKD2L1/PKD1L3 off-response can be repeated and is not followed by a desensitization period, compared to PKD2L1 Ca^{2+}-induced activation. Moreover, Inada *et al.* (*141*) also reported that PKD2L1/PKD1L3 off-response current inactivation was markedly enhanced in the presence of extracellular Ca^{2+}.

Mouse PKD2L1 (mPKD2L1) is sensitive to alkalization in a bimodal manner (*144*). Shimizu and colleagues reported (*144*) that homomeric PKD2L1 NP_o was increased by raising the pH to 8.0 - 9.0 and accordingly increased its current, while raising it to 10.0 has an inhibitory and inactivating effects. In the same study, PKD2L1 was proposed to be activated by alkalization for the robust current observed upon the wash of pH 10.0 with neutral pH, which may be simply explained by the removal of the inhibitory effect of pH 10.0. Moreover, current simulation studies assumed that PKD2L1 as part of PKD2L1/PKD1L3 channel complex is an alkali-activated cation channel (*145*).

1.4.2 Ca^{2+} regulation

Ca^{2+} activation and cation permeability are the first PKD2L1 channel properties to be reported soon after its discovery in 1998 (*117*). Ca^{2+}-induced activation was detected in heterologously expressed human PKD2L1 (hPKD2L1) in *Xenopus* oocytes. It was followed by a reversible desensitization period that may last up to 10 min. The study of PKD2L1 splice variants led to the discovery that the C-terminus EF-hand is not essential for either the initiation of channel activity or its activation, but it rather augments the inactivation process (*18*).

hPKD2L1 showed Ca^{2+}-induced activation when the channel was expressed in *Xenopus* oocytes (*117*), but not HEK293T cells (*23;140*). The latter was characterized by an outwardly rectifying current when expressing mPKD2L1 (*140;144*) or hPKD2L1 (*23*). HEK expressing mPKD2L1 was constitutively active, highly permeable to Ca^{2+} and its currents were inhibited by the high extracellular Ca^{2+} (*140*). DeCaen and others

(*23*) reported that hPKD2L1 expressed in HEK cells is not activated by high extracellular Ca^{2+}, but rather it forms homomeric channels that conduct large non-selective cation current with moderate Ca^{2+} selectivity.

PKD2L1/PKD1L1 channel complex is a main ciliary channel that maintains a surprisingly high Ca^{2+} concentrations (≈ 600 nM) inside the cilium, distinct from the resting cytoplasmic Ca^{2+}concentrations (≈ 100 nM) (*102*). The cilia from human retina pigmented epithelium cell line (hRPE) were found to possess a non-inactivating outwardly rectifying current that is 56 fold higher than that produced from the hRPE cell bodies (*23*). Such current was moderately selective to Ca^{2+} and heat while not sensitive to pressure and mechanical stimuli (*23*). This channel activity is thought to keep high levels of Ca^{2+} in primary cilia at rest and allow the regulation of certain hedgehog signalling components (*102*).

1.5 PKD2L1 functional modulation

1.5.1 Chemical modulators

PKD2L1 was inhibited by amiloride and analogs in a reversible manner. Such an inhibition affected the channel MOT and NP_o, but not the single channel conductance (*146*). Moreover, PKD2L1 was inhibited by external application of Mg^{2+} in a voltage-dependent manner (*124*) and ciliary PKD2L1 currents were sensitive to ruthenium red (*23*). Additionally, PKD2L1 was reversibly inhibited by the Chinese herb *Sparganum stoloniferum* Buch.-Ham. (*147*)

The channel was also inhibited by NMDG, choline, La^{3+}, Gd^{3+}, and large organic cations including tetraethylammonium (TEA), tetrapropylammonium (TPA), tetrabutylammonium (TBA) and tetrapentylammonium (TPeA), while not sensitive to Co^{2+}, Pb^{2+}, Zn^{2+}, and Cd^{2+} (*117;123;124*). Large organic cations have been reported to act in two different mechanism; so it either affects the single channel conductance without affecting the channel MOT and NP_o (e.g; TBA), or it can affect the channel MOT and NP_o (e.g; TEA, TPA, and TPeA) without affecting the single channel conductance (*123*). The former mechanism suggests that the inhibitor acts on the pore domain and affects the permeation filter, while the latter affects the channel gating mechanism (*123*). Inhibition was found to be correlated with the size of the organic cation.

PKD2L1 expressed in HEK cells was modulated by cell volume changes, with a mechanism that involves phospholipase A_2 (PLA_2). Application of the non-selective PLA_2 inhibitor, 4-bromophenacyl bromide (pBPB), abolished PKD2L1 currents and application of 10 μM arachidonic acid increased them (*140*). This study points to the

role of lipid messengers in modulating PKD2L1 activity. In addition, CaM antagonists and calmidazolium activated/augmented PKD2L1 channel conductance in primary cilia (*23*).

1.5.2 Oligomerization

Molland and colleagues (*47*) identified a structural motif in the C-terminus of PKD2 and PKD2L1 that is responsible for trimerization and Ca^{2+} binding. More specifically the CCD (CC2) domain from F839 to K876 and G692 to K741 in PKD2 and PKD2L1, respectively, was identified as a Ca^{2+}-independent trimerization domain (*47*). A subsequent study from the same group identified a conserved structural motif responsible for this observed PKD2L1 trimerization (*48*). This motif is composed of the residues R–h–x–x–h–E (where "R" is Arg, "E" is Glu, "h" is a hydrophobic residue, and "x" is any residue) as shown in Figure 1-6. An arginine from one molecule extends around the exterior of the helix to form an ionic interaction with a glutamic acid from the adjacent molecule through a salt bridge (*48*). However, the fact that the function of PKD2L1 does not depend on this domain challenges its importance (*18;45*).

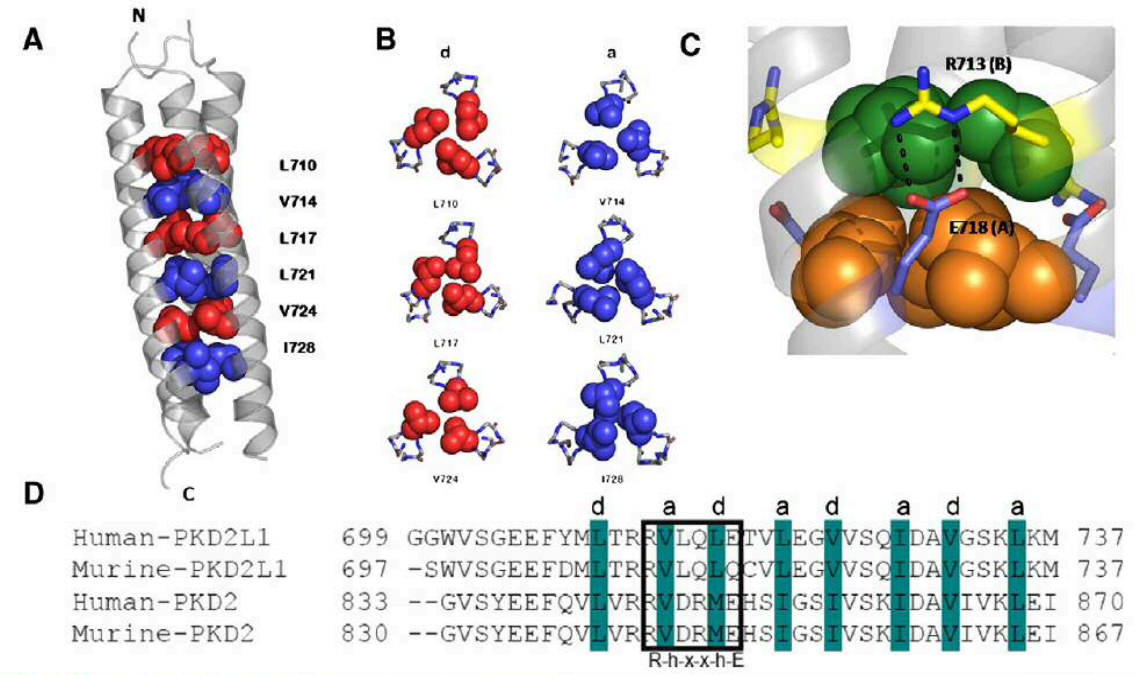

Figure 1-6 PKD2L1 CRD trimerization is promoted by specific conserved residues. (**A**) PKD2L1 CC2 structure with residues at "a" and "d" positions of the heptad repeat coloured blue and red, respectively. (**B**) Acute packing geometry of individual coiled-coil layers with backbone atoms shown as sticks and side chains shown as spheres with same coloring as in (**A**). (**C**) Magnification of "R–h–x–x–h–E" trimerization motif in which R713 from chain B forms a salt bridge (dashed black lines) with E718 from chain A. (**D**) Sequence alignment of the of crystallized region (first line) with other polycystins. Conservation of residues at "a" and "d" positions of coiled coil highlighted in teal and conserved salt bridge outlined by a black box. Reprinted, with permission, from Molland *et al.* (2012) *(47)*.

1.5.3 Protein partners of PKD2L1

PKD2L1 interacts and is functionally modulated by a number of proteins, including, PKD1 (*122*), PKD1L1 (*23*), PKD1L3 (*45;130;134;135*), α-actinin (*132*), troponin-I (*139*) and RACK1 (*121*).

Troponin-I

Troponin-I (TnI) was the first protein partner interacting with PKD2L1 to be identified (*139*). Li *et al.* (*139*) showed that skeletal and cardiac TnI isoforms reduced PKD2L1 channel function, with an inward rectification at negative membrane potentials, without affecting its PM targeting. This modulation of the channel function was through direct interaction between the two proteins, as revealed under *in vivo* and *in vitro* conditions. Native human PKD2L1 interacts with skeletal and cardiac TnI under normal conditions (*139*). PKD2L1 C-terminus likely mediated this interaction through its EF-hand and CCD with two TnI CCDs (*139*). Knowing that TnI is an important regulatory protein in the actin cytoskeleton system, this study established the association of PKD2L1 with the actin cytoskeleton.

PKD1 family members

While PKD1 family members are described as polycystins, for their founding member PKD1 causing ADPKD (*148*), due to their limited structural similarity to TRPs they are not considered members of the TRP superfamily (*149*). PKD1 family members (PKD1, PKD1L1, PKD1L2, PKD1L3, PKDREJ) are large proteins that have different topology from PKD2 channels with 11 TMs and a long extracellular N-

terminus. The long extracellular N-terminus has multiple domains that allow for protein-protein, protein-carbohydrate interactions, as well as a G-protein coupled receptor (GPCR) proteolytic site (GPS) domain. The last 5 TMs proximal to the C-terminus are similar to TRP channels (*150*). Figure 1-7 illustrates one member of the PKD1 family, mPKD1L3. Of note that human PKD1L3 does not contain S/P-rich repeats (*151*). PKD2L1 interacts with PKD1 family members PKD1, PKD1L1 and PKD1L3.

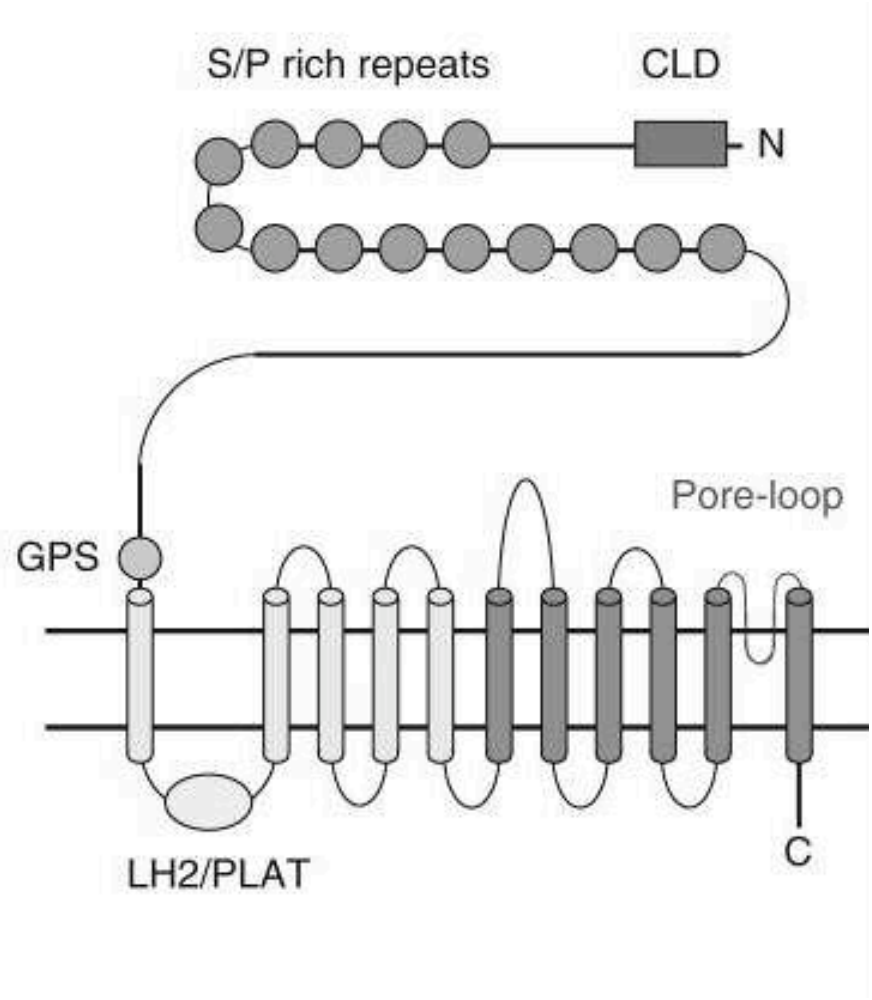

Figure 1-7 Schematic drawing illustrating conformational structures of mPKD1L3. mPKD1L3 is predicted to have 11 transmembrane domains, and contains an N-terminal CLD, 29 S/P-rich repeats, a GPS, and a PLAT/LH2 domain. CLD, C-type lectin domain; S/P-rich

repeats, serine/proline-rich repeats; GPS, G-protein-coupled receptor proteolytic site; PLAT, polycystin-1-lipoxygenase-alpha toxin; LH2, lipoxygenase homology 2 *(151)*.

Murine PKD2L1 can form a functional channel with PKD1 that is responsive to hypo-osmotic solution. PKD2L1 C-terminal CCD mediated this interaction, which was believed important for PKD2L1 PM trafficking. The same study identified and highlighted the essential role of PKD2L1 ER retention sequence (*122*). Another study showed that PKD2L1 colocalizes with PKD1 in the same complex in cell-to-cell contact, specifically in desmosomes, as well as in the cilia (*138*).

PKD2L1/PKD1L3 channel complex was extensively studied for its role in sour tasting and pH sensing (*45;120;134;141-143;152*). It was determined that the heteromeric channel have a similar unitary Na^+ conductance (144 pS) (*141*) to that initially reported for PKD2L1 when expressed alone in *Xenopus* oocytes (137 pS) (*117*). The two proteins interact through different sites, including the C-terminus as well as several TMs (*42;45*).

PKD2L1/PKD1L1 is the most recent channel complex that has been deemed important for controlling Ca^{2+} levels in primary cilia and regulating the sonic hedgehog signalling proteins (*23;102*). While homomeric PKD2L1 channels were still fully functional when knocking down PKD1L1, but the proposed channel unitary conductance suggested that the main functional channel *in vivo* is the heteromeric one (*23*).

α-actinin

In vivo and *in vitro* evidence showed that α-actinin binds to the C-terminus of PKD2L1 in a Ca^{2+}-independent manner (*132*). Co-immunoprecipitation (co-IP) from human kidney, human heart, mouse brain, HEK and MDCK cells showed an

interaction between PKD2L1 with muscular and non-muscular types of α-actinin in native and transfected tissue and cells (*132*). Such an interaction enhanced PKD2L1 plasma membrane presence and channel open probability and functional activity.

RACK1

RACK1 is a scaffolding protein that belongs to the tryptophan-aspartate repeat (WD-repeat) family. It is homologous to the β subunit of G-proteins and implicated in many cellular physiological processes; for example, cell proliferation and migration, transcription, protein synthesis and neuronal functions (*153*). RACK1 physically interacts with PKD2L1 through the last WD motifs of RACK1 and the first 45 aa residues in the N-terminus of PKD2L1 (*121*). RACK1 was found to significantly inhibit PKD2L1 channel function and reduces its PM population.

1.6 PKD2L1-associated clinical manifestations

While PKD2L1 has a high similarity and sequence identity to PKD2, there is no evidence that it shares in the progression of the ADPKD. To date, there is no clear genetic disease linked to PKD2L1 mutations or absence, however, there are some worthy observations that will be covered here.

PKD2L1, as a candidate receptor for sour taste, was linked to sour taste disorders. The sense of taste in mice lacking PKD1L3 was similar to wild-type (WT) mice but targeting of PKD2L1 was accompanied by a substantial reduction (25%-45%) in sour tasting (*154*). Similarly, two patients with sour ageusia (i.e.; inability to taste sour) had undetectable levels of transcripts coding acid sensing ion channels (ASICs) and PKDs (especially PKD2L1) when biopsies from human lingual fungiform papillae were tested (*103*). Additionally, genetic ablation of the PKD2L1-expressing TRCs in mice abolished their ability to taste sour while it did not affect sensing any of the other taste qualities (*130*).

PKD2L1 knockout mice ($PKD2L1^{-/-}$) are apparently healthy with a moderate taste disorder as discussed earlier (*154*). Another malformation observed in 50% of the PKD2L1-deficient mice was intestinal malrotation, a developmental defect associated with the subsequently affected SHH signalling pathway (*102*). In addition, unpublished observations from my own work include 1) loose cell-to-cell contact in $PKD2L1^{-/-}$ heart tissue sections compared to the WT control hearts; noteworthy, PKD2L1 presence in desmosomes is evident with a not-yet-defined function (*138*), and 2) hair loss in some body areas of $PKD2L1^{-/-}$ mice accompanied by the urge to itch and dermatitis.

Although Gilliam and Wensel detected a weak Northern blot signal of PKD2L1 in the mouse retina (*155*), human and mouse RPEs have a dense population of heteromeric PKD2L1/PKD1L1 on their primary cilia (*23*). This may point to the tight translational regulation of PKD2L1 according to the cellular compartment. A previous report proved such conditional translational regulation to the parent homologue PKD2 (*100*). Moreover, downregulation of PKD2L1 was detected and changed proportional to the stage of human retinal detachment and was proposed as a biomarker for the retinal detachment process (*104*).

1.7 Thesis rationale

Mammalian cells expression systems would be better choices compared to *Xenopus* oocytes. However, the ion channel protein PKD2L1 we study mostly localizes to the intracellular endoplasmic reticulum membrane in these cells. We choose oocytes that have been shown to be able to target PKD2L1 to the surface membrane, so that we can employ electrophysiology approaches to study the function and regulation of the channel.

1.8 Thesis objectives

The main purpose of the current study was to gain a better understanding of the factors regulating the TRP-type channel, PKD2L1. For this, my first objective was to determine whether PKD2L1 acid-induced activity requires the protein partner PKD1L3. My second objective was to investigate the C-terminus structure/function relationship involved in channel activity and their subsequent effect on oligomerization. My third objective was to study the role of lipid messengers and potential phosphorylation sites involved in PKD2L1 channel regulation.

Our hypotheses were that 1) PKD2L1 off-response property does not require the presence of the protein partner PKD1L3, 2) PKD2L1 C-terminus contains an important domain (K575-T622) that is essential for both channel function and oligomerization, and 3) PKD2L1 is regulated downstream of phospholipase C pathway, with the subsequent activation of protein kinase C is accompanied by channel inhibition/inactivation.

CHAPTER 2

2. RESULT #1 Acid-induced off-response of PKD2L1 channel in *Xenopus* oocytes and its regulation by Ca^{2+}

2.1 INTRODUCTION

Polycystic kidney disease (PKD) protein 2 Like 1 (PKD2L1) belongs to the transient receptor potential (TRP) superfamily of which members are implicated in a number of sensory functions, such as detection of light, force, osmolarity, temperature, odor, taste and pain *(1;2)*. Human PKD2L1 gene is a homologue of PKD protein 2 (PKD2) and was first identified in 1998 *(3)*. While mutations in PKD protein 1 (PKD1) and PKD2 account for about 80% and 15% of the cases in autosomal dominant PKD (ADPKD) *(4)*, respectively, PKD2L1 does not seem to be involved in the disease. In 1999, Chen *et al*. discovered the Ca^{2+}-regulated non-selective cation permeability of PKD2L1 *(5)*. We previously reported that human PKD2L1 expressed alone in *Xenopus* oocytes targets to the plasma membrane (PM) and shows the regulation of Ca^{2+}-induced channel activation (on-response) by a number of factors including Ca^{2+}, voltage, pH, amiloride analogs, large monovalent organic cations, troponin I, α-actinin, and receptor for activated protein kinase 1 (RACK1) *(5-12)*.

In mammalian cells, outward rectifying cation permeability of PKD2L1, with or without co-expression of PKD protein 1 Like 1 (PKD1L1, a homologue of PKD1), was recently reported *(13)*. This group of researchers found that PKD2L1, present in primary cilia, regulates the ciliary Ca^{2+} concentration and sonic hedgehog signalling. Lack of PKD2L1 in mice was associated with defective hedgehog signalling and development of inverted colon *(13;14)*. In mammalian cells and oocytes, PKD2L1, in complex with PKD protein 1 Like 3 (PKD1L3, another PKD1 homologue), was activated by acids in an off-response manner, i.e., the PKD2L1/PKD1L3 channel complex mediated a large current only after the removal of the extracellular acid

(15;16). These and subsequent studies *(17;18)* indicated that PKD2L1 or PKD1L3 forms a novel extracellular acid sensor. Forming a candidate for sour taste sensation, PKD2L1 was shown to interact with PKD1L3 *(18)* in a subset of murine taste receptor type III cells. PKD2L1 and PKD1L3 were co-expressed around the pore region of taste buds in mouse circumvallate and foliate papillae *(19)*, but only PKD2L1 was found in other areas, including the fungiform and palate taste buds *(15;18)*. The involvement of the PKD2L1/PKD1L3 complex in sour tasting remains controversial as studies using knockout mice showed that PKD2L1, but not PKD1L3, is involved in sour tasting and acid sensing *(17;20;21)*. Further, these taste buds, regardless of whether expressing PKD1L3 or not, still have similar distribution patterns of PKD2L1 with a specific localization to the pore region *(18;21)*. The PM localization of PKD2L1 alone was reported in both HEK cells and *Xenopus* oocytes by immunofluorescence, surface biotinylation and/or electrophysiology *(5;12;13;16;22)* . Co-expression of PKD1L3 substantially increased PKD2L1 PM targeting, which presumably allowed the channel function to be observed more easily *(15;16;23;24)*.

PKD2L1/PKD1L3 channel complex responded to both weak and strong acids. It was reported that weak acids, such as citric acid, induce larger off-response currents in HEK cells expressing the PKD2L1/PKD1L3 complex than strong acids, such as HCl, at the same pH. All these acids possessed similar activation threshold values of around pH 3.0 *(18)*. Controversially, it was reported later that the induced off-response for PKD2L1/PKD1L3 by strong (HCl and sulphuric) and weak (citric, malic, phosphoric, succinic and tartaric) acids are not significantly different in HEK cells *(15)*. In intact biological systems, PKD2L1-expressing cells were associated with activation

thresholds of higher pH values. For example, the threshold value for taste receptor cells (TRCs) was found to be around pH 5.0 *(20;25)*. Murine cerebrospinal fluid contacting neurons (CSFcN), expressing endogenous PKD2L1, were very sensitive to changes in extracellular pH, in the pH range of 6.5-7.4 *(20)*. Moreover, two negatively charged residues in the PKD2L1 pore loop, D523 *(26)* and D525 *(16)*, have been identified to affect Ca^{2+} permeation and cation selectivity of the PKD2L1/PKD1L3 channel complex. Such studies are important to determine the mechanism of channel gating and selectivity.

Despite recent significant progresses towards understanding the biological and physiological roles of PKD2L1 and PKD1L3, how PKD2L1 and/or PKD1L3 sense acid is not fully understood. In the current study, we employed *Xenopus* oocyte expression model to examine how acids and PKD1L3 modulate PKD2L1 channel activity. In addition, we tried to understand the roles of Ca^{2+} and intra-membrane acidic residues in this modulation. For this we utilized two-microelectrode voltage clamp in combination with mutagenesis, Western blotting, RT-PCR and immunofluorescence.

2.2 MATERIALS AND METHODS

2.2.1 Preparation of *PKD2L1* plasmid constructs

Human PKD2L1 gene was cloned as previously described *(6)*. Mutations of aspartic and glutamic acid residues to the neutral residues asparagine or glutamine were performed using QuikChange Lightning site-directed mutagenesis kit (Agilent Technologies, La Jolla, CA, USA). Primer design and procedure was performed following the manufacturer's protocol.

2.2.2 mRNA preparation and micro-injection into *Xenopus laevis* oocytes

Plasmids pCHGF harbouring wild type (WT) or a mutant *PKD2L1* cDNA were linearized with Mlu I, followed by phenol/chloroform purification and ethanol precipitation. Linearized plasmids were used to *in vitro* synthesize capped mRNAs using the T7 mMessage mMachine™ kit (Ambion, Austin, TX, USA). Stage V-VI oocytes were isolated from *Xenopus laevis* under an approved institutional protocol. Defolliculation of oocytes was performed through incubation in Barth's solution *(6)* containing Type 2 collagenase (2 mg/mL) (Worthington, Lakewood, NJ, USA) at room temperature (RT) for 1.5 hours (hr). Oocytes were then incubated at 16-18 ºC in Barth's solution supplemented with 1% antibiotics (penicillin/streptomycin) (GIBCO™, Life Technologies, Burlington, ON, Canada) for at least 3 hr before injection of 50 nL H_2O containing 25-50 ng mRNAs or as stated in the experiment. An equal volume of H_2O was injected into control oocytes. Injected oocytes were incubated at 16-18 ºC in Barth's solution, for 2-4 days prior to experiments. For intracellular Ca^{2+} chelation studies, oocytes were injected with 50 nL of 50 mM ethylene glycol tetra-acetic acid (EGTA) tetra-sodium salt (Sigma-Aldrich, Oakville,

ON, Canada) to allow a final intracellular concentration of ~5 mM 1 hr prior to recordings.

2.2.3 Western blotting

Western blotting was performed as previously described *(6)*. Briefly, 10-20 μg of purified oocyte proteins were resolved on SDS PAGE (8%) gel, transferred to nitrocellulose membrane. Membranes were blocked with 3-5% skim milk in Tris Buffered Saline, 1% Tween 20 (TBST) for 1 hr at room temperature. This was followed by a 4 ºC overnight incubation with rabbit anti-PKD2L1 polyclonal antibody (cat# PAB5914, Abnova, Taipei, Taiwan) diluted 1:1000 in the blocking buffer. Loading control β-actin was detected using a mouse monoclonal antibody (cat# sc-47778, Santa Cruz Biotechnology, Dallas, TX, USA). Secondary horseradish peroxidase (HRP) - coupled anti-mouse and anti-rabbit were purchased from GE Healthcare (Baie d'Urfe, QC, Canada).

2.2.4 Immunofluorescence

Xenopus oocytes were washed in PBS, fixed in 3% paraformaldehyde (PFA) for 15 min, and washed 3 times in PBS plus 50 mM NH_4Cl, and then permeabilized with 0.1% Triton X-100 for 4 min. Oocytes were then washed 3 times in PBS for 5 min each time, blocked in 3% skim milk in PBS for 30 min, and then incubated overnight with the PKD2L1 polyclonal antibody. This was followed by 3 times 10 min washes in PBS. The oocytes were then incubated with a secondary AlexaFluor 488-conjugated donkey anti-rabbit antibody (Jackson ImmunoResearch Laboratories, West Grove, PA, USA) for 30 min, followed by 3 times washes in PBS and mounting in Vectashield (Vector labs, Burlington, ON, Canada). The slides were examined on an AIVI spinning disc

confocal microscopy (Cell Imaging Facility, Faculty of Medicine and Dentistry, University of Alberta).

2.2.5 Solution preparation

The standard extracellular solution contained (in mM): 100 NaCl, 2 KCl, 1 $MgCl_2$, 10 HEPES adjusted to pH 7.5 by TRIS base. Low pH (2.5-4.5) standard solutions were prepared from the standard solution adjusted by HCl. Solutions containing extracellular Ca^{2+} were prepared from the standard solution with the addition of $CaCl_2$.

2.2.6 Electrophysiology

Current and voltage signals were measured with the conventional two-microelectrode voltage clamp technique with a commercial amplifier (TEV-200A, Dagan, Minneapolis, MN, USA). Electrodes were fabricated from borosilicate glass (Warner Instruments, Hamden, CT, USA) by a micropipette puller (P-87, Sutter Instruments, Novato, CA, USA) and filled with 3 M KCl with typical tip resistance of 0.5-3 MΩ. Digidata 1320A converter and pClamp 9.2 (Axon Instruments, Union City, CA, USA) were used for data acquisition and analysis, respectively. In experiments using a ramp or gapfree protocol *(5)*, current/voltage signals were digitized at 200 ms/sample. Recorded tracings were then analyzed using pClamp 9.2 and plotted using SigmaPlot 12 (Systat Software, San Jose, CA, USA). Absolute amplitudes of channel activity were collected and normalized to the average activity of PKD2L1 wild-type obtained under the same day, condition and group. Normalized values were then expressed as a percentage value and plotted using SigmaPlot 12.

2.2.7 Reverse Transcriptase –Polymerase Chain Reaction (RT-PCR)

Total RNAs were prepared from female *Xenopus laevis* oocytes, tongue, kidney, and brain tissues. Oocytes were collected as described above. Tissues were washed in PBS and kept on ice. RNAs were then extracted at room temperature with TRIzol reagent (Invitrogen, Life Technologies, Burlington, ON, Canada). According to the manufacturer's manual, 1 mL TRIzol was used to homegenize 50-100 mg of tissue. Chloroform was used to isolate the RNA followed by precipitation, wash and resuspension steps. One-step RT-PCR was carried out using SuperScript®III One-step RT-PCR kit (Invitrogen Life Technologies, Burlington, ON, Canada) by following the instruction manual. The oligonucleotide primers for *Xenopus laevis β-actin* and *PKD1L3* for the first PCR were as follows: *β-actin*, sense GAGATGAAGCTCAAAGCAAAAG and antisense CAGGATTCCATACCAAGGAAAG; *PKD1L3* sense GCAGATTGTGAGGAAGAAAGG and antisense TGCTGAGAGCTGGTAGGGTAGT. 10X diluted first *PKD1L3* PCR products were used as templates to run second (nested) PCR using inner primers to increase PCR specificity and efficiency. Sequences of the *PKD1L3* inner primers were: sense AGATTGTGAGGAAGAAAGGGGG and antisense TTTGCTAAAGTCTGGTGGGTTG.

2.2.8 Statistical analysis

Data were presented as mean ± standard error of the mean (SEM). All data were collected from at least three different experiments. Student's t-test was used to compare

two groups of data for statistical significance indicated by a p value. P values of less than 0.05 and 0.01 were considered significant and very significant, respectively.

2.3 RESULTS

2.3.1 Acid-induced off-response currents in oocytes expressing PKD2L1 with or without PKD1L3

Although reported acid-dependent off-response properties have so far all been associated with the co-expression of PKD2L1 and PKD1L3 *(15;18;23-28)*, it has remained unclear as to the role of PKD2L1 in acid sensing and induction of the off-response. We employed the two-microelectrode voltage clamp (TVMC) electrophysiology to determine how PKD2L1 expressed alone in *Xenopus* oocytes responds to acidic stimuli. In the absence of extracellular Ca^{2+} (to avoid the on-response effect of Ca^{2+} on PKD2L1), we found that increasing extracellular acidity (from pH 7.5 to pH 2.5-4.5) to PKD2L1-expressing or control oocytes does not induce appreciable currents. However, in PKD2L1-expressing, but not water-injected control, oocytes voltage clamped at -50 mV a large inward current was elicited following substitution of an acidic extracellular solution with a control solution at pH 7.5 (Figure 2-1 A). This large current induced in an off-response manner resembles those associated with PKD2L1/PKD1L3 co-expressed in HEK cells, oocytes and TRCs *(15;16;18;25)*. This indicates that PKD2L1 alone is able to exhibit off-response activation. We also voltage clamped oocytes at other membrane potentials using a voltage ramp protocol, which produced the acid-elicited off-response currents as function of the membrane potential (I-V curves) (Figure 2-1 B).

To examine whether any oocyte endogenous PKD1L3 contributed to our observed off-response currents we performed RT-PCR assays using total RNAs isolated from oocytes and various *Xenopus* tissues including tongue, kidney and brain.

No PKD1L3 or PKD2L1 signal was detected in oocytes in the first round of the RT-PCR (Figure 2-1 C). We followed up with nested PCR assays which revealed a weak PKD2L1 signal in oocytes and brain, but still no detectable PKD1L3 signal in oocytes (Figure 2-1 C and D). Thus, the off-response observed in PKD2L1-expressing oocytes is independent of *Xenopus* PKD1L3.

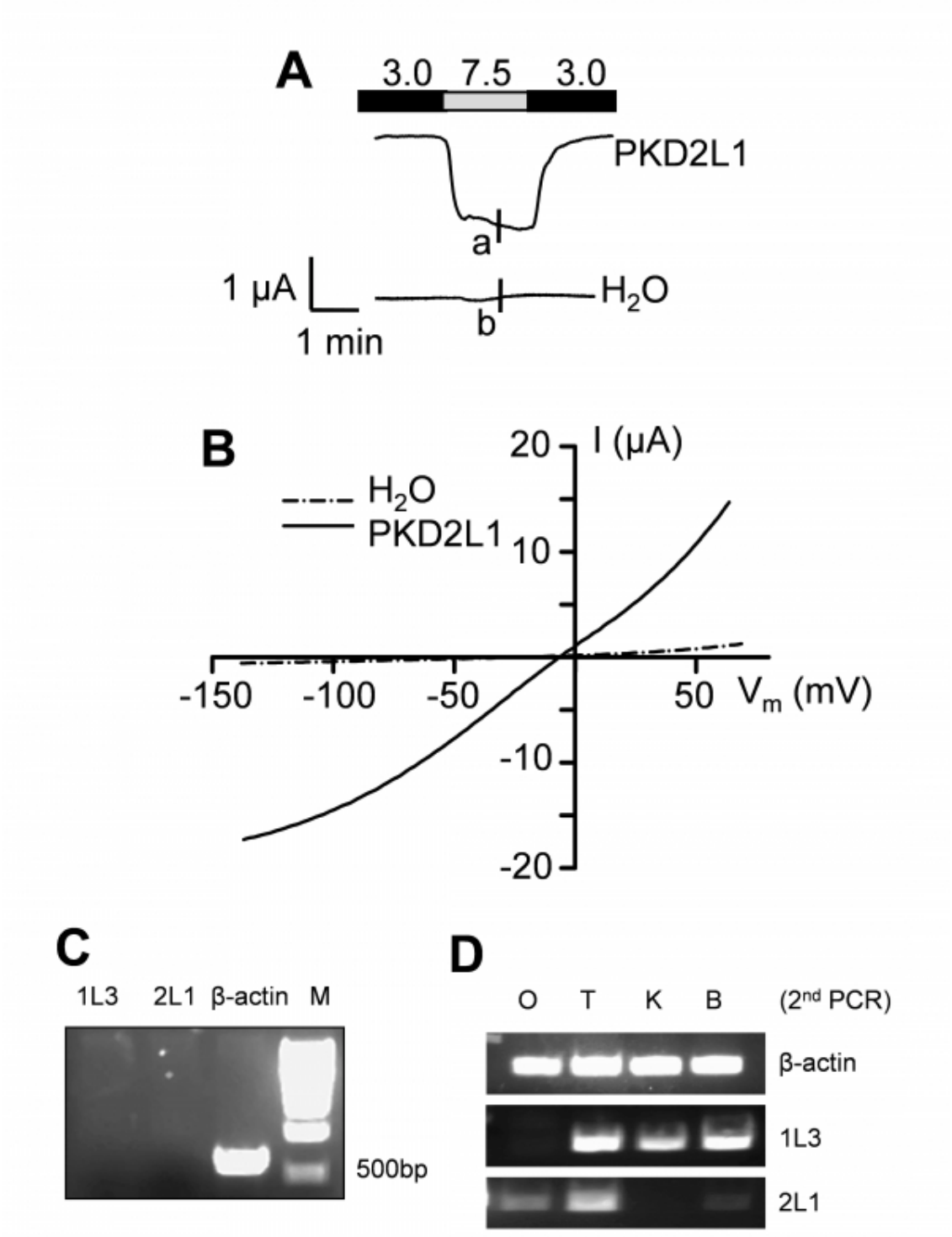

Figure 2-1 Acid-induced off-response currents in *Xenopus laevis* oocytes over-expressing human PKD2L1. (**A**), Representative currents recorded by the two-microelectrode voltage clamp at -50 mV from an oocyte expressing human PKD2L1 or a water-injected oocyte (as a control). An off-response current is defined as the difference between the current amplitudes at

pH 7.5 and the acidic pH 3.0. The pH values of the standard extracellular solutions are indicated. (**B**), Representative current–voltage relationship curves obtained using a voltage ramp protocol at the time points indicated by 'a' and 'b' in the panel **A** tracings. (**C**) RT-PCR using *Xenopus* oocytes detecting the RNA signals of PKD2L1 (2L1), PKD1L3 (1L3) and β-actin. The predicted sizes are 658 bp, 706 bp and 718 bp for β-actin, PKD1L3 and PKD2L1, respectively. (**D**) Second (nested) PCR detecting PKD1L3 signals using *Xenopus* oocytes (O), tongue (T), kidney (K) and brain (B). β-actin signals served as positive controls.

We next examined the effect of PKD1L3 co-expression on PKD2L1-induced off-responses. In oocytes injected with a small amount (4 ng) of PKD2L1 mRNA the off-response was observed only in the presence of PKD1L3 co-expression (at 25 ng mRNA per oocyte) (Figure 2-2 A and B). Our immunofluorescence experiments showed that PKD1L3 co-expression increases the PM localization of PKD2L1 (Figure 2-2 C). These data are in agreement with a previous report in which similar amounts of mRNAs were injected *(16)*. In oocytes injected with a larger amount (25 ng) of PKD2L1 mRNA, co-expression of PKD1L3 still increased off-response currents and PKD2L1 PM localization (Figure 2-2). Thus, taken together, our data indicated that PKD2L1 exhibits the off-response when its PM localization exceeds a certain threshold level and that PKD1L3 enhances the off-response amplitude likely through increasing the PM population of PKD2L1.

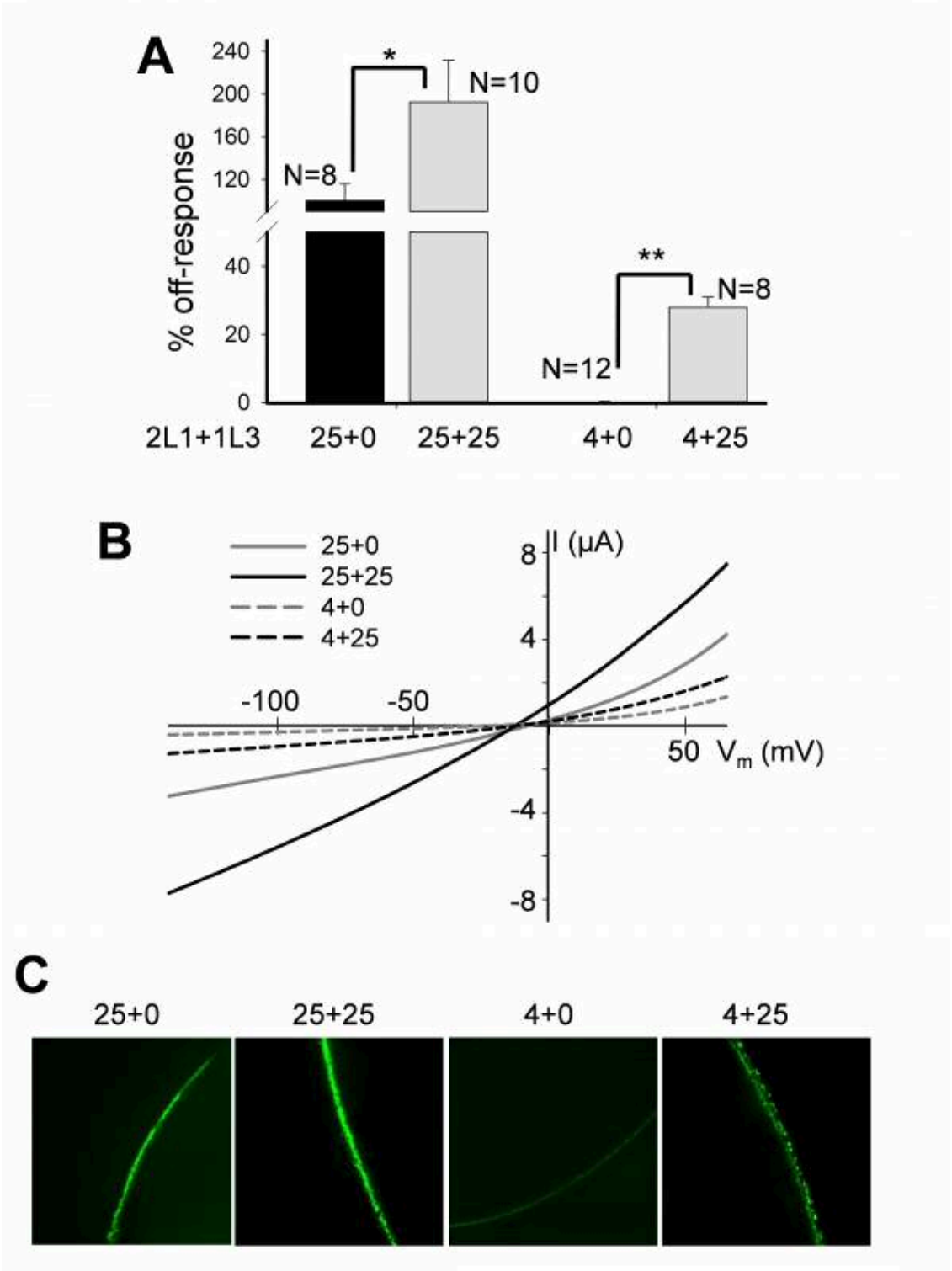

Figure 2-2 Off-response currents in oocytes expressing PKD2L1 with or without PKD1L3. (**A**) Averaged and normalized off-response currents elicited by extracellular pH3.0 from oocytes injected with 4 or 25 ng of PKD2L1 (2L1) mRNA alone or co-injected with 25 ng

of PKD1L3 (1L3) mRNA, and voltage clamped at -50 mV. Shown are off-response currents averaged from different numbers of oocyte, as indicated. *$p \leq 0.05$ and **$p \leq 0.01$. (**B**) Representative off-response I-V curves obtained using a ramp protocol under the same conditions as in panel A. (**C**) Representative immunofluorescence data showing the PM intensity of PKD2L1 protein in oocytes injected with different amounts of mRNAs, as indicated.

2.3.2 Effects of acid dose, application time, and type on the PKD2L1 off-response

Our voltage clamp data showed that the PKD2L1-associated off-response is dose-dependent with half maximal activation value of pH 3.5 ± 0.5 (N = 5-9) in PKD2L1- expressing oocytes voltage clamped at -50 mV (Figure 2-3 A and B). Previous studies also found dose-dependent off-responses, with cell-type dependent half maximal activation pH values. PKD2L1/PKD1L3 expressed in HEK cells responded to pH 3.0 or less *(15;18;24)*, taste cells responded to solutions of pH 5.0 or less *(19;20)*, while mouse CSF-cN neurons responded to changes in extracellular pH in the 6.5 to 7.4 range *(20)*.

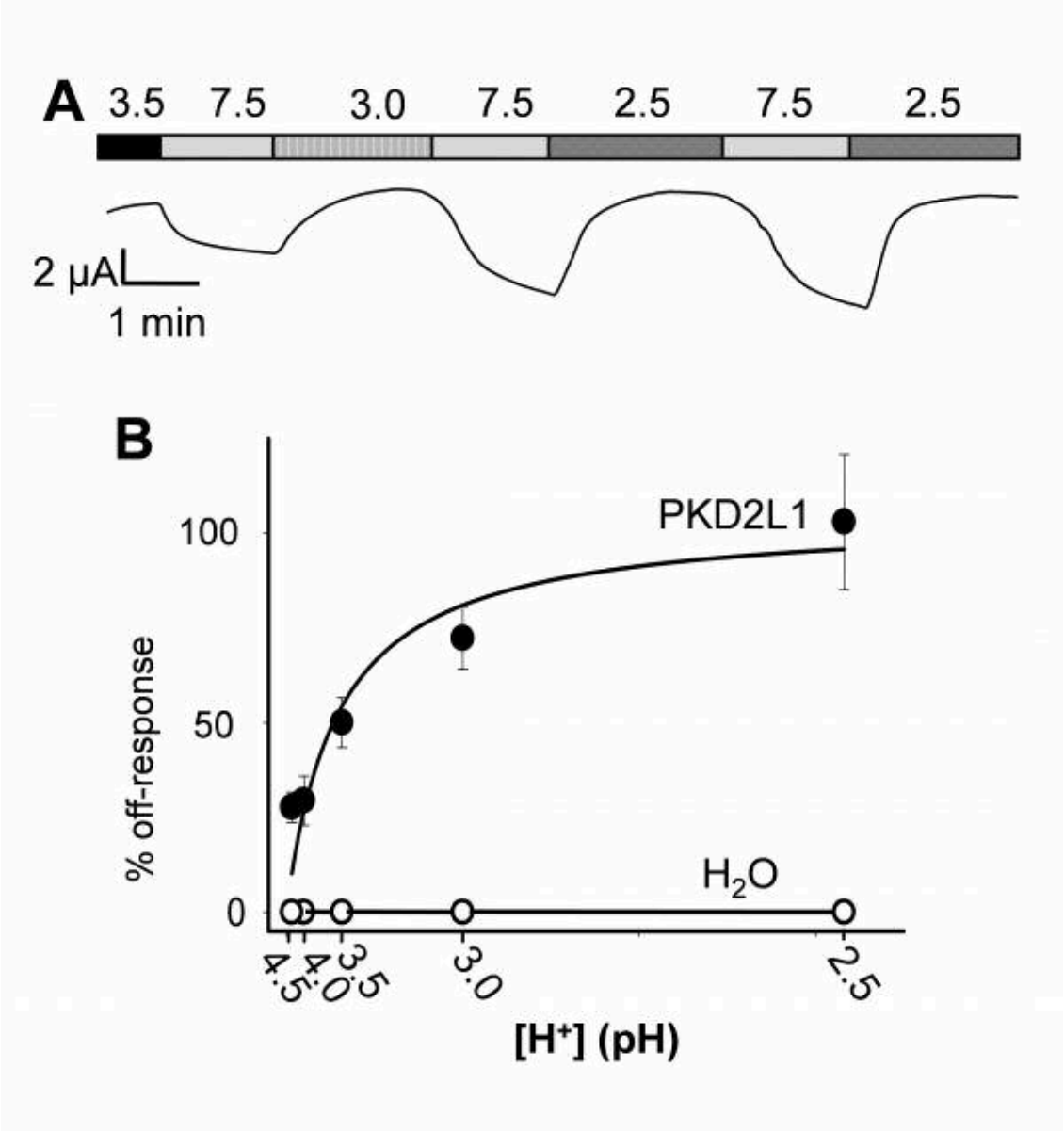

Figure 2-3 Dose dependence of the acid-induced off-response. (**A**) Representative current recorded at -50 mV and different extracellular pH, as indicated, from a PKD2L1-expressing oocyte. (**B**), pH dose dependence of the off-response currents for oocytes injected with PKD2L1 mRNA or water. [H+] indicates protons concentration. Data points represents average values from N= 5-9 with SEM and were fitted to the Michaelis Menton Equation, which produced a K_m value of pH 3.5 ± 0.5.

In order to determine whether the off-response is sensitive to the duration of acid application, we applied a solution of pH 3.0 for different periods of time. We found that oocytes over-expressing PKD2L1 exhibit similar off-response amplitudes for different application durations, ranging from 10 sec to 1 min (Figure 2-4 A). Our data indicated that acid application time is rather not a determinant of the off-response amplitude, resembling the previously reported duration-independent characteristic of the PKD2L1/PKD1L3 channel complex *(15)*.

Further, we investigated whether there is any difference between weak and strong acids with respect to the amplitude of off-response current. For this we compared the effects of acetic and citric acids with HCl, using 50 mM Na-acetate or Na-citrate to replace 50 mM NaCl in the standard solution. These solutions were adjusted to pH 3.0 by titrating against HCl. Considering the pK_a values of both acids, the resulting solutions contain 49.1 and 12.9 mM of the undissociated membrane-permeable form of acetic and citric acids, respectively. Additionally, we found that the off-response current induced by acetic acid, but not citric acid, is significantly larger than that induced by HCl (60%, $p \leq 0.001$) (Figure 2-4 B and C). This pattern of increase is comparable to the response in the chorda tympani of rat TRCs by acetate, citric and hydrochloric acids at the same pH *(29)*.

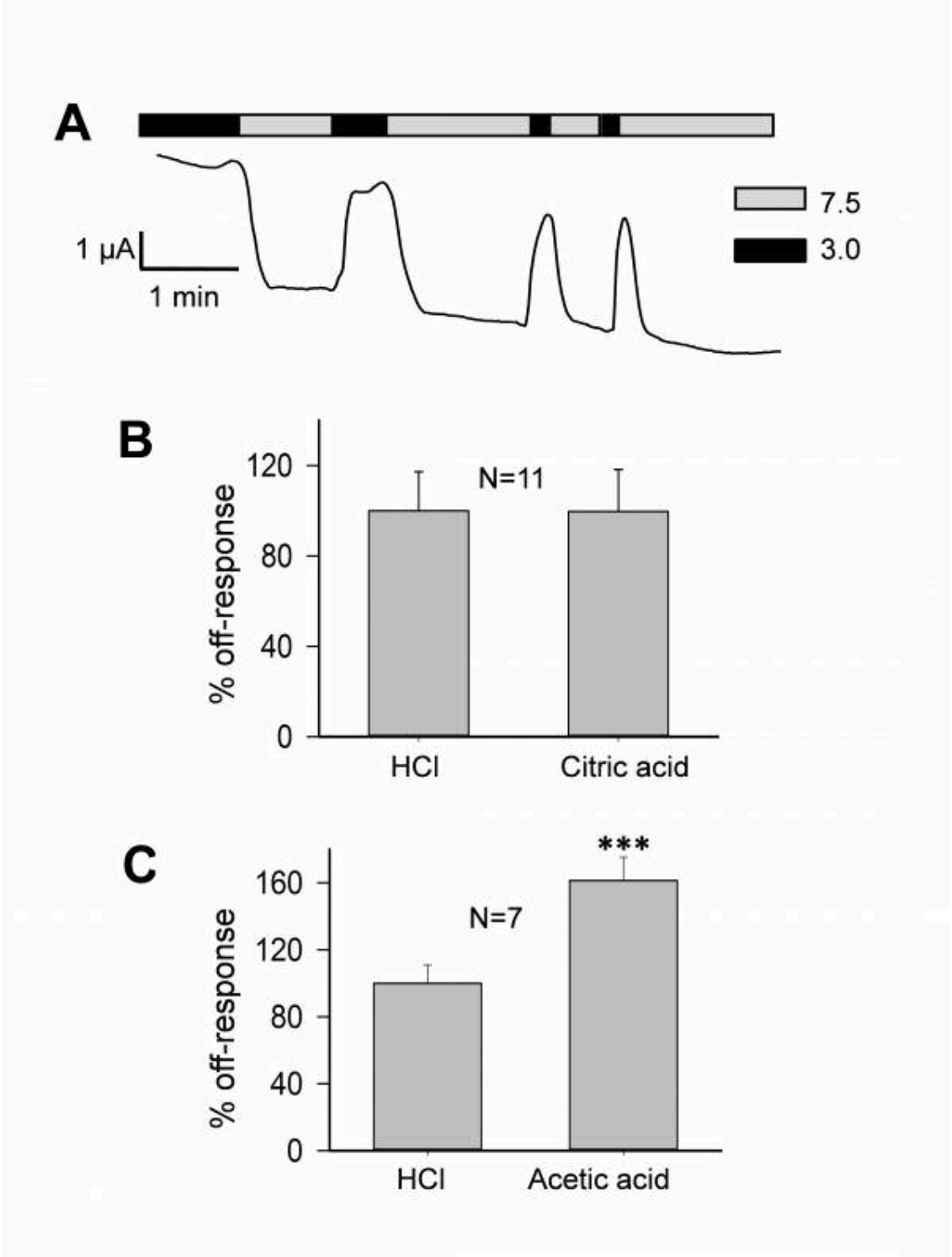

Figure 2-4 Effects of acid application time and type on the off-response. (**A**) Representative current recorded at -50 mV and with the application of the standard solution with pH 3.0 for different time intervals in an oocyte expressing PKD2L1. (**B**) Averaged and normalized off-response currents elicited by HCl or citric acid at pH 3.0 were compared from the same

oocytes. (**C**) Averaged and normalized off-response currents elicited by HCl or acetic acid at pH 3.0 were compared from the same oocytes (***$p \leq 0.001$, by paired t-test).

2.3.3 Roles of extracellular protons in modulating PKD2L1 on-response

Application of extracellular Ca^{2+} induces PKD2L1 channel activation followed by an ensuing channel inactivation *(5)*. In contrast, an acid-induced off-response did not display an ensuing inactivation under Ca^{2+}-free conditions (Figure 2-5 A). Thus, the same channel expressed in oocytes exhibits two apparently distinct properties: Ca^{2+}-induced on-response with inactivation and acid-induced off-response (in the absence of Ca^{2+}) without inactivation.

We previously showed that extracellular low pH significantly reduces Ca^{2+}-induced PKD2L1 activation *(5)*. Consistently, here we found that the Ca^{2+}-induced activation is completely abolished when extracellular pH drops to pH 3.0 (Figure 2-5 B). Similar conclusion can be made by comparing between the on-response current-voltage relationships obtained at pH 7.5 and 3.0 (Figure 2-5 C). Thus, the off-response activator, acid, played an inhibitory role in the on-response.

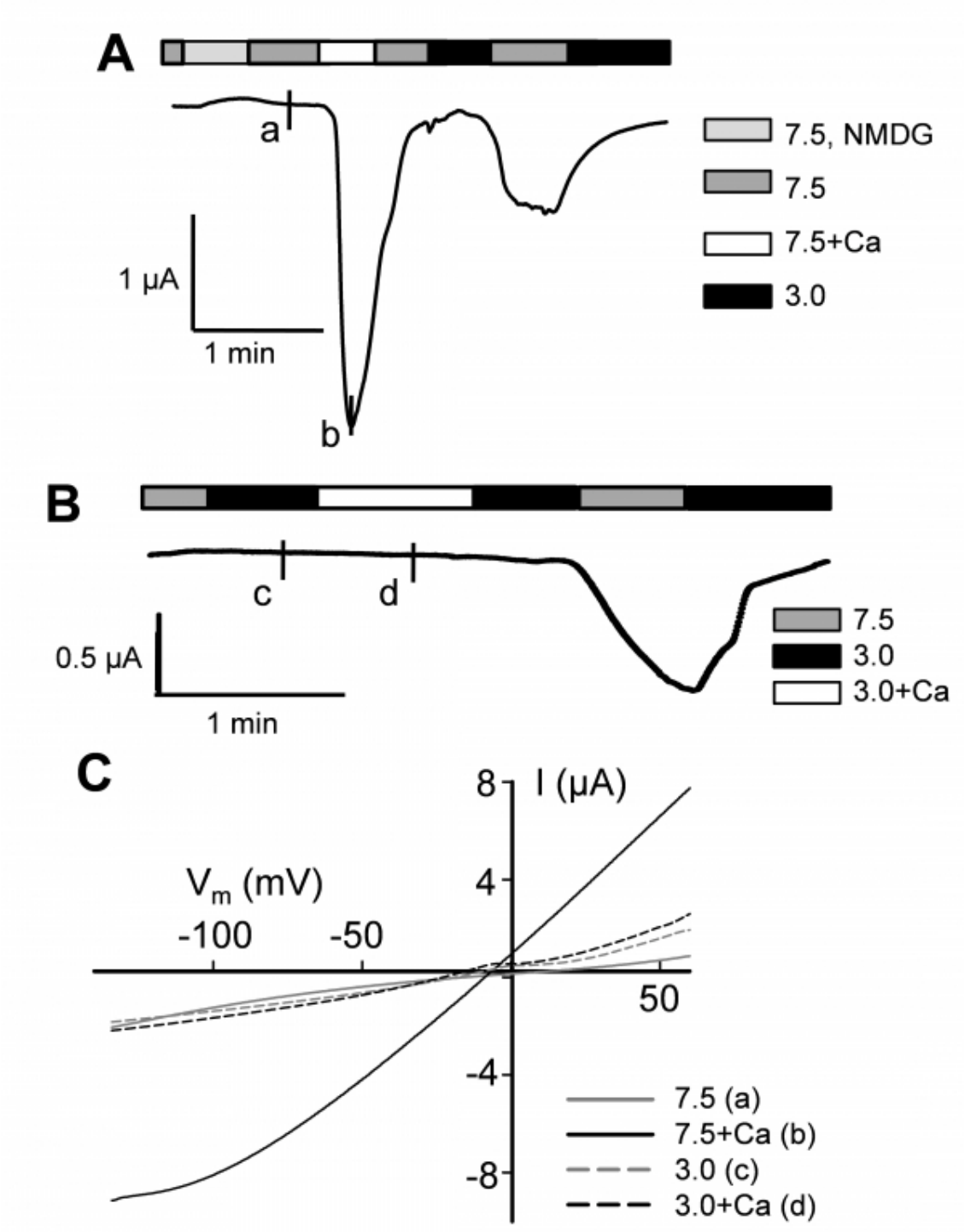

Figure 2-5 Acid-induced vs Ca^{2+}-induced channel activation of PKD2L1. (**A**) Representative current recorded at -50 mV in a PKD2L1-expressing oocyte to show the on-response induced by 5 mM extracellular Ca^{2+} (and pH 7.5) and the subsequent off-response induced by extracellular pH 3.0 (no extracellular Ca^{2+}). (**B**) Representative current recorded at -50 mV in a PKD2L1-expressing oocyte to show the on-response induced by 5 mM

extracellular Ca^{2+} (and pH 3.0) and the subsequent off-response induced by extracellular pH 3.0 (no extracellular Ca^{2+}). (**C**) I-V curves generated at the time points ('a' - 'd') indicated in panels **A** and **B**.

2.3.4 Roles of Ca^{2+} ion in modulating PKD2L1 off-response

Conversely, we wondered whether and how the on-response activator Ca^{2+} plays a role in the off-response. So far, we have performed all the off-response experiments in Ca^{2+}-free extracellular environments, in part to avoid the Ca^{2+}-induced on-response. Interestingly, in the presence of extracellular Ca^{2+} (5 mM), PKD2L1-expressing oocytes responded with a robust off-response current followed by channel inactivation, forming a spike of current (Figure 2-6 A) that has a similar shape as those previously published using HEK cells expressing PKD2L1/PKD1L3, also in the presence of Ca^{2+} *(15)*. Thus, compared with the presence of a sustained off-response current plateau in the absence of Ca^{2+} (see Figure 2-1 A and 2-4 A), our data together suggest that the off-response inactivation is attributed to Ca^{2+}. Indeed, consistently, we found that sustained off-response currents were abolished by the addition of Ca^{2+} (Figure 2-6 B). Thus, the on-response activator Ca^{2+} played an inhibitory role in the off-response.

Because of the permeability of PKD2L1 to Ca^{2+} we wondered whether the Ca^{2+}- induced inhibition/inactivation is due to an increase in the intracellular Ca^{2+} concentration ($[Ca^{2+}]_i$). For this, we pre-injected *Xenopus* oocytes over-expressing PKD2L1 with 50 nL of 50 mM ethylene glycol tetra-acetic acid (EGTA) tetra –sodium salt solution 1 hr before the same electrophysiological measurements as those for Figure 2-6 B, to chelate the intracellular Ca^{2+}. We found that while EGTA pre-injection does not prevent PKD2L1 from exhibiting the off-response, it substantially reduces the ability of extracellular Ca^{2+} to inhibit the off-response (Figure 2-6 C to E). On average, EGTA pre-injection resulted in similar off-response currents compared with the control

condition (115.8 ± 27.1%, N = 8-12, p = 0.6) while it reduced the Ca^{2+} inhibition ability to 23.1 ± 12.0% (N = 8-12, p = 0.0007, unpaired t-test) (Figure 2-6 D and E). These results suggest that the increase in $[Ca^{2+}]_i$ is critical for the extracellular Ca^{2+}-induced inhibition, but not for the activation of the off-response.

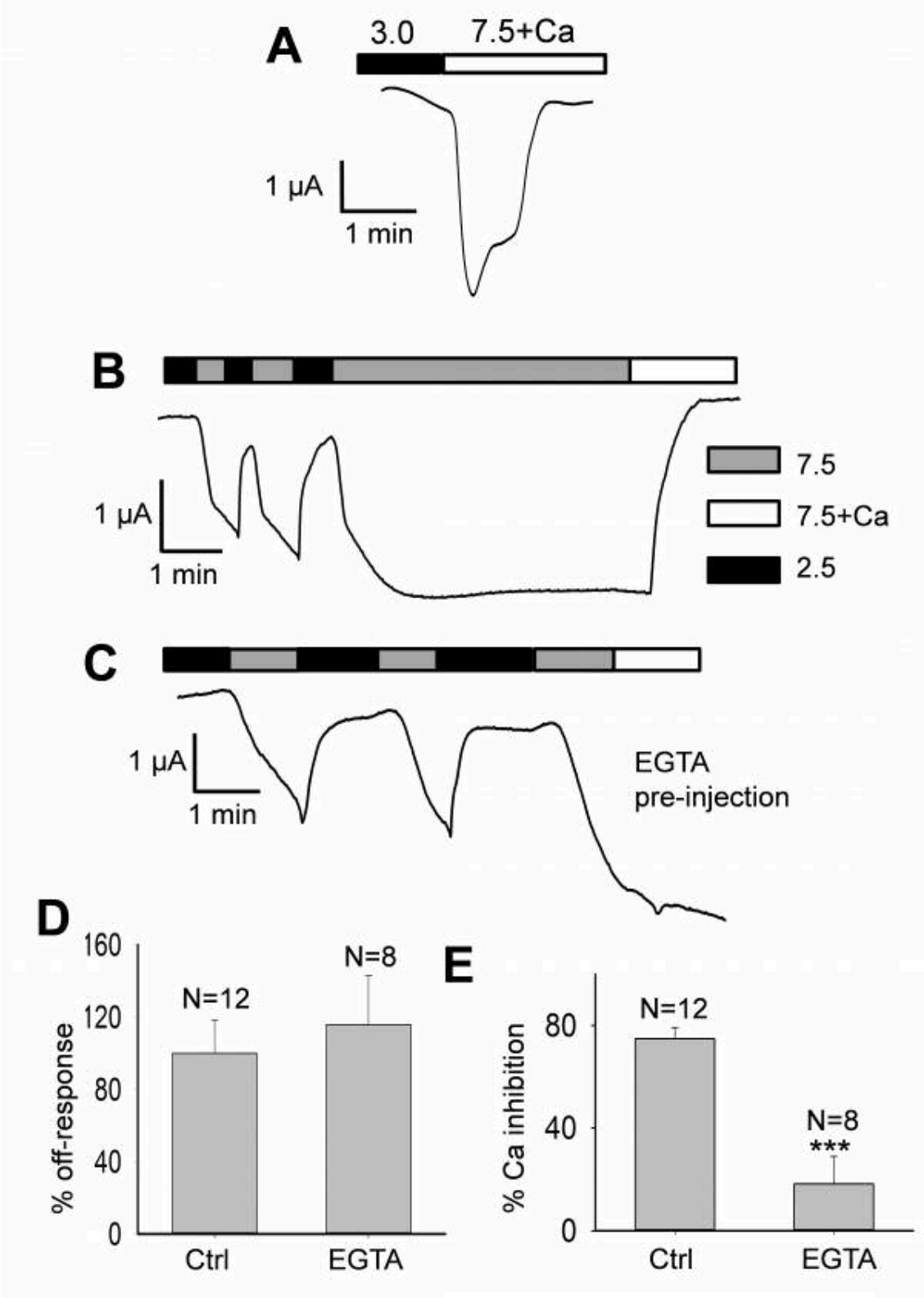

Figure 2-6 Roles of Ca^{2+} ions in the PKD2L1 off-response. (**A**) Representative tracing recorded at -50 mV, showing the off-response activation and ensuing inactivation in the

presence of extracellular Ca^{2+} (5 mM). (**B**) Representative current recorded at -50 mV in aPKD2L1-expressing oocyte, showing the inhibition of the off-response current by extracellular Ca^{2+} (5 mM). (**C**) Representative current recorded at -50 mV in a PKD2L1-expressing oocyte 1 hr after injection of 50 nL of 50 mM EGTA, showing the effect of extracellular Ca^{2+} (5 mM). (**D**) Averaged and normalized off-response currents with EGTA or water (control) pre-injection. (**E**) Averaged percentage of the off-response current inhibition by extracellular Ca^{2+} with EGTA or water pre-injection. ***p = 0.0007, unpaired t-test.

We also used EGTA to chelate extracellular Ca^{2+}. We added 1 mM EGTA to our extracellular solutions to chelate any trace amounts of Ca^{2+} ion and consistently this resulted in 36.7 ± 3.8% (N = 11, p = 0.04, unpaired t-test) increase in the off-response current (Figure 2-7 A and B).We then further wanted to determine the K_i value of the extracellular Ca^{2+}concentration ($[Ca^{2+}]_o$) for the Ca^{2+} inhibition by applying different $[Ca^{2+}]_o$ values, as shown in Figure 2-7 A. We found that 1 mM $CaCl_2$ is sufficient to completely inhibit the off-response current and that K_i for $[Ca^{2+}]_o$ is equal to 167 ± 33 μM (N = 11) for the off-response current generated from pH 3.0 to 7.5 (Figure 2-7 C). This K_i value was obtained by fitting experimental data to the equation

$$I = I_{off} \times [Ca]_o \div (K_i + [Ca]_o) \qquad 1$$

where I_{off} represents the off-response current and I is the inhibited fraction of I_{off} . Of note, we think that the presence of trace amounts of 'contaminating' Ca^{2+} in extracellular solutions (~5 μM, based on data sheets of MgCl, NaCl and KCl) may account, at least in part, for the difference in the off-response currents with and without extracellular EGTA (Figure 2-7 A).

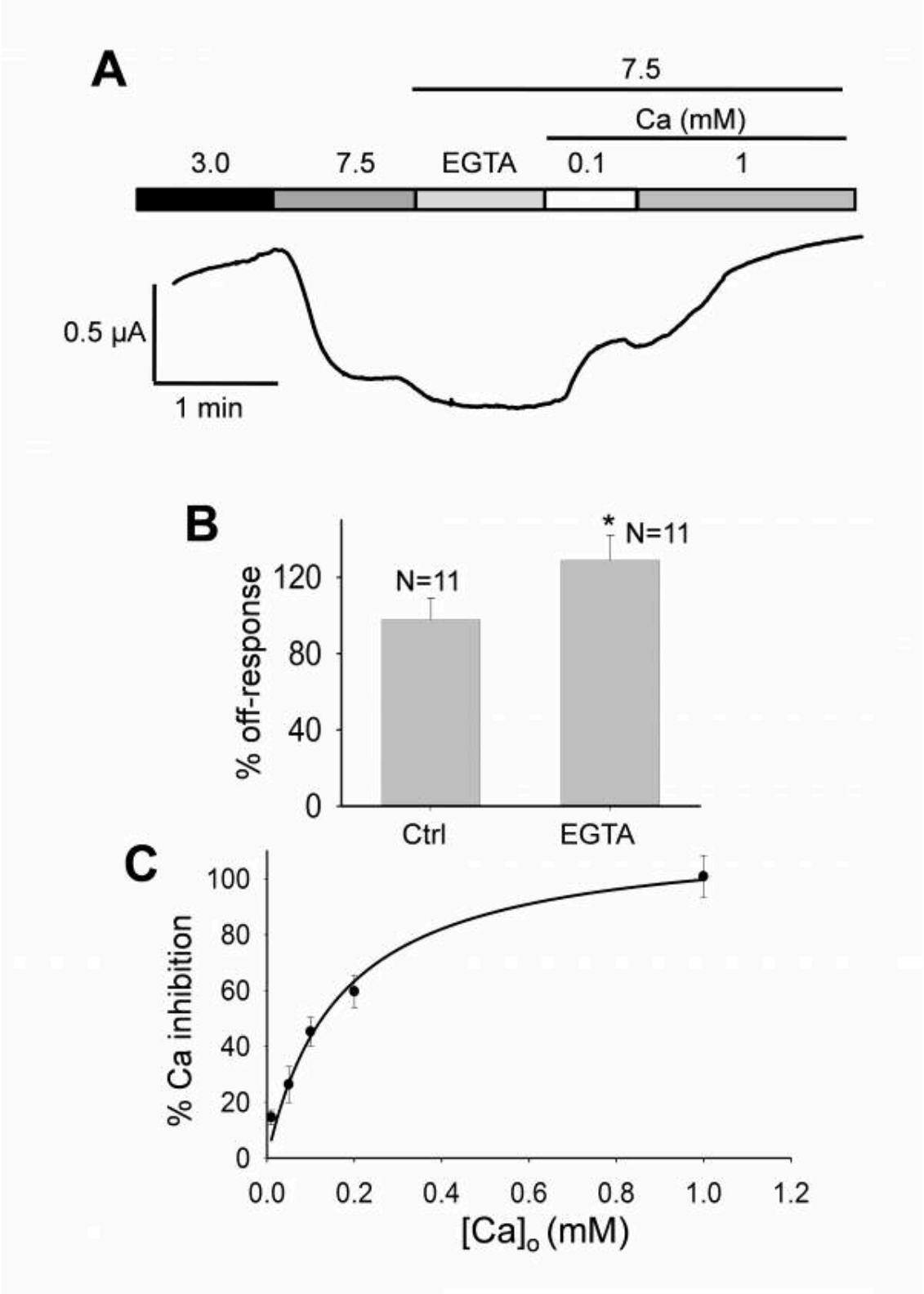

Figure 2-7 Role of extracellular Ca^{2+} ions in the PKD2L1 off-response. (**A**) Representative current recorded at -50 mV in a PKD2L1-expressing oocyte under various extracellular

conditions, as indicated. (**B**) Based on experiments described in panel **A**, averaged data to show the effect of extracellular EGTA (1 mM). *p = 0.04. (**C**) Dose-dependence of the relative Ca^{2+} inhibition of the off-response current. Data were averaged from 11 oocytes and the curve is the fit of the data to Equation 1, with K_i value of 167 ± 33 μM.

2.3.5 Roles of acidic residues in PKD2L1 on- and off-responses

Previous reports found the importance of the aspartic acid residue D523 in human PKD2L1 for the Ca^{2+} permeability *(13)* as well as for the off-response of the PKD2L1/PKD1L3 complex *(16;26)*. We wanted to explore whether this mutation affects the Ca^{2+}-induced on-response as well. We found that the D-to-N mutation inhibits the on- and off-response currents by 104.0 ± 1.6 % (N = 20, p = 3.0e-6, unpaired t-test) and 77.2 ± 2.8 % (N = 8, p = 0.002, unpaired t-test), respectively (Figure 2-8 A and B). We verified by Western blotting and immunofluorescence that the mutant is expressed on the PM to a similar extent as the wild type (WT) PKD2L1 (Figure 2-8 C and D). Thus, our studies found that residue D523 is essential for both on- and off-responses of PKD2L1.

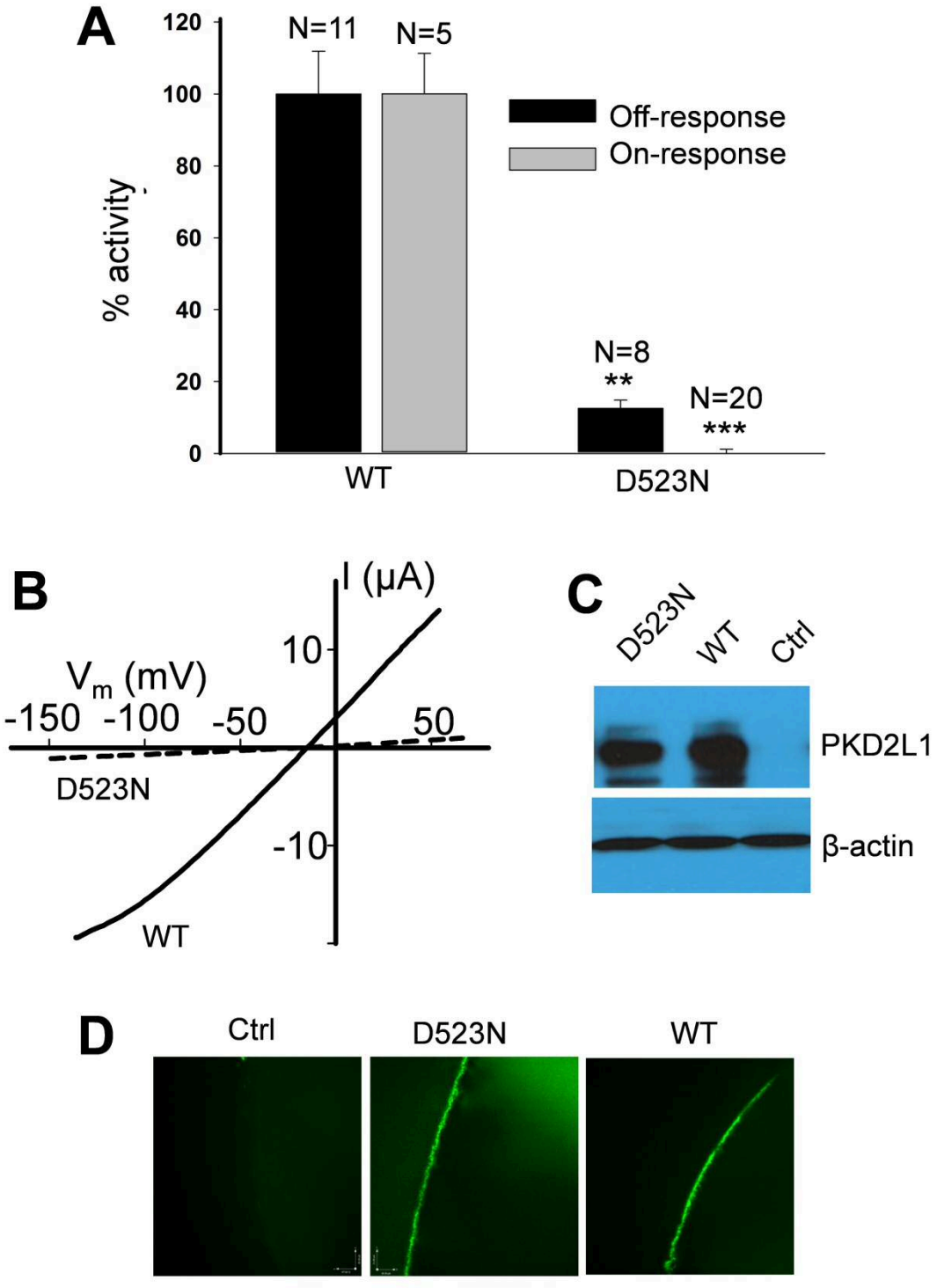

Figure 2-8 Effects of mutation D523N on the PKD2L1 on- and off-responses. (**A**) Averaged and normalized on- and off-response currents elicited by extracellular 5 mM Ca^{2+} and pH 3.0,

respectively, from oocytes expressing WT or mutant PKD2L1 voltage clamped at -50 mV. Shown are on- (***p = 3.0e-6) and off-response currents (**p = 0.002) averaged from different numbers of oocyte, as indicated. (**B**) Representative off-response I-V curves obtained by a ramp protocol under the same condition as in panel **A**. (**C**) Western blotting data showing the protein expression of WT and mutant PKD2L1 in expressing or water-injected (Ctrl) oocytes. (**D**) Representative immunofluorescence data showing the PM localization of WT and mutant PKD2L1 in oocytes.

We next examined the importance of intra-membrane acidic residues for PKD2L1 on- or off-response properties. For this we mutated eight such residues into their corresponding neutral residues: E103Q and D113N in TM1, D349N, E356N, E369Q and E370Q in TM3, D390N in TM4, and D476N in TM5 and then examined their expression and channel function in oocytes. We found that mutants E369Q, D390N and D476N have no detectable protein expression although their mRNA is normal (Figure 2-9 A), possibly rapidly degraded due to mis-folding. While the function of mutants E103Q, D113N and E370Q were similar to that of the WT channel, we found that the function of mutants D349N and E356N is significantly reduced (Figure 2-9 B). As our immunofluorescence data indicated that their PM levels are not affected (Figure 2-9 C), our electrophysiology data indicated that residues D349 and E356 in TM3 are critical for both the Ca^{2+}-induced on-response and H^{+}-induced off-response, possibly through interaction with Ca^{2+} or protons. Of note, the loss of function by point mutations D523N, D349N and E356N further supports the specificity of the off-response currents observed for the WT PKD2L1 in oocytes.

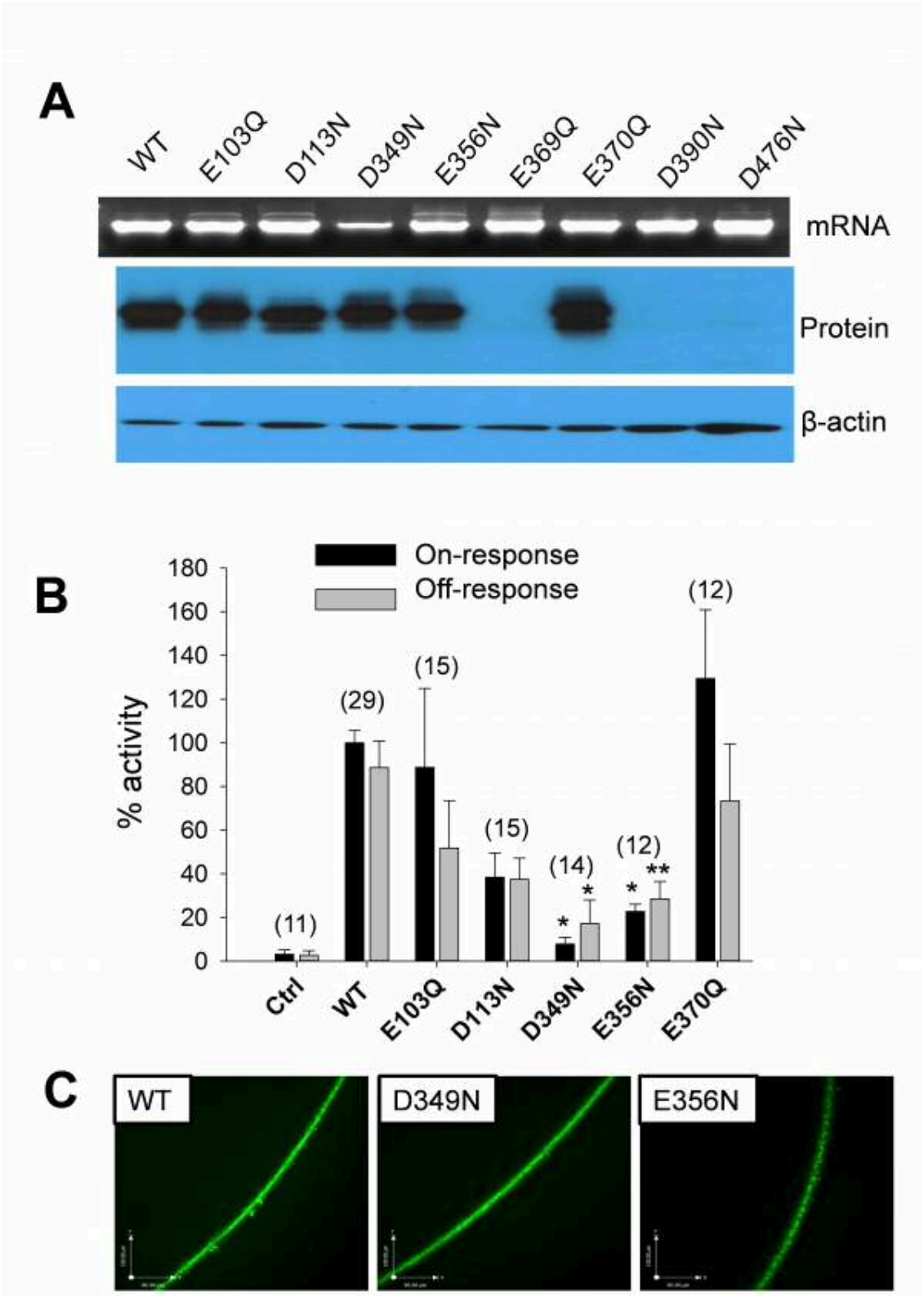

Figure 2-9 Effects of the negatively charged intramembrane residues on the PKD2L1 on- and off-responses. (**A**) Representative data showing mRNA and protein bands that were

revealed in 1% agarose gel and 8% SDS-PAGE, respectively. (**B**) Averaged and normalized on- and off-response currents elicited by extracellular 5 mM Ca^{2+} and pH 3.0, respectively. Oocytes expressing WT, mutants or in water-injected oocytes (Ctrl) were voltage clamped at -50 mV. The number of each group is indicated in a bracket. On-response currents were significantly reduced with *p = 0.03 and 0.05 (unpaired t-test) in D349N and E356N, respectively. Off-response currents were also significantly reduced with *p = 0.05 and **p = 0.01 (unpaired t-test) in D349N and E356N, respectively. (**C**) Representative immunofluorescence data showing the PM localization of PKD2L1 (WT), D349N and E356N expressed in oocytes.

2.4 DISCUSSION

In the present study we have examined acid-dependent properties of human PKD2L1 expressed in *Xenopus* oocytes using the two-microelectrode voltage clamp electrophysiology, together with molecular biology and mutagenesis techniques. We found that PKD2L1 over-expressed alone in oocytes exhibits acid-induced off-response characteristics, such as pH dependence, activation by strong and weak acids, and I-V relationships, that are comparable to those previously reported for the PKD2L1/PKD1L3 complex in HEK cells and oocytes. Given the non-detectable endogenous PKD1L3 in oocytes, this indicates that PKD1L3 is not required for the acid sensation of PKD2L1. PKD2L1 off-response was inhibited and regulated by an increase in intracellular Ca^{2+}. Moreover, the intra-membrane residues D349 and E356 were found to be essential for channel function.

Previous reports showed that PKD1L3 is essential for the off-response through increasing the targeting of PKD2L1 to the PM *(15;16;23;24)*. Nonetheless, the functional roles of PKD1L3 in the channel activity of the PM PKD2L1/PKD1L3 channel complex remain unclear. It was proposed that the PKD1L3 long extracellular N-terminus is involved in sensing extracellular pH *(15)*. While PKD2L1 knockout mice have defective sour tasting, PKD1L3 knockout mice do not exhibit tasting abnormality *(17;21)*. This fact appears to be controversial and argues that PKD1L3 does not play a significant role in the PKD2L1/PKD1L3 complex in terms of sensing acid in the tongue. Studies by Yu and colleagues *(16)* nicely supported our finding that PKD2L1 alone in oocytes is expressed on the PM. However, injection of ~4 ng mRNA of PKD2L1 into each oocyte did not result in measurable PKD2L1-associated currents in

our study as well as in a previous report *(16)*. This is likely due to an insufficient PM population of PKD2L1. Co-expression of PKD1L3 much increased the PM level of PKD2L1, allowing PKD2L1 to exhibit the off-response *(16)*. In fact, this report showed that tetrameric PKD2L1 is present on the PM even with a small mRNA amount injected and in the absence of PKD1L3. In addition, the same report indicated that PKD1L3 alone does not target to the PM or exhibit channel activity *(16)*. Therefore, these data together suggest that PKD2L1, rather than PKD1L3, may possess an acid sensing capability and defines the basic channel properties of PKD2L1/PKD1L3. However, we could not exclude the possibility that an endogenous partner protein participates in the acid sensing in cells expressing PKD2L1 alone or complex PKD2L1/PKD1L3. In addition to the chaperone role, it is nevertheless possible that PKD1L3 modulates PKD2L1 channel properties. It is noted that another PKD1 homologue PKD1L1 indeed modulates the single-channel conductance of PKD2L1 in mammalian cells, though PKD2L1 alone exhibits channel function on the PM *(13)*

PKD2L1 was first reported in 1999 to be a non-selective cation channel activated by and highly permeable to Ca^{2+} in *Xenopus* oocytes *(5)*, a property that we call here a Ca^{2+}-induced on-response. Its Ca^{2+} permeability in mammalian cilium membrane is important for regulating ciliary Ca^{2+} concentration and Ca^{2+}-dependent hedgehog signalling. However, distinct channel properties were observed in the primary cilium, such as outward rectification and absence of Ca^{2+}-induced channel activation *(13;14)*. Whether the Ca^{2+}-induced on-response and acid-induced off-response share part of the molecular mechanisms, this remains unknown. However, some different properties between the on- and off-responses are noted. For example,

after an on-response a waiting/recovery period of 5-8 minute was required for the induction of a new on-response *(5)*. In contrast, as shown here, the off-responses (at least under Ca^{2+}-free conditions) can be repeatedly induced immediately one after another. Further, Ca^{2+}-induced channel activation was followed by channel inactivation while acid-induced channel activation was sustained without inactivation in the absence of Ca^{2+}. These data also suggest that the Ca^{2+}-dependent on-response and acid-dependent off-response are not completely governed by the same mechanism.

In fact, acid-induced off-response activation in PKD2L1-expressing oocytes occurred in the absence of extracellular Ca^{2+} and reached a plateau, similar to reported data using oocytes *(16)*. In fact, in the presence of extracellular Ca^{2+}, the off-response was still present but was followed by an ensuing inactivation, producing a current spike that is similar to the reported observations in HEK cells for PKD2L1/PKD1L3 under a comparable condition *(15)*. Furthermore, if Ca^{2+} was added during an off-response activation, then an immediate inhibition of the off-response current was observed, with a K_i value (50% inhibition) for $[Ca^{2+}]_o$ of only 0.17 mM. These data together indicated that extracellular Ca^{2+} regulates (somehow inhibits) the off-response currents. In contrast, other previous reports using HEK cells expressing PKD2L1 and PKD1L3 stated that the acid-induced off-response requires the presence of extracellular Ca^{2+} and results in an increase in $[Ca^{2+}]_i$ *(25)*. The discrepancy in the role of extracellular Ca^{2+} will have to be clarified in further studies.

Interestingly, while preloading oocytes with Ca^{2+} chelator did not significantly alter the off-response, it abolished the ability of extracellular Ca^{2+} to inhibit the off-response. This suggests that an increase in the intracellular free Ca^{2+} is required to

inhibit the off-response activation. On the other hand, we previously reported that an increase in intracellular Ca^{2+} is required for both the Ca^{2+}-induced on-response activation and the ensuing inactivation *(5)*. In terms of the effect of intracellular protons, our data and previous report *(29)* using weak and strong acids support that acid-induced off-responses positively correlate with increased intracellular H^+ concentrations. Putting all data together, although Ca^{2+} and acid distinctly induce PKD2L1 channel activations they seem to share the same or similar way of inactivation, i.e., by an increase in $[Ca^{2+}]_i$.

It has remained unclear as to how Ca^{2+} and proton ions trigger channel activations although Ca^{2+} plays roles in both phenomena. It is worthy to note that the PKD2L1 C-terminus possesses an EF hand, a coiled-coil domain, a cytoplasmic regulatory domain (CRD, aa 561-805) and phosphorylation sites *(30;31)*. PKD2L1 CRD was shown to be related to channel inactivation *(32)*, maybe through direct binding to Ca^{2+}, or through activating downstream signalling molecules. More recently, CRD binding to Ca^{2+} was reported to change the α-helical property of the C-terminus *(30)*, which may explain the desensitization/inactivation phenomenon that follows the Ca^{2+}-induced activation. However, whether the same domain is involved in the Ca^{2+} inhibition associated with acid-dependent off-response needs further studies. On the other hand, we found two negatively charged residues D349 and E356 to be critical for both on- and off-response functions. Because aspartate and glutamate residues have their pK_a values of pH 3.7 and pH 4.0, respectively, which are well within the pH range in which PKD2L1 exhibits the off-response, our work suggests that protons may interact with these residues as part of the off-response activation process. Further,

because of their importance for the Ca^{2+}-induced on-response activation, these acidic residues may also interact with Ca^{2+} during the on-response process.

In summary, in the present study we discovered that PKD2L1 expressed alone in *Xenopus* oocytes exhibits extracellular acid-induced off-responses with characteristics resembling those associated with PKD2L1/PKD1L3 and that this off-response is inhibited by an increase in the intracellular Ca^{2+}. Further studies will help in better understanding how PKD1L3 and Ca^{2+} modulate the PKD2L1 channel function.

.

2.5 REFERENCES

1. Naziroglu, M., Dikici, D. M., and Dursun, S. (2012) Role of oxidative stress and Ca^{2+}signaling on molecular pathways of neuropathic pain in diabetes: focus on TRP channels, *Neurochem. Res. 37*, 2065-2075.

2. Venkatachalam, K. and Montell, C. (2007) TRP channels, *Annu. Rev. Biochem. 76*, 387-417.

3. Nomura, H., Turco, A. E., Pei, Y., Kalaydjieva, L., Schiavello, T., Weremowicz, S., Ji, W., Morton, C. C., Meisler, M., Reeders, S. T., and Zhou, J. (1998) Identification of PKDL, a novel polycystic kidney disease 2-like gene whose murine homologue is deleted in mice with kidney and retinal defects, *J. Biol. Chem. 273*, 25967-25973.

4. Pei, Y. (2003) Molecular genetics of autosomal dominant polycystic kidney disease, *Clin. Invest Med. 26*, 252-258.

5. Chen, X. Z., Vassilev, P. M., Basora, N., Peng, J. B., Nomura, H., Segal, Y., Brown, E. M., Reeders, S. T., Hediger, M. A., and Zhou, J. (1999) Polycystin-L is a calcium-regulated cation channel permeable to calcium ions, *Nature 401*, 383-386.

6. Yang, J., Wang, Q., Zheng, W., Tuli, J., Li, Q., Wu, Y., Hussein, S., Dai, X. Q., Shafiei, S., Li, X. G., Shen, P. Y., Tu, J. C., and Chen, X. Z. (2012) Receptor for activated C kinase 1 (RACK1) inhibits function of transient receptor potential (TRP)-type channel Pkd2L1 through physical interaction, *J. Biol. Chem. 287*, 6551-6561.

7. Liu, Y., Li, Q., Tan, M., Zhang, Y. Y., Karpinski, E., Zhou, J., and Chen, X. Z. (2002) Modulation of the human polycystin-L channel by voltage and divalent cations, *FEBS Lett.525*, 71-76.

8. Li, Q., Liu, Y., Shen, P. Y., Dai, X. Q., Wang, S., Smillie, L. B., Sandford, R., and Chen, X. Z. (2003) Troponin I binds polycystin-L and inhibits its calcium-induced channel activation, *Biochemistry 42*, 7618-7625.

9. Li, Q., Dai, X. Q., Shen, P. Y., Wu, Y., Long, W., Chen, C. X., Hussain, Z., Wang, S., and Chen, X. Z. (2007) Direct binding of alpha-actinin enhances TRPP3 channel activity, *J. Neurochem. 103*, 2391-2400.

10. Dai, X. Q., Karpinski, E., and Chen, X. Z. (2006) Permeation and inhibition of polycystin-L channel by monovalent organic cations, *Biochim. Biophys. Acta 1758*, 197-205.

11. Dai, X. Q., Ramji, A., Liu, Y., Li, Q., Karpinski, E., and Chen, X. Z. (2007) Inhibition of TRPP3 channel by amiloride and analogs, *Mol. Pharmacol. 72*, 1576-1585.

12. Shimizu, T., Janssens, A., Voets, T., and Nilius, B. (2009) Regulation of the murine TRPP3 channel by voltage, pH, and changes in cell volume, *Pflugers Arch. 457*, 795-807.

13. DeCaen, P. G., Delling, M., Vien, T. N., and Clapham, D. E. (2013) Direct recording and molecular identification of the calcium channel of primary cilia, *Nature 504*, 315-318.

14. Delling, M., DeCaen, P. G., Doerner, J. F., Febvay, S., and Clapham, D. E. (2013) Primary cilia are specialized calcium signalling organelles, *Nature 504*, 311-314.

15. Inada, H., Kawabata, F., Ishimaru, Y., Fushiki, T., Matsunami, H., and Tominaga, M. (2008) Off-response property of an acid-activated cation channel complex PKD1L3-PKD2L1, *EMBO Rep. 9*, 690-697.

16. Yu, Y., Ulbrich, M. H., Li, M. H., Dobbins, S., Zhang, W. K., Tong, L., Isacoff, E. Y., and Yang, J. (2012) Molecular mechanism of the assembly of an acid-sensing receptor ion channel complex, *Nat. Commun. 3*, 1252.

17. Horio, N., Yoshida, R., Yasumatsu, K., Yanagawa, Y., Ishimaru, Y., Matsunami, H., and Ninomiya, Y. (2011) Sour taste responses in mice lacking PKD channels, *PLoS. One. 6*, e20007.

18. Ishimaru, Y., Inada, H., Kubota, M., Zhuang, H., Tominaga, M., and Matsunami, H. (2006) Transient receptor potential family members PKD1L3 and PKD2L1 form a candidate sour taste receptor, *Proc. Natl. Acad. Sci. U. S. A 103*, 12569-12574.

19. Kataoka, S., Yang, R., Ishimaru, Y., Matsunami, H., Sevigny, J., Kinnamon, J. C., and Finger, T. E. (2008) The candidate sour taste receptor, PKD2L1, is expressed by type III taste cells in the mouse, *Chem. Senses 33*, 243-254.

20. Huang, A. L., Chen, X., Hoon, M. A., Chandrashekar, J., Guo, W., Trankner, D., Ryba, N. J., and Zuker, C. S. (2006) The cells and logic for mammalian sour taste detection, *Nature 442*, 934-938.

21. Nelson, T. M., Lopezjimenez, N. D., Tessarollo, L., Inoue, M., Bachmanov, A. A., and Sullivan, S. L. (2010) Taste function in mice with a targeted mutation of the pkd1l3 gene, *Chem. Senses 35*, 565-577.

22. Shimizu, T., Higuchi, T., Fujii, T., Nilius, B., and Sakai, H. (2011) Bimodal effect of alkalization on the polycystin transient receptor potential channel, PKD2L1, *Pflugers Arch. 461*, 507-513.

23. Ishimaru, Y., Katano, Y., Yamamoto, K., Akiba, M., Misaka, T., Roberts, R. W., Asakura, T., Matsunami, H., and Abe, K. (2010) Interaction between PKD1L3 and PKD2L1 through their transmembrane domains is required for

localization of PKD2L1 at taste pores in taste cells of circumvallate and foliate papillae, *FASEB J. 24*, 4058-4067.

24. Ishii, S., Misaka, T., Kishi, M., Kaga, T., Ishimaru, Y., and Abe, K. (2009) Acetic acid activates PKD1L3-PKD2L1 channel--a candidate sour taste receptor, *Biochem. Biophys. Res. Commun. 385*, 346-350.

25. Kawaguchi, H., Yamanaka, A., Uchida, K., Shibasaki, K., Sokabe, T., Maruyama, Y., Yanagawa, Y., Murakami, S., and Tominaga, M. (2010) Activation of polycystic kidney disease-2-like 1 (PKD2L1)-PKD1L3 complex by acid in mouse taste cells, *J. Biol. Chem. 285*, 17277-17281.

26. Fujimoto, C., Ishimaru, Y., Katano, Y., Misaka, T., Yamasoba, T., Asakura, T., and Abe, K. (2011) The single pore residue Asp523 in PKD2L1 determines Ca2+ permeation of the PKD1L3/PKD2L1 complex, *Biochem. Biophys. Res. Commun. 404*, 946-951.

27. Lopezjimenez, N. D., Cavenagh, M. M., Sainz, E., Cruz-Ithier, M. A., Battey, J. F., and Sullivan, S. L. (2006) Two members of the TRPP family of ion channels, Pkd1l3 and Pkd2l1, are co-expressed in a subset of taste receptor cells, *J. Neurochem. 98*, 68-77.

28. Ishii, S., Kurokawa, A., Kishi, M., Yamagami, K., Okada, S., Ishimaru, Y., and Misaka, T. (2012) The response of PKD1L3/PKD2L1 to acid stimuli is inhibited by capsaicin and its pungent analogs, *FEBS J. 279*, 1857-1870.

29. Lyall, V., Alam, R. I., Phan, D. Q., Ereso, G. L., Phan, T. H., Malik, S. A., Montrose, M. H., Chu, S., Heck, G. L., Feldman, G. M., and DeSimone, J. A. (2001) Decrease in rat taste receptor cell intracellular pH is the proximate stimulus in sour taste transduction, *Am. J. Physiol Cell Physiol 281*, C1005-C1013.

30. Molland, K. L., Paul, L. N., and Yernool, D. A. (2012) Crystal structure and characterization of coiled-coil domain of the transient receptor potential channel PKD2L1, *Biochim. Biophys. Acta 1824*, 413-421.

31. Murakami, M., Ohba, T., Xu, F., Shida, S., Satoh, E., Ono, K., Miyoshi, I., Watanabe, H., Ito, H., and Iijima, T. (2005) Genomic organization and functional analysis of murine PKD2L1, *J. Biol. Chem. 280*, 5626-5635.

32. Li, Q., Liu, Y., Zhao, W., and Chen, X. Z. (2002) The calcium-binding EF-hand in polycystin-L is not a domain for channel activation and ensuing inactivation, *FEBS Lett. 516*, 270-278.

CHAPTER 3

3. RESULT #2 A novel PKD2L1 C-terminal domain critical for trimerization and channel function

3.1 INTRODUCTION

Eight members in the polycystic kidney disease (PKD) family of proteins have so far been identified: PKD1,-1L1, -1L2, -1L3, -REJ; PKD2, -2L1 and -2L2. Among them, only PKD1 and PKD2 are mutated in autosomal dominant PKD (ADPKD) *(1;2)*. PKD2, -2L1 and -2L2 form the transient receptor potential (TRP) polycystin (TRPP) subfamily and are called TRPP2, 3 and 5, respectively. Members of the TRP superfamily are cation channels and play critical roles in sensory physiology *(3;4)*. PKD2L1 and PKD2 share 50% sequence identity and 71% similarity and are predicted to have similar membrane architecture: six transmembrane (TM) segments flanked by the intracellular amino- (N-) terminus (NT, M1-Y96) and carboxyl- (C-) terminus (CT, E566-S805), with a pore loop between TM5 and TM6. Sharing these topological features with other TRP members TRPP channels are presumably organized as homotetramers *(5-7)*. When over-expressed in *Xenopus* oocytes alone, PKD2L1 channel was found to traffic to the plasma membrane and be activated by Ca^{2+} and permeable to Ca^{2+} *(8;9)*. PKD2L1 also acts as a Ca^{2+} channel on the mammalian cell surface membrane and primary cilia where it regulates Ca^{2+} concentration and Ca^{2+}-dependent hedgehog signalling *(10;11)*. The same studies found that PKD2L1 knockout (KO) mice exhibit defective intestinal development. When over-expressed in human embryonic kidney (HEK) cells, PKD2L1 is regulated by extracellular pH and cell swelling *(12)*. In addition, PKD2L1 is expressed in bipolar neurons in the tongue taste buds and neurons surrounding the central canal of spinal cord where it responds to a decrease in extracellular pH *(13)*. In fact, the same study found that genetic ablation of cells expressing PKD2L1 eliminates gustatory nerve response to sour stimuli in

mice. The involvement of PKD2L1 in sour tasting was later confirmed using KO mouse models *(14)*.

There are theoretically 15 possible ways of complexion between a PKD1 and a PKD2 homologue, which may nicely respond to various tissue-specific needs of sensory functions and regulations. E.g.; the PKD2/PKD1 and PKD2L1/PKD1L3 channel complexes were reported to sense fluid flow and acid, in primary cilia and surface membrane, respectively *(15;16)*. PKD1 and PKD2L1 were also reported to form a channel complex when co-expressed in HEK cells, but the physiological role has remained unknown *(17)*. At least when co-expressed in HEK cells, PKD2L1 also interacts with PKD1L3 such that both efficiently traffic to the surface membrane where they act as an extracellular acid-induced off-response cation channel, i.e. activation occurred only after low extracellular pH was removed *(15;18)*. Further, they are co-expressed in mouse circumvallate and foliate papillae although only PKD2L1 is found in other taste bud areas, including fungiform and palate taste buds *(15;18)*. These *in vitro* and *in vivo* data suggest that PKD2L1 and PKD1L3 are synergistically involved in acid sensing pathways. However, unlike PKD2L1 KO mice, PKD1L3 KO mice were not found to have defects in sour tasting *(19)*, arguing against the assumption that they are in the same pathway in the tongue. In primary cilia PKD2L1 and PKD1L1 form a Ca^{2+} channel that regulates the ciliary Ca^{2+} concentration and Ca^{2+}-dependent hedgehog signalling pathway, which seems to be developmentally important *(10;11)*. In these studies, PKD1L1 was found to regulate the single-channel conductance of PKD2L1. However, it remains to be determined whether PKD1L1 KO mice also display similar developmental defects as those observed in PKD2L1 KO mice. Optimistically, more

diverse functions and regulations associated with pairs of PKD proteins will be discovered in near future.

How does a PKD2 homologue complex with a PKD1 homologue? Studies using mammalian cell and *Xenopus* oocyte expression showed that both the PKD2/PKD1 and PKD2L1/PKD1L3 complexes form heterotetramers with 3:1 stoichiometry, i.e. one PKD2 (or PKD2L1) trimer paired with one PKD1 (or PKD1L3) monomer *(20;21)*. Although no corresponding information for PKD2L1/PKD1 and PKD2L1/PKD1L1 is available it is reasonable to speculate that they are also organized with the same stoichiometry. The PKD2L1 C-terminal coiled-coil 2 domain (CC2, G699-W743) was found to homotrimerize *in vitro* and be important for PKD2L1 homomeric assembly and PKD2L1/PKD1L3 surface expression in *Xenopus* oocytes *(21-23)*. However, a previous study found that PKD2L1 truncation mutants lacking CC2 possess similar Ca^{2+}-activated channel function as wild-type (WT) PKD2L1. PKD2L1 and PKD1L3 interact with each other through their TMs, which is required for PKD2L1/PKD1L3 surface expression in HEK cells *(24)*. This study also showed that cells still respond to 25 mM citric acid solution when co-expressed full-length PKD1L3 with PKD2L1 truncation mutant lacking either CC2 (PKD2L1ΔCC, M1-E653) or both CC2 and the EF hand domain (PKD2L1ΔEF-CC, M1-F621), but little response was observed with PKD2L1 truncation mutant lacking the entire C-terminus (PKD2L1ΔCT, M1-I560), despite robust cell surface expression. This suggests the importance of a domain within I560-F621 for channel function *(25)*.

Based on the tetrameric assembly of PKD2 *(26;27)* and other TRP channels *(5-7)* it is likely that PKD2L1 also possesses tetrameric organization. It may be speculated that a TRP homotetrameric channel is formed through dimerization of two homodimers. If such speculation would be true for PKD2L1, then it should possess two distinct domains, for dimerization of two monomers and of two homodimers, respectively, and these domains should also be distinct from a trimerization domain, e.g. CC2. Unfortunately, it has so far remained unknown as to which PKD2L1 domains are critical for both its homomerization and channel function. In the present study, through the use of mutagenesis, non-reducing SDS-PAGE, blue native PAGE (BN-PAGE) and electrophysiology, among others, we discovered that a novel C-terminal domain called C1 (K575-T622) is essential for both homotrimerization and channel function, challenging the speculation that a functional homotetrameric TRP channel is formed through two consecutive steps of homodimerization.

3.2 MATERIALS AND METHODS

3.2.1 Plasmid construction

Human full-length PKD2L1 cDNA was amplified from pCHGF *(9)* by PCR and subcloned into pcDNA3.1(+) and pEGFP-C2 for mammalian cell expression. Flag tag was inserted 5' of the PKD2L1 coding region in pcDNA3.1(+). Mouse PKD1L3 plasmid was a kind gift of Dr. H. Matsunami from Duke University. All mutations were made with QuikChange Lightning Site-Directed Mutagenesis kit (Agilent Technologies, La Jolla, CA) and confirmed by sequencing.

3.2.2 Cell culture and transfection

HeLa and HEK cells were cultured in Dulbecco's modified Eagle's medium (DMEM) supplemented with 10% fetal bovine serum (FBS) and 1% penicillin/streptomycin (Sigma, St. Louis, MO). Cells of less than 25 passages were cultured to full confluence before collection. Transient transfection was performed on cells cultured to 70%–90% confluence using Lipofectamine 2000 (Invitrogen, Carlsbad, CA) according to the manufacturer's instruction.

3.2.3 Western Blotting (WB)

Protein samples were separated on 8% SDS-PAGE gels. For the non-reducing SDS-PAGE, samples were mixed with SDS loading buffer without reducing reagents and kept on ice for 5 minutes (min) prior to electrophoresis. For the reducing SDS-PAGE, samples were mixed with loading buffer supplemented with 0.5 M dithiothreitol (DTT) or 5% 2-mercaptoethanol (2-ME), and subjected to heating at 65 °C for 5 min. 30 μg of total protein was loaded per lane. Flag and GFP (B-2) antibodies

were purchased from Santa Cruz Biotechnology (Santa Cruz, CA). PKD2L1 antibody (H00009033) was purchased from Abnova (Taipei, Taiwan) for tissue detection. Rabbit antibody against PKD2L1 (PR71) was custom made and used previously *(42)*. Secondary antibodies were purchased from GE Healthcare (Baie d'Urfe, QC, Canada). Band intensity was analyzed with the software ImageJ (NIH, Bethesda, MD).

3.2.4 BN-PAGE

HeLa cell lysates for BN-PAGE were prepared with NativePAGE Sample Prep Kit (Invitrogen) according to the manufacturer's protocol. Coomassie blue G-250 was added to supernatants at 8:1 detergent:G-250 ratio. Protein complexes were separated at 150 V for 90 min using NativePAGE Novex 3–12% BisTris gels (Invitrogen). For immunoblotting, gel was incubated in 20 mM Tris-HCl (pH 8.3), 0.15 M glycine, and 0.02% SDS for 5 min at room temperature. Proteins were then transferred to polyvinylidene difluoride membranes (at 150 mA for 90 min and 4 °C). Membranes were blocked with 3% skim milk in PBS buffer with 0.1% tween-20 for 40 min at room temperature and then incubated with antibodies.

3.2.5 Dot blot

Lysates of *Xenopus* oocytes were spotted onto a nitrocellulose membrane and then let the membrane dry. Glutaraldehyde fixation was applied as previously described *(43)* to enhance the retention of short peptides on the membrane. Briefly, membrane was immersed in PBS containing 0.5% (v/v) glutaraldehyde for 5 min and moved to a fresh PBS/glutaraldehyde solution for 10 min, followed by placement in PBS containing 50 mM glycine to stop cross-linking reaction. Membrane was then washed once with PBS buffer and subjected to normal WB procedure.

3.2.6 Immunofluorescence

Xenopus oocytes were washed in PBS, fixed in 3% paraformaldehyde for 15 min, washed 3 times in PBS plus 50 mM NH_4Cl, and then permeabilized with 0.1% Triton X-100 for 4 min. Oocytes were then washed 3 times in PBS for 5 min each time, blocked in 3% skim milk in PBS for 30 min, and then incubated overnight at 4 °C with the rabbit anti-PKD2L1 polyclonal antibody (cat# PAB5914, Abnova). This was followed by 3 times 10-min washes in PBS. Oocytes were then incubated with a secondary AlexaFluor 488-conjugated donkey anti-rabbit antibody (Jackson ImmunoResearch Laboratories, West Grove, PA) for 30 min, followed by 3-time washes in PBS and mounting in Vectashield (Vector Labs, Burlington, ON). The slides were examined on an AIVI spinning disc confocal microscopy (Cell Imaging Facility, Faculty of Medicine and Dentistry, University of Alberta). Plasma membrane intensity of WT or mutant PKD2L1 was assessed by quantifying the plasma membrane immunofluorescence using Volocity 6.2 (Perkin Elmer, Waltham, MA). Background fluorescence was subtracted and data were normalized to the average PKD2L1 WT intensity.

3.2.7 Co-immunoprecipitation (Co-IP)

Co-IP was performed using lysates of HeLa cells over-expressing GFP-PKD2L1 and Flag-tagged mutant PKD2L1 constructs. HeLa cell monolayer in 100 mm dishes was washed twice with PBS and solubilized in ice-cold CellLytic-M lysis buffer supplemented with protease inhibitor mixture (Sigma). Supernatants were collected following centrifugation at 16,000 × *g* for 15 min. Equal amounts of total proteins from postnuclear supernatants were pre-cleared for 1 hour (hr) with protein G-Sepharose

(GE Healthcare), and then incubated for 4 hr at 4 °C with the antibody against GFP. After the addition of 100 μl of 50% protein G-Sepharose, the mixture was incubated overnight with gentle shaking at 4 °C. The immune complexes adsorbed to protein G-Sepharose were washed five times with Nonidet P-40 lysis buffer (50 mM Tris, pH 7.5, 150 mM NaCl, 1% Nonidet P-40) with protease inhibitors and eluted by SDS loading buffer. Precipitated proteins were analyzed by WB using the antibodies against Flag or GFP.

3.2.8 Protein expression in and purification from *E. coli*

DNA fragment encoding C1 was inserted into pET28a(+) that contains upstream GFP gene. BL21 (DE3) strain (Novagen, Darmstadt, Germany) was used for expression. Following growth at 37 °C to an optical density (OD) of 0.6, cultures were cooled to 30°C, induced with 1 mM isopropyl β-D-thiogalactoside and incubated for 6 hr. Cell lysates from 50 mL culture were prepared with CellLytic-B lysis buffer (Sigma) according to the manufacturer's instruction. Proteins were pulled down with Ni-NTA resin (Qiagen, Venlo, Netherlands) and eluted from beads with 250 mM imidazole by following the manufacturer's manual.

3.2.9 Preparation of mRNAs and microinjection into oocytes

Capped mRNAs of WT or mutant PKD2L1 were synthesized by *in vitro* transcription from a linearized template in the pCHGF vector using the mMESSAGE mMACHINE kit (Ambion, Austin, TX). Stage V–VI oocytes were isolated from *Xenopus laevis*. Defolliculation of oocytes was performed through incubation in Ca^{2+}-free Barth's solution *(24)* containing collagenase (2 mg/ml) at RT for 2–2.5 hr. Oocytes were then incubated at 18 °C in the Barth's solution for at least 3 hr before injection of

50 nl RNase-free water containing 50 ng mRNAs. An equal volume of water was injected into each control oocyte. The present study was approved by the Ethical Committee for Animal Experiments of the University of Alberta, and was carried out in accordance with the Guidelines for Research with Experimental Animals of the University of Alberta and the Guide for the Care and Use of Laboratory Animals (NIH Guide) revised in 1996. Injected oocytes were incubated at 16–18 °C in the Barth's solution supplemented with antibiotics for 2–4 days prior to experiments.

3.2.10 Two-microelectrode voltage clamp (TMVC)

Two-microelectrode voltage clamp experiments were performed as described before *(9)*. Briefly, the two electrodes (Capillary pipettes, Warner Instruments, Hamden, CT) impaling oocytes were filled with 3 M KCl to form a tip resistance of 0.3–2 MΩ. The standard extracellular solution (pH 7.5) containing 100 mM NaCl, 2 mM KCl, 1 mM $MgCl_2$ and 10 mM HEPES was used. The solution containing extracellular Ca^{2+} was prepared from the standard solution with the addition of $CaCl_2$ to a final concentration of 5 mM. Duration of application of Ca^{2+} medium was indicated in time course recordings. Oocyte whole-cell currents were recorded using a Geneclamp 500B amplifier and Digidata 1322A AD/DA converter (Molecular Devices, Union City, CA). The pClamp 9 software (Axon Instruments, Union City, CA) was applied for data acquisition and analysis. Currents and voltages were digitally recorded at 200 μs/sample and filtered at 2 kHz through a Bessel filter. SigmaPlot 12 (Systat Software, San Jose, CA) was used for data fitting and plotting.

3.2.11 Dynamic light scattering (DLS)

DLS experiments were performed using a Malvern Zetasizer Nano ZS instrument (Malvern, Worcestershire, UK) at 25 °C, as described previously *(44)*. Freshly purified PKD2L1 CT and deletion mutants from *E. coli* in a solution containing 50 mM NaH_2PO_4, 300 mM NaCl and 250 mM imidazole, pH 8.0 were passed through a 0.22 μm filter to remove large particles or aggregates and diluted to 0.4 mg/ml before measurements. Correlation data obtained with DynaLS software (Malvern) were fitted using SigmaPlot 12 (Systat Software) to derive the average apparent hydrodynamic diameter.

3.2.12 Statistical analysis

Data were analyzed and plotted using SigmaPlot 12 (Systat Software), and expressed as mean ± SEM (N), where SEM stands for the standard error of the mean and N indicates the number of experimental repeats. Paired or unpaired Student t-test was used to compare two sets of data. A probability value (P) of less than 0.05, 0.01 and 0.001 was considered statistically significant and indicated by *, ** and ***, respectively.

3.3 RESULTS

3.3.1 Oligomeric state of PKD2L1 in mouse tissues and human cells

Previous studies on PKD2L1 oligomerization were limited to *in vitro* conditions, including trimerization of its purified C-terminus or of the full-length protein over-expressed in *Xenopus* oocytes *(21-23)*. In order to determine the oligomeric states of PKD2L1 under more *in vivo* and physiological conditions, we performed Western Blot (WB) experiments using mouse tissues under non-reducing and reducing conditions. We found that in the kidney, testis and brain under non-reducing condition, endogenous PKD2L1 displays similar oligomeric patterns from which the bands' sizes suggest the presence of PKD2L1 homodimers, -trimers and -tetramers, or its heteromerization with endogenous interacting partner proteins (Figure 3-1 A). These oligomer bands disappeared in the presence of a reducing condition. To provide further documentations regarding whether these bands correspond to PKD2L1 homo- or heterooligomers we over-expressed human PKD2L1 in HEK (HEK293T) and HeLa cells in which partners of PKD2L1 were assumed to have little influence due to their absence or relatively low expression levels. In both HEK and HeLa cells under the non-reducing condition, we still detected four bands (Figure 3-1 B and C) that were comparable to the patterns obtained using mouse tissues. We thus tentatively assigned them as monomer, dimer, trimer and tetramer. Interestingly, under the reducing condition, a significant portion of trimers remained while all tetramers and the majority of dimers were absent. These data indicated that the oligomerization strength follows an order of trimer $\gg$ dimer > tetramer, consistent with a previous finding that PKD2L1 CT forms very stable trimers *in vitro (22;23)*.

Because oligomerization may occur through a disulfide bond between two cysteine residues during lysate preparations or SDS-PAGE under denaturing conditions, and there are several cysteine residues in PKD2L1, we wondered whether disulfide bonds formed by these residues under oxidative conditions account for the observed oligomers. For this we included 10 mM N-ethylmaleimide (NEM) in cell lysis buffer to inhibit disulfide bond formation by modifying free cysteine residues. We found that the amount of oligomers decreases with the NEM treatment in HEK cells but does not further decrease with additional reducing agents (Figure 3-1 D), indicating that the observed oligomers in Figure 3-1 B and C are partially due to disulfide bond formation during sample preparations and/or electrophoresis, and that the oligomers detected in the presence of the NEM treatment are formed through peptide-peptide interactions.

We also employed BN-PAGE to check PKD2L1 oligomeric state under the non-denaturing condition. No disulfide bonds would be formed during sample preparation and/or electrophoresis with BN-PAGE. Our data indicated that PKD2L1 is mainly present as homotrimers, and possibly also as homotetramers or hetero-oligomers with its partner proteins, while monomers and dimers are still detectable under this condition (Figure 3-1 E). Only monomers were observed in the presence of SDS and DTT, while dimers were detectable if only SDS was applied (Figure 3-1 E). Previous studies showed that peptide-peptide interaction mediated oligomers of some membrane proteins, especially multiple-transmembrane proteins, can also be detected with non-reducing SDS-PAGE under denaturing conditions *(28-30)* because SDS as a detergent may form micelles, similar to lipid vesicles, at certain concentrations to hold

denatured oligomers by binding to hydrophobic transmembrane domains rather than to disrupting them into monomers *(31)*. However, since there is no SDS in the gel or running buffer on BN-PAGE, compared with SDS-PAGE, these oligomers/SDS micelle complexes may be dissociated once the samples are loaded into the gel. That may be the reason why no trimers were detected on BN-PAGE with SDS while trimers can still be observed on non-reducing SDS-PAGE. Taken together, our data using over-expressed PKD2L1 together with our *in vivo* data using mouse tissues strongly indicated that PKD2L1 forms homodimers, -trimers and -tetramers.

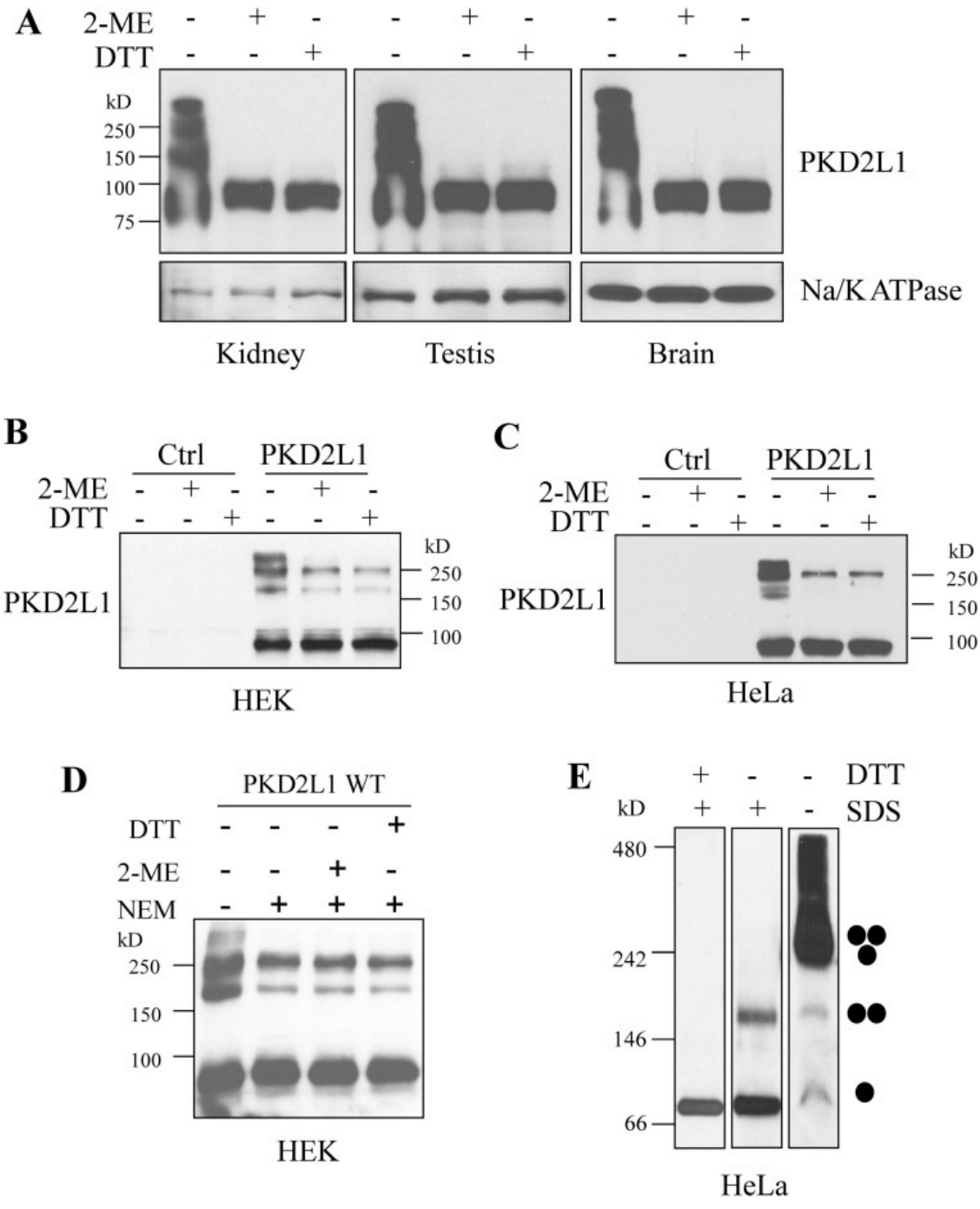

Figure 3-1 Oligomers of PKD2L1 in mouse tissues and human cell lines. (**A**) Detection of PKD2L1 in mouse kidney, testis, and brain tissues by WB. Samples were prepared with SDS loading buffer under the non-reducing and reducing (supplemented with 5% 2-ME or 0.5 M DTT) conditions. PKD2L1 was detected with an antibody from Abnova. Na/K ATPase was used as a loading control. Detection of over-expressed human PKD2L1 in HEK (**B**) and HeLa cells (**C**). pcDNA3.1(+) containing human PKD2L1 or empty vector (Ctrl) was transfected into

HEK and HeLa cells. Cell lysates were collected 48 hr after transfection. Samples for SDS-PAGE were prepared under non-reducing or reducing condition. (**D**) Detection of over-expressed human PKD2L1 in HEK cells under non-reducing and reducing conditions. Samples were prepared with or without treatment by 10 mM NEM. (**E**) WB analysis after BN-PAGE of Flag-tagged PKD2L1 over-expressed in HeLa cells. Samples were prepared with or without 2.5% SDS, or with 2.5% SDS plus 0.1 M DTT. An anti-Flag antibody was used for WB detection. Putative PKD2L1 monomer, dimer and trimer are indicated.

3.3.2 Effects of intracellular N- and C-termini of PKD2L1 on its channel function and homomerization

PKD2L1 was first found to act as a Ca^{2+}-activated non-selective cation channel when over-expressed in *Xenopus* oocytes in which PKD2L1 traffics to the plasma membrane *(8;9)*. Previous studies demonstrated that the PKD2L1 C-terminal domain CC2 formed a trimer *in vitro (22;23)* but truncation mutant channels T622X and V670X that do not contain CC2 are still functional *(24)*, indicating that CC2 is not important for PKD2L1 channel function. On the other hand, mutant PKD2L1 lacking CT is still able to oligomerize *(25)*, indicating that a domain outside CT mediates the oligomerization. In an effort to identify domain(s) that are important for both PKD2L1 homomerization and channel function we first set to examine the effects of the PKD2L1 CT and NT on its channel function. For this we over-expressed PKD2L1 truncation mutant with deletion of CT (named ΔCT) or NT (named ΔNT) in *Xenopus* oocytes, and measured Ca^{2+}-induced channel activation currents with the two-microelectrode voltage clamp. We found that both the ΔCT and ΔNT mutants are functionally dead although they continue to traffic to the plasma membrane (Figure 3-2 A–E), which is consistent with previous findings that PKD1L3/PKD2L1 ΔCT or PKD1L3/PKD2L1 ΔNT complex shows no response to 25 mM citric acid *(25)*.

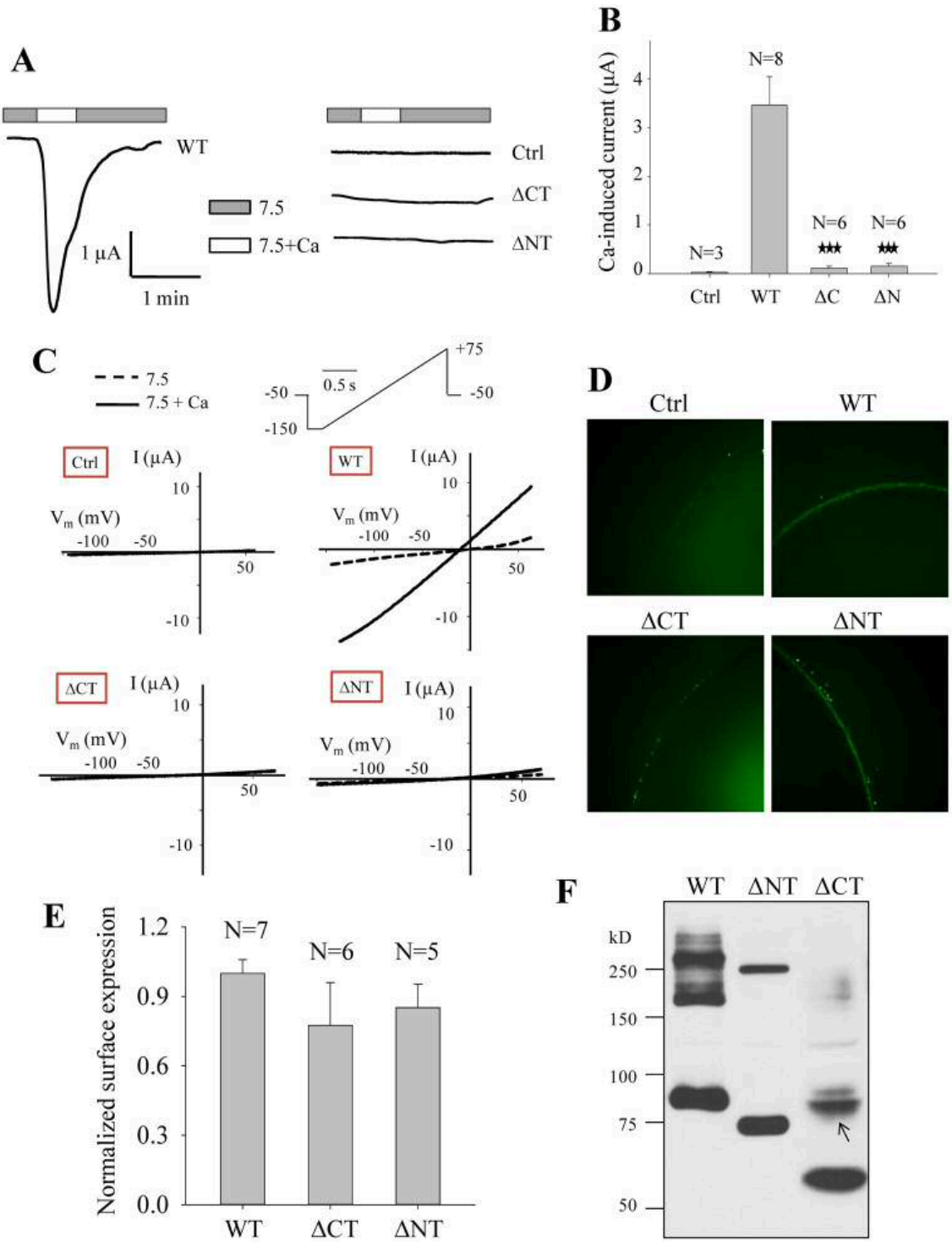

Figure 3-2 Roles of the human PKD2L1 N- and C-termini in its channel activity and oligomerization. (**A**) Representative whole-cell current tracings obtained from *Xenopus* oocytes expressing PKD2L1 WT, mutant ΔCT (deletion of E566-S805) or ΔNT (deletion of M1-Y96) using the two-microelectrode voltage clamp technique. Oocytes were voltage

clamped at −50 mV. Data from a water-injected oocyte served as a negative control (Ctrl). Currents were measured using standard extracellular solution pH 7.5 (7.5) or standard extracellular solution containing 5 mM $CaCl_2$ (7.5+Ca). (**B**) Averaged currents obtained from oocytes expressing PKD2L1 WT, ΔCT, ΔNT or water (Ctrl). Currents were averaged from different numbers of oocytes, as indicated. ***$p \leq 0.001$ compared to WT data. (**C**) Representative current–voltage relationship curves obtained using a voltage ramp protocol, as indicated, before (7.5) and after addition of 5 mM $CaCl_2$ (7.5+Ca). (**D**) Representative immunofluorescence data showing the plasma membrane expression of PKD2L1 WT, ΔCT and ΔNT in oocytes. (**E**) Averaged and normalized surface expression of PKD2L1 WT, ΔCT and ΔNT in oocytes. Surface expressions were averaged from indicated numbers of oocytes and normalized to that of PKD2L1 WT. (**F**) WB detection of Flag-tagged human PKD2L1 WT, ΔNT and ΔCT over-expressed in HeLa cells under the non-reducing condition. A band (indicated by an arrow), that is unlikely a dimer based on its size and remained unaccounted for, was detected with the CT deletion. The data in this figure were generated by me except for data in **F**.

We next wanted to determine whether NT is important for oligomerization using HeLa cells. Absence of NT in mutant ΔNT abolished the oligomers except trimers with both SDS-PAGE (Figure 3-2 F) and BN-PAGE (Figure 3-3 B), suggesting that NT mediates homodimerization. Interestingly, deletion of CT resulted in loss of all trimers and most of dimers (Figure 3-2 F), suggesting the possibility that the dimerization is dependent, at least in part, on trimerization. Because we showed that part of dimers is due to disulfide bond formation during lysate preparations or SDS-PAGE under denaturing conditions (Figure 3-1 D), and there are four cysteine residues in NT, we wondered whether disulfide bonds formed by these residues under oxidative conditions account for the observed dimerization. For this we mutated one or more of these cysteine residues to alanine and found that the mutation C38A, but not any of the other three mutations (C60A, C70A and C74A), substantially reduces the dimer band (Figure 3-3 A). Further, inclusion of NEM in cell lysis buffer exhibited a similar effect (Figure 3-3 A), which was confirmed with BN-PAGE (Figure 3-3 B). These data together showed that part of the dimer band observed under SDS-PAGE attributes to the disulfide bond formed between two C38 residues during the denaturing step and indicated that the rest of the dimer band is due to specific dimerization of NT *in vivo*.

To gain insights into domains responsible for trimerization without ‘contamination' of di- and tetramerization we thus utilized the Flag-tagged ΔNT mutant to construct plasmids with deletion of C-terminal fragments. We found that while the mutant with T622X truncation from ΔNT (named ΔNT/T622X) still forms trimers, the mutant with the entire CT deleted from ΔNT (named ΔNT/ΔCT) has no trimer (Figure 3-3 D). Since no cysteine residue is present in the CT, the observed trimer band likely

corresponds to the specific trimerization of PKD2L1 *in vivo*. Because domain CC2 is absent in these mutants, and ΔCT and T622X are dead (Figure 3-2 B) and functional mutants *(24)*, respectively, our data indicated that the C-terminal fragment E566-T622 contains a novel domain that is critical for both PKD2L1 trimerization and channel function.

3.3.3 Identification of a C-terminal domain critical for both PKD2L1 homotrimerization and channel function

For WT or a mutant PKD2L1 channel to be functional it is necessary that they are in a correct oligomeric state. In an effort to identify a PKD2L1 domain that is essential for both trimerization and channel function we first made two deletion mutants with C1 or CC2 deleted from truncation mutant Flag-ΔNT (see Figure 3-3 A for a schematic illustration of the C1 and CC2 positions in CT), and performed WB experiments under the non-reducing condition. We found that while CC2 deletion significantly reduces the trimerization C1 deletion has a more substantial effect (Figure 3-3 E). Consistently, double deletion of C1 and CC2 completely abolished the trimer band. These data indicated that there exist two domains, C1 and CC2 *(22;23)* in CT, that are essential for trimerization. Human PKD2L1 C1 is a 48-amino-acid peptide containing 16 highly hydrophobic residues and 7 and 8 negatively and positively charged residues, respectively. Sequence alignment showed that C1 is the most conserved part in CT and shares overall 62.5% identity among different species (Figure 3-3 F), suggesting its importance in the PKD2L1 assembly and/or function.

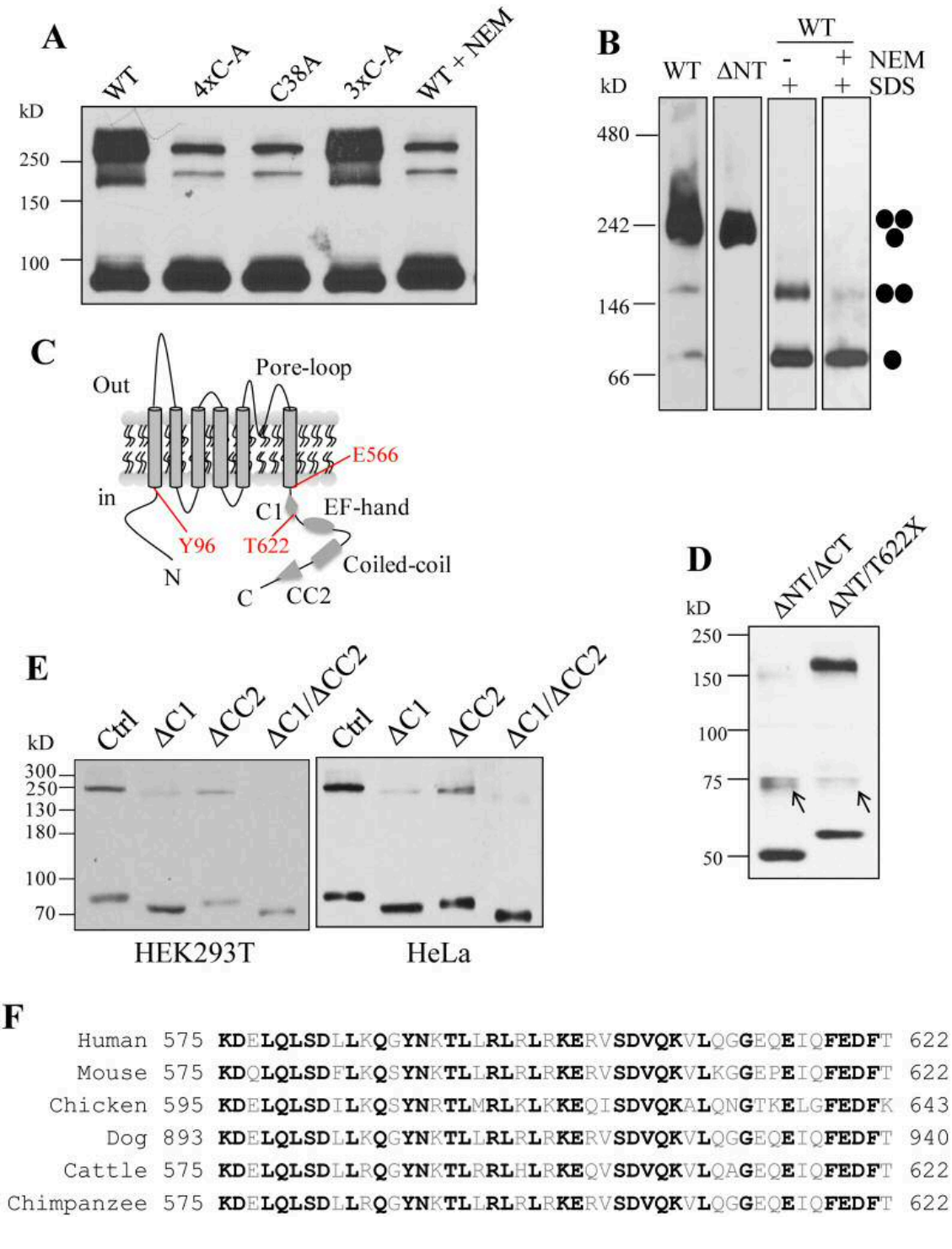

Figure 3-3 Identification of domain C1 of PKD2L1 critical for its trimerization. (**A**) WB detection of over-expressed Flag-tagged PKD2L1 WT, without or with 10 mM NEM treatment, or mutants 4×C-A (quadruple C38A, C60A, C70A and C74A mutations), C38A and 3×C-A (triple C60A, C70A and C74A mutations) under non-reducing condition. (**B**) WB analysis after BN-PAGE of Flag-tagged PKD2L1 WT and ΔNT over-expressed in HeLa cells. WT samples

were prepared with or without 2.5% SDS, or with 2.5% SDS plus 10 mM NEM. Putative PKD2L1 monomer, dimer and trimer are indicated. (**C**) Schematic illustration of PKD2L1 membrane topology. TMs, pore-loop, C1, CC2, EF-hand, coiled-coil domains, and positions of residues Y96, E566 and T622 are indicated. (**D**) WB detection of Flag-tagged PKD2L1 mutants ΔNT/ΔCT (M1-Y96 and E566-S805 double deletion) and ΔNT/T622X (M1-Y96 and T622-S805 double deletion) over-expressed in HeLa cells under the non-reducing condition. Two unknown bands similar to one in Figure 3-2 F remained unaccounted for. (**E**) WB detection of over-expressed Flag-tagged PKD2L1 mutants in HEK or HeLa cells. All constructs were made from ΔNT. These included Ctrl (ΔNT), ΔC1 (C1, K575-T622, deletion from ΔNT), ΔCC2 (CC2, G699-W743, deletion from ΔNT), or ΔC1/ΔCC2 (C1 and CC2 double deletion from ΔN). (**F**) Amino acid sequence alignment of PKD2L1 C1 from indicated species. National Center for Biotechnology Information accession number for sequences used here are NP_057196 (human), NP_852087 (mouse), XP_426509 (chicken), XP_005637930 (dog), XP_002698535 (cattle), and XP_001168415 (chimpanzee). Identical residues among the species are indicated by black bold letters.

We next performed electrophysiological experiments using various C-terminal deletion and truncation mutations of PKD2L1. We found that any domain after T622 is not important for the channel function, as supported by functional mutant V670X and T622X channels. In contrast, truncation mutant S581X and the mutant with C1 deletion did not exhibit channel function (Figure 3-4 A–C). Our immunofluorescence data indicated that all these mutants target to the plasma membrane (Figure 3-4 D and E). These data together demonstrated that C1, but not CC2, is critical for PKD2L1 channel function. Thus, we have discovered for the first time a domain in PKD2L1, C1, that is essential for both homotrimerization and channel function. Interestingly, Ishimaru *et al.* also found that PKD1L3/PKD2L1 M1-F621 responds to citric acid while PKD1L3/PKD2L1 M1-I560 shows no response, suggesting that domain C1 is also important for PKD1L3/PKD2L1 complex off-response channel function *(25)*.

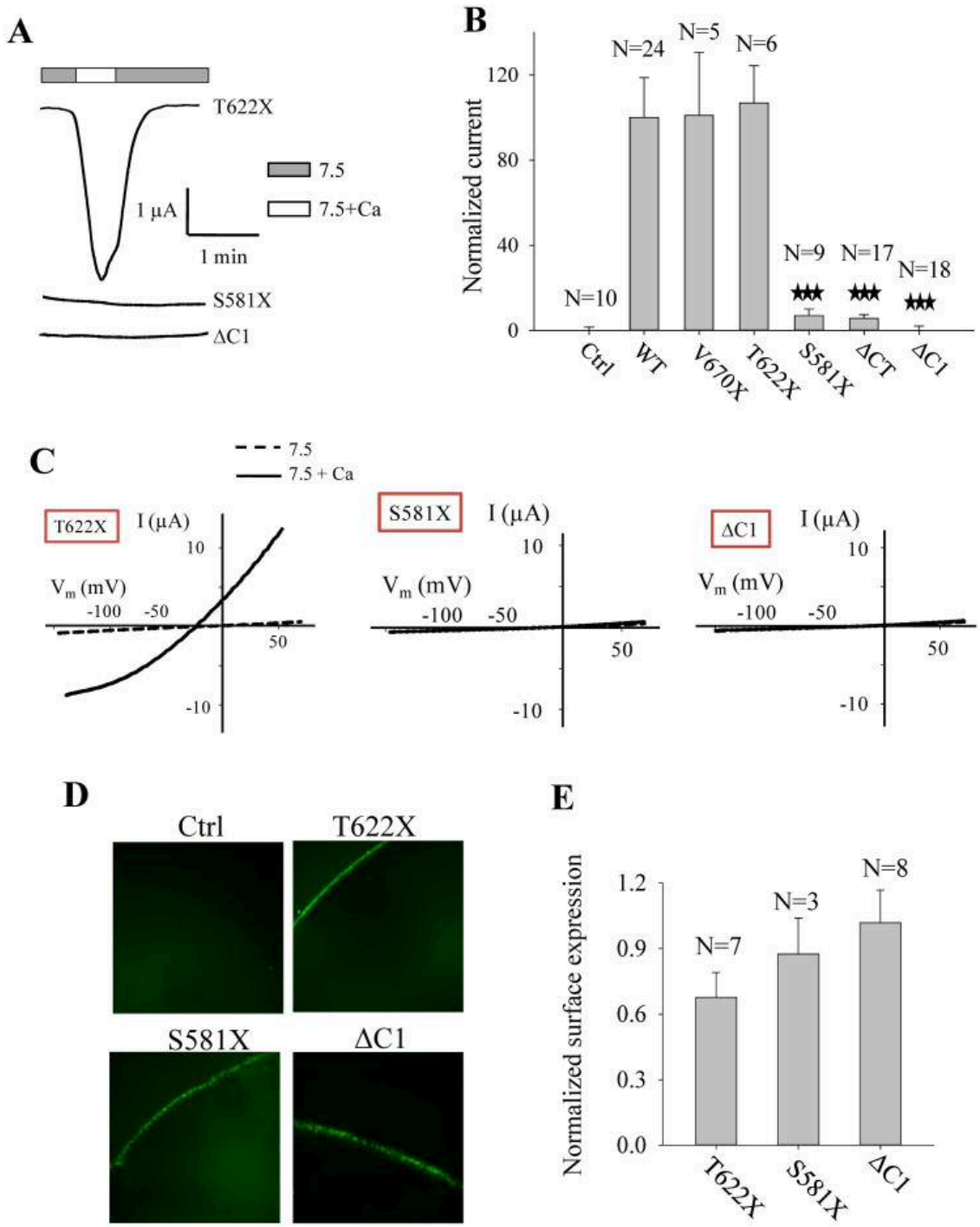

Figure 3-4 Identification of domain C1 of PKD2L1 critical for its channel function. (**A**) Representative whole-cell current tracings obtained from *Xenopus* oocytes expressing PKD2L1 truncation mutant T622X, S581X, or deletion mutant ΔC1 (C1 deletion from PKD2L1 WT) using the two-microelectrode voltage clamp technique under similar experimental conditions as those for Figure 3-2. (**B**) Averaged currents obtained from oocytes expressing PKD2L1 WT or

truncation/deletion mutants, as indicated. Currents at −50mV were averaged from indicated numbers of oocytes and normalized to that of PKD2L1 WT. Water-injected oocytes were used as control (Ctrl). ***p ≤ 0.001 compared to WT. (**C**) Representative current–voltage relationship curves obtained using a voltage ramp protocol, as indicated in Figure 3-2 C, before (7.5) and after addition of 5 mM $CaCl_2$ (7.5+Ca). (**D**) Representative immunofluorescence data showing the plasma membrane expression of mutants T622X, S581X and ΔC1 expressed in oocytes, or those injected with water (Ctrl). (**E**) Surface membrane expression of mutants T622X, S581X and ΔC1 were averaged from the indicated numbers of oocytes and normalized to that of PKD2L1 WT. The data in this figure were generated by me.

3.3.4 Further characterization of C1-involved trimerization

To provide further documentations on the involvement of C1 in trimerization we first employed co-IP assays to determine the effect of C1 on the interaction between two differently tagged WT or mutant PKD2L1 proteins. To enhance the co-expression efficiency, HeLa cells were transfected with GFP-WT first, then 12 hr later with Flag-T622X or -K575X. We collected cell lysates 30 hr after the second transfection. We found that the strength of the interaction of WT with K575X (that lacks C1), assessed by the immunoblotting band after normalization by input bands, is 36.5 ± 6.8% (N = 3, $P < 0.001$, by paired t-test) less than the interaction with T622X (Figure 3-5 A and B). We believe that the interaction between WT PKD2L1 and K575X is largely mediated through their N-terminus. In summary, our *in vitro* data were in support of the involvement of C1 in trimerization.

Further, we employed the DLS technique to examine the role of C1 in the trimerization of purified CT in solution. DLS assesses a protein's apparent hydrodynamic diameter (D_H) as being the size of a hypothetical hard sphere that diffuses in the same fashion as the hydrated protein being measured. We expressed and purified CT and its deletion mutants CT-ΔC1 (with C1 deletion) and CT-Δdouble (with both C1 and CC2 deletions) from *E. coli* (Figure 3-5 C). We found that the D_H of CT measured by DLS is 8.88 ± 0.26 nm (N = 6), which is significantly reduced to 5.80 ± 0.17 nm (N = 5, $P < 0.001$) and 5.49 ± 0.05 nm (N = 5, $P < 0.001$) for C1 and double deletions, respectively (Figure 3-5 D). Using the Mark-Houwink-Sakurada equation, molecular weight = $a(D_H)^b$, where parameters a and b were found to be 0.41 ± 0.05 and 2.48 ± 0.04, respectively, for proteins in the range of 17–440 kD *(32)*, the

corresponding molecular weights deduced from these D_H values are 93 ± 6 kD, 32 ± 2 kD and 28 ± 1 kD, for CT, CT-ΔC1 and CT-Δdouble, respectively, indicating a predominant trimeric structure for CT and monomeric structures for the two deletion mutants under this experimental condition. These data indicated that C1 deletion significantly breaks down trimerization of CT, in support of the importance of C1 for oligomerization.

Next, we examined whether peptide C1 is sufficient to form trimers by itself. For this we first expressed C1 in and purified it from *E. coli*. Because C1 was not detectable when expressed alone, presumably due to its small size and/or instability, we utilized fusion protein GFP-C1 for *E. coli* expression. As a negative control, we expressed and purified GFP protein fused with human eukaryotic initiation factor 4E binding protein 1 (4EBP1) fragment M1-T50 (GFP-Ctrl) of a similar size. We then carried out BN-PAGE experiments which indeed revealed the presence of a trimer band for GFP-C1 but not for GFP-Ctrl (Figure 3-5 E). Of note, the trimer band was relatively weak, which may be due to the added coomassie blue G-250 that gave negative changes to C1 and reduced its trimerization during sample preparation for BN-PAGE. As a comparison and control, we carried out SDS-PAGE analysis as well and found no trimer band for C1 under this condition (Figure 3-5 E). Therefore, our data showed that purified C1 itself forms trimers. We also noted visible weak bands below and above the trimer band, which may represent a dimer due to the well-known weak dimerization of GFP and a hexamer due to GFP dimerization plus C1 trimerization, respectively.

3.3.5 Role of C1 as a blocking peptide

We reasoned that C1 may disrupt the oligomerization of full-length PKD2L1 through competitive binding, thereby inhibiting channel function. To test this, we applied a similar blocking peptide strategy that we described previously *(9)*. First, we co-transfected PKD2L1 ΔNT with HA-tagged C1 or control plasmid encoding HA-T622-E657 (negative Ctrl), that has no overlap with C1 or CC2. Indeed, we found that co-expression of C1 decreases ΔNT trimerization to 42.7 ± 7.5% ($N = 3$, $P < 0.001$, by paired t-test) (Figure 3-5 F).

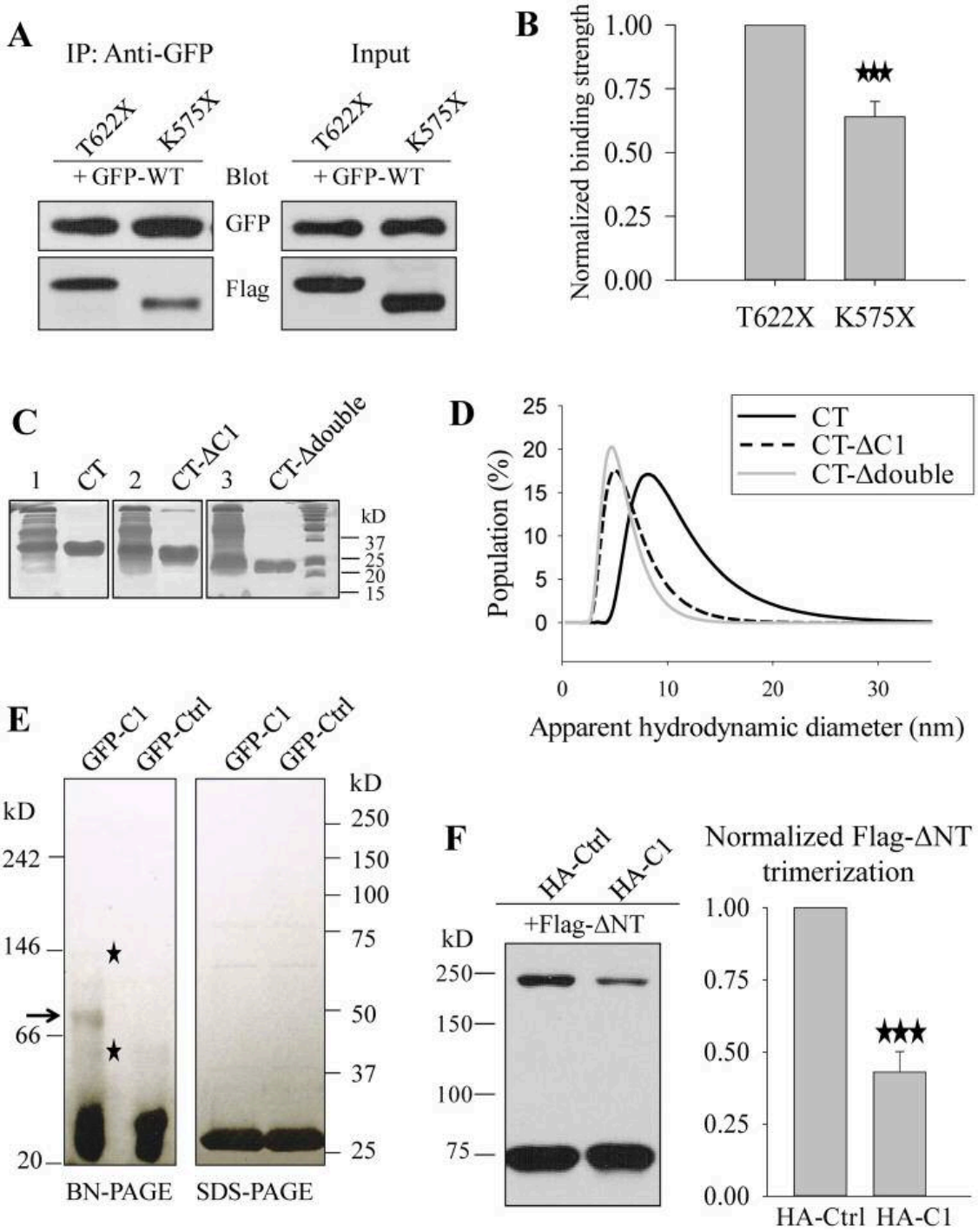

Figure 3-5 Further evidence for C1 involvement in trimerization. (**A**) Effect of C1 on the interaction between two PKD2L1 proteins assessed by co-IP. Left panel: representative data showing the interaction of GFP-PKD2L1 (GFP-WT) with Flag-T622X or Flag-K575X in HeLa cells. GFP-WT was first transfected, followed by transfection of T622X and K575X 12 hr later. Right panel: representative input data by WB showing the expression of WT, T622X and

K575X. (**B**) Data from experiments in panel **A** were quantified, averaged, normalized, and then compared by paired t-test (***p ≤ 0.001, N = 3). (**C**) Coomassie blue staining of purified PKD2L1 C-terminus (CT, E566-S805), CT-ΔC1 (C1 deletion from CT), and CT-Δdouble (C1 and CC2 double deletion from CT) from *E. coli*. Data using crude lysates are shown on their left (lanes 1, 2 and 3). (**D**) Analysis of size distribution of purified CT, CT-ΔC1, and CT-Δdouble fragments by DLS experiments. (**E**) Coomassie blue staining analysis of BN-PAGE or SDS-PAGE of purified protein GFP-C1 or GFP-Ctrl (human 4EBP1 M1-T50 fragment). Putative GFP-C1 trimer is indicated by an arrow on BN-PAGE. The faint bands below and above the putative trimer are indicated with stars. (**F**) Left panel: WB detection of over-expressed Flag-ΔNT with co-expression of HA-tagged blocking peptide C1 (HA-C1) or control peptide T622-E675 (HA-Ctrl) in HeLa cells under the non-reducing condition. 200ng Flag-ΔNT plasmid and 1000ng HA-C1 or HA-Ctrl plasmid were used in the co-transfection. Right panel: trimer bands were quantified, averaged, normalized, and compared by paired t-test (***p ≤ 0.001, N = 3).

Next, using oocyte expression and electrophysiology, we found that expression of C1 substantially inhibits the channel function of PKD2L1 alone and in complex with PKD1L3 (Figure 3-6 A, B and D). Our WB assays using similarly prepared oocytes showed that C1 expression significantly reduces the formation of PKD2L1 oligomers but not monomers, regardless whether PKD1L3 was co-expressed or not (Figure 3-6 C). Of note, due to its small size of only about 5 kD, we carried out dot blot assays and confirmed its expression (Figure 3-6 C). Our immunofluorescence data indicated that over-expression of C1 reduces PKD2L1 surface expression (Figure 3-6 E and F), which may be the reason why reduction in the trimer band did not result in an increase in the monomer band in our WB experiments (Figure 3-6 C).

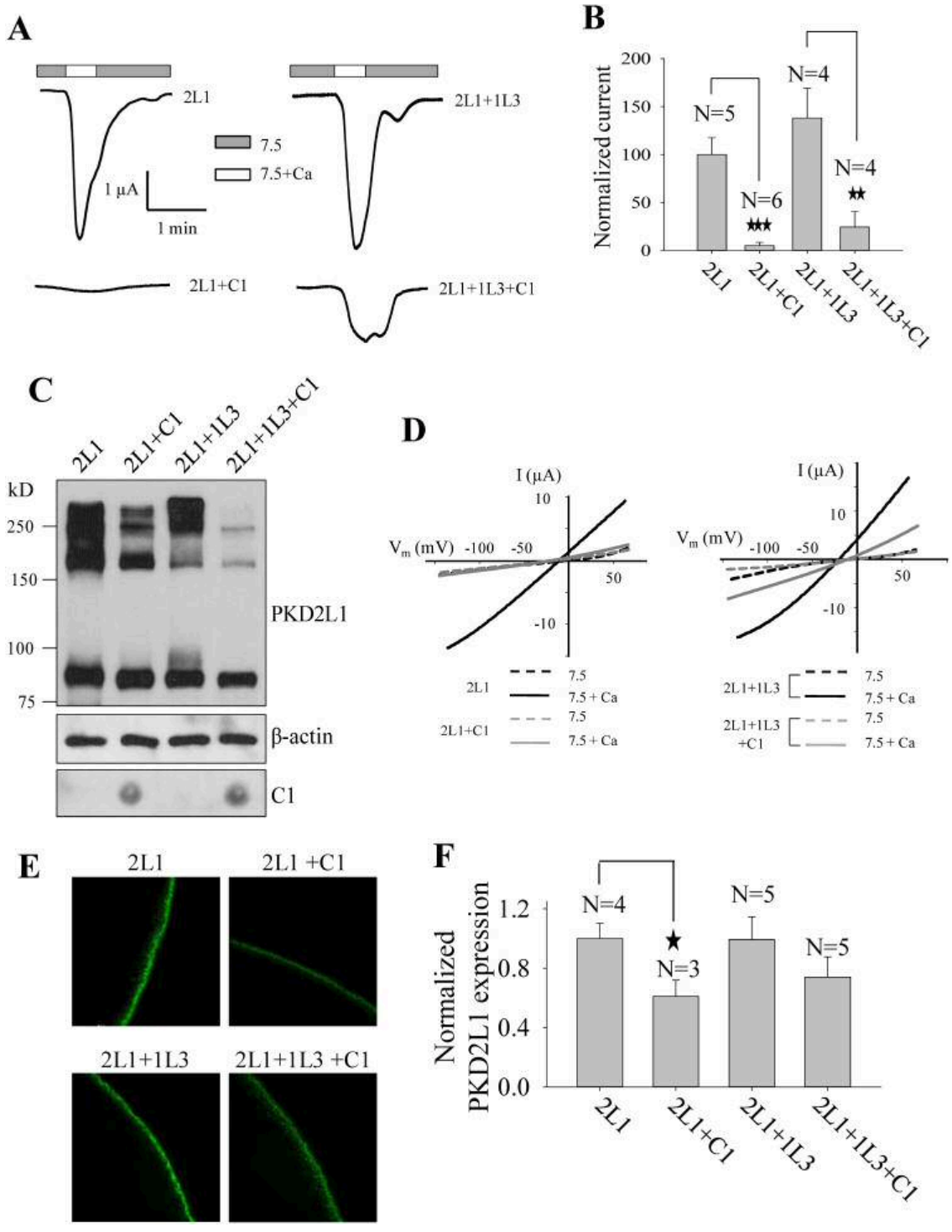

Figure 3-6 Effect of C1 on PKD2L1 trimerization and function. (**A**) Representative whole-cell current tracings from *Xenopus* oocytes expressing PKD2L1 (2L1) or PKD2L1/PKD1L3 (2L1+1L3), with or without C1 using the two-microelectrode voltage clamp technique under similar conditions as for Figure 3-2. (**B**) Averaged currents elicited by extracellular 5 mM Ca^{2+}

from oocytes expressing 2L1 or 2L1+1L3, with or without C1, and voltage clamped at −50 mV. Currents were averaged from different numbers of oocytes, as indicated, and normalized to that of WT PKD2L1 alone. (**C**) WB detection of PKD2L1 expression or dot blot detection of C1 expression in oocytes. (**D**) Representative current–voltage relationship curves obtained using a voltage ramp protocol, as indicated in Figure 3-2 C, before (7.5) and after addition of 5 mM $CaCl_2$ (7.5+Ca). (**E**) Representative immunofluorescence data showing the oocyte plasma membrane expression of 2L1 and 2L1+1L3, with or without C1. (**F**) Surface expression was quantified and averaged from the indicated numbers of oocytes, and normalized to that of 2L1. The data in this figure were generated by me except for data in **C**.

3.4 DISCUSSION

Because the function of an ion channel presumably relies on its intact oligomeric state deletion of or alterations in an oligomerization domain would substantially affect the channel architecture and consequently channel activity. Up to now it has remained unknown as to which domain of PKD2L1 that is important for both oligomerization and function. Previous studies identified CC2 as a trimeric domain in CT that is important for the surface membrane expression of PKD2L1 and complex PKD2L1/PKD1L3 *(21-23)*. However, using the *Xenopus* oocyte expression system, it was previously shown that PKD2L1 with truncation either before or after the CC2 domain does not significantly affect the channel function *(24)*, which is also confirmed by the current study (Figure 3-4 B), indicating that CC2 is not required for PKD2L1 channel function. The reported 3:1 oligomeric assembly for PKD2L1/PKD1L3 channel complex and our current *in vivo* data from mouse tissues showing the presence of trimeric assembly indicate the presence of a yet to-be-identified domain(s) important for a functional PKD2L1 trimeric state. Indeed, our current studies using a combination of *in vitro* expression in mammalian cells and *Xenopus* oocytes, electrophysiology, mutagenesis, protein-protein interaction, and dynamic light scattering identified the C-terminal C1 domain as the most conserved in CT and critical for both PKD2L1 trimerization and channel function.

Our non-reducing SDS-PAGE with mouse tissues showed the same oligomers pattern in kidney, testis and brain and these oligomers were reduced to monomer with reducing agents (Figure 3-1 A). This would suggest that all PKD2L1 oligomers in the tissues are generated through cysteine-cysteine disulfide bonds since reducing agents

are expected to only disrupt oligomerization mediated by disulfide bonds. However, for some unknown reasons, reducing agents may also disrupt oligomerization mediated by peptide-peptide interactions, at least for some multiple-transmembrane proteins. For example, Feng *et al.* showed that dimers of PKD2 truncation mutant PKD2-L703X detected with non-reducing SDS-PAGE disappeared by the addition of reducing agents and that these dimers are indeed formed by a peptide-peptide interaction in the N-terminus of PKD2 *(26)*. Further, oligomers formed through peptide-peptide interactions under non-reducing SDS-PAGE may be more vulnerably disrupted by reducing agents in tissue lysates than in cell line lysates for unclear reasons. For example, almost all PKD2 oligomers were reduced into monomers with addition of reducing agents in human kidney tissues, but the effect of reducing agents were only moderate in cell lines *(33)*. In the case of PKD2L1, previous studies by other groups have reported the presence of PKD2L1 homooligomers through its C-terminal peptide-peptide interactions, e.g., through CC2 trimerization *(21)* and PKD2L1/PKD1L3 heterooligomerization at 3:1 stoichiometry through peptide-peptide interaction *(25)*. Together with our current data on its C-terminal C1 trimerization, we think that part of PKD2L1 oligomers detected with non-reducing SDS-PAGE using tissue lysates should be mediated by peptide-peptide interactions, possibly the C1-C1 interaction, and reduced to monomers by reducing agents.

TRPC, TRPM and TRPN channels were found to contain a conserved intracellular TRP domain downstream of TM6, which is similarly located as C1. This TRP domain was proposed to participate in subunit assembly and/or allosteric modulation of channel gating *(34)*. Interestingly, the recently resolved TRPV1 structure

showed that charged side chains within the TRP domain interact with pre-S1 helix in the N-terminus through hydrogen bonding and salt bridging *(35)*. It is possible that C1 shares some functional similarities and plays corresponding roles in PKD2L1. For example, in addition to its trimerization role, it seemed to regulate PKD2L1 dimerization formed by PKD2L1 NT (see Figure 3-2 F). Future studies will need to address this by providing more direct evidence.

We wondered why PKD2L1 needs two distinct trimerization domains in CT of PKD2L1. PKD2L1 channel is activated by Ca^{2+} followed by channel inactivation, presumably through an increase in the intracellular Ca^{2+} concentration *(8)*, but it remains unclear whether Ca^{2+} regulates PKD2L1 channel activity through direct binding. CT contains a Ca^{2+}-binding EF hand motif (E637-L665) that negatively regulates the ability of PKD2L1 channel to be activated by Ca^{2+}, suggesting that Ca^{2+} binds to this domain to prevent the channel from over-activation *(24)*. Direct binding of Ca^{2+} to CT was indeed reported *(23)* although it remains unknown whether and how this binding is relevant to channel function. At least, this same study showed that Ca^{2+} binding is not affected by mutations of 6 residues to alanine within CC2, suggesting that CC2 is not involved in Ca^{2+} binding. More importantly, our previous and current studies both demonstrated that CC2 is not important for PKD2L1 channel function. Although arguably, CC2 was found to be important for surface expression of PKD2L1 and complex PKD2L1/PKD1L3 in *Xenopus* oocytes *(21)* whether it promotes the trafficking to, or prevents the retrieval from, the surface membrane remains unknown. In contrast, although C1 did not seem to affect the PKD2L1 surface membrane expression (Figure 3-4 E) it is critical for the channel function. It is possible that nature

chooses to have two trimerization domains that together ensure proper surface membrane configuration and stability, as well as channel function.

Members of the TRP superfamily including PKD2 and PKD2L1 are assumed to assemble into homo- and/or hetero-tetramers with either a PKD1 homologue or another TRP protein, but the molecular mechanisms underlying these assemblies are still unclear. Like PKD2L1, the PKD2 C-terminus was found to form trimers *(20;22)*. The trimerization of the PKD2 or PKD2L1 C-termini seems to nicely explain the tetrameric organization of the PKD2/PKD1 or PKD2L1/PKD1L3 complex with a trimer/monomer assembly *(20;21)*. Based on our current data we propose that a functional PKD2L1 homotetramer can be formed either through C-terminal trimerization followed by N-terminal dimerization of a fourth subunit with a subunit in the trimer or through dimerization followed by trimerization (see model in Figure 3-7). Thus, we think that, under physiological conditions, depending on the availability of a co-localized PKD1 homologue, PKD2L1 forms homo- or heterotetramers by a shared way, namely, homotrimerization of PKD2L1 and heterodimerization of PKD2L1-PKD1 homologue (Figure 3-7). We should however bear in mind that interaction forces involved in the organization of TMs for a pore forming architecture are important as well although they are not discussed here.

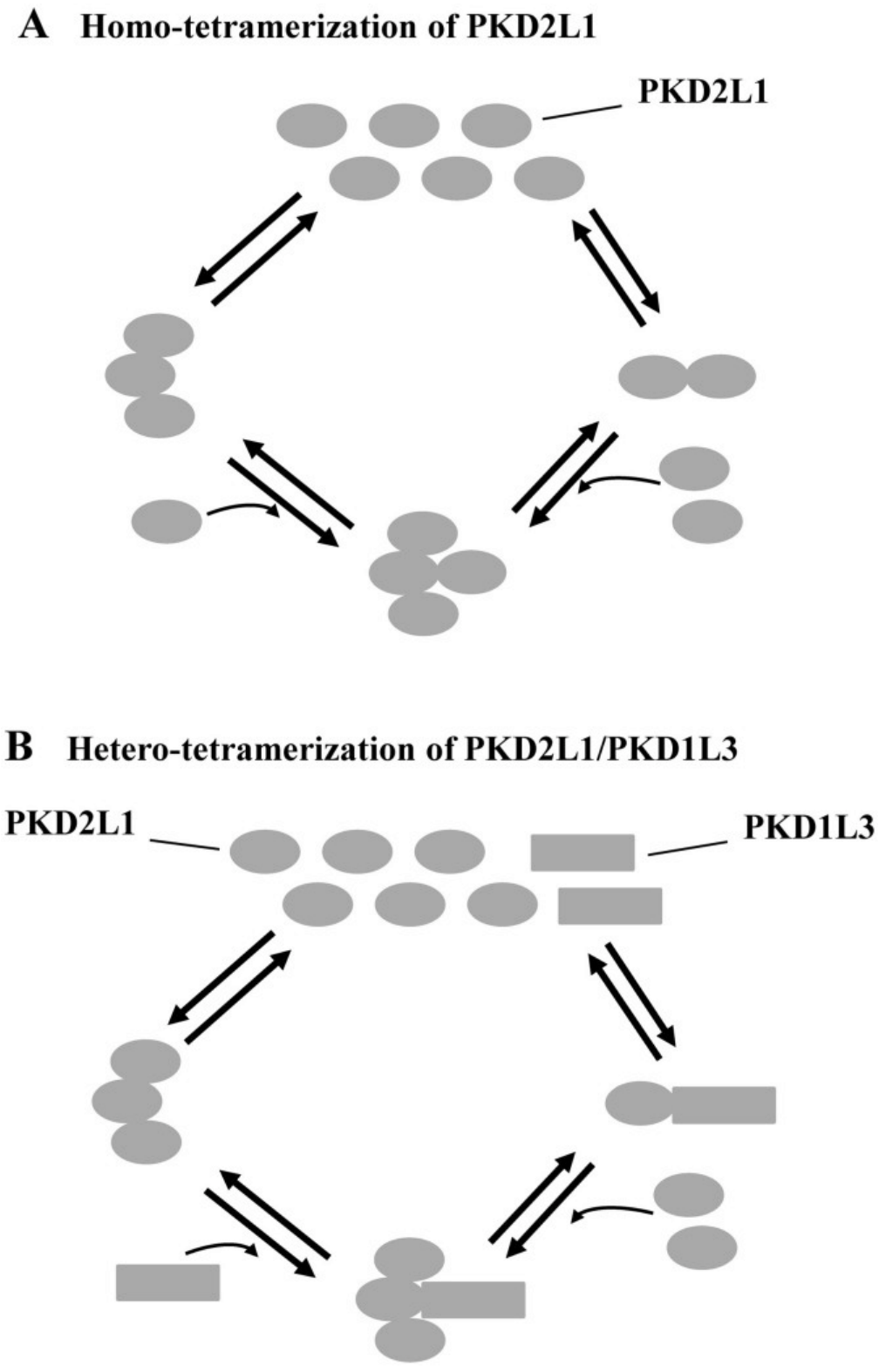

Figure 3-7 Model illustrating how a PKD2L1 homo- or heterotetramerer can be formed. (**A**) A PKD2L1 (oval) homotetramer can be formed either through first homotrimerization

followed by recruitment of a fourth subunit to the trimer by dimerization or through first homodimerization followed by recruitment of two subunits to form a trimer with a subunit in the dimer. Of note, 1) the illustration is only to indicate trimeric and dimeric binding and does not intend to show how the pore region is organized; and 2) the drawn trimer does not intend to mean that there are two points of contact. (**B**) A PKD2L1 heterotetramer can be formed with a PKD1 homologue (square), eg, PKD1L3 or PKD1L1, through first trimerization of PKD2L1 and then recruitment of a PKD1 homologue, or reversely, through first heterodimerization between PKD2L1 and a PKD1 homologue, followed by the recruitment of two PKD2L1 subunits to form a trimer with the existing PKD2L1 subunit.

It is noted that such a 3 + 1 assembly protocol for forming homo- and heterotetramers has been reported for other channels. For example, the cytoplasmic C-terminal leucine zipper domain (G488-Y526) of small conductance voltage-gated Ca^{2+}-activated K^+ channel (SK_{Ca}) forms trimers, as shown by crystallographic analyses *(36)* while the functional full-length SK_{Ca} channel forms homotetramers *(37)*. Similarly, a C-terminal domain (R583-D611) of voltage-gated K^+ channel $K_v7.1$ was shown to trimerize but the full-length channel forms tetramers *(38)*. Under physiological conditions, cyclic-nucleotide-gated channels are more likely heterotetramers consisting of the A and B subtypes with the A-trimer:B-monomer assembly when both are present. In cells over-expressing the A subtype, homotetramers were found *(39-41)*. Therefore, PKD2L1 as a TRP superfamily member may possess a strategy of oligomeric assembly that is shared by other families of ion channel.

In summary, our study has found that endogenous PKD2L1 in mouse tissues exhibits oligomeric states including dimers, trimers and tetramers. We identified a novel PKD2L1 C-terminal C1 domain that is associated with stronger trimerization than the previously reported CC2 domain. Importantly, C1 represents the first oligomerization domain critical for PKD2L1 channel function. We thus propose that functional PKD2L1 channel assembly involves both trimerization and dimerization, a mechanism possibly shared by some non-TRP types of ion channel.

3.5 REFERENCES

1. Tan Y. C., Blumenfeld J. and Rennert H. (2011) Autosomal dominant polycystic kidney disease: genetics, mutations and microRNAs. *Biochim. Biophys. Acta. 1812,* 1202–1212.

2. Wilson P. D. (2004) Polycystic kidney disease. N. Engl. J. Med. 350, 151–164.

3. Montell C. (2005) The TRP superfamily of cation channels. Sci. STKE.2005, re3.

4. Eijkelkamp N., Quick K. and Wood J. N. (2013) Transient receptor potential channels and mechanosensation. Annu. Rev. Neurosci. 36, 519–546.

5. Wu L. J., Sweet T. B. and Clapham D. E. (2010) International Union of Basic and Clinical Pharmacology. LXXVI. Current progress in the mammalian TRP ion channel family. Pharmacol. Rev. 62, 381–404.

6. Owsianik G., D'hoedt D., Voets T. and Nilius B. (2006) Structure-function relationship of the TRP channel superfamily. Rev. Physiol Biochem. Pharmacol. 156, 61–90.

7. Venkatachalam K. and Montell C. (2007) TRP channels. Annu. Rev. Biochem. 76, 387–417.

8. Chen, X. Z., Vassilev, P. M., Basora, N., Peng, J. B., Nomura, H., Segal, Y., Brown, E. M., Reeders, S. T., Hediger, M. A., and Zhou, J. (1999) Polycystin-L is a calcium-regulated cation channel permeable to calcium ions, Nature 401, 383-386.

9. Yang, J., Wang, Q., Zheng, W., Tuli, J., Li, Q., Wu, Y., Hussein, S., Dai, X. Q., Shafiei, S., Li, X. G., Shen, P. Y., Tu, J. C., and Chen, X. Z. (2012) Receptor for activated C kinase 1 (RACK1) inhibits function of transient receptor potential (TRP)-type channel Pkd2L1 through physical interaction, *J. Biol. Chem. 287*, 6551-6561.

10. DeCaen P. G., Delling M., Vien T. N. and Clapham D. E. (2013) Direct recording and molecular identification of the calcium channel of primary cilia. *Nature 504*, 315–318.

11. Delling M., DeCaen P. G., Doerner J. F., Febvay S. and Clapham D. E.(2013) Primary cilia are specialized calcium signalling organelles. *Nature 504*, 311–314.

12. Shimizu T., Janssens A., Voets T. and Nilius B.(2009) Regulation of the murine TRPP3 channel by voltage, pH, and changes in cell volume. *Pflugers Arch. 457*, 795–807.

13. Huang, A. L., Chen, X., Hoon, M. A., Chandrashekar, J., Guo, W., Trankner, D., Ryba, N. J., and Zuker, C. S. (2006) The cells and logic for mammalian sour taste detection, *Nature 442*, 934-938.

14. Horio, N., Yoshida, R., Yasumatsu, K., Yanagawa, Y., Ishimaru, Y., Matsunami, H., and Ninomiya, Y. (2011) Sour taste responses in mice lacking PKD channels, *PLoS. One. 6*, e20007.

15. Inada, H., Kawabata, F., Ishimaru, Y., Fushiki, T., Matsunami, H., and Tominaga, M. (2008) Off-response property of an acid-activated cation channel complex PKD1L3-PKD2L1, *EMBO Rep. 9*, 690-697.

16. Nauli S. M. Alenghat F.J., Luo Y., Williams E., Vassilev P., Li X., Elia A.E., Lu W., Brown E.M., Quinn S.J., Ingber D.E.and Zhou J.(2003) Polycystins 1 and 2 mediate mechanosensation in the primary cilium of kidney cells. *Nat. Genet. 33*, 129–137.

17. Murakami, M., Ohba, T., Xu, F., Shida, S., Satoh, E., Ono, K., Miyoshi, I., Watanabe, H., Ito, H., and Iijima, T. (2005) Genomic organization and functional analysis of murine PKD2L1, *J. Biol. Chem. 280*, 5626-5635.

18. Ishimaru, Y., Inada, H., Kubota, M., Zhuang, H., Tominaga, M., and Matsunami, H. (2006) Transient receptor potential family members PKD1L3 and PKD2L1 form a candidate sour taste receptor, *Proc. Natl. Acad. Sci. U. S. A 103*, 12569-12574.

19. Nelson, T. M., Lopezjimenez, N. D., Tessarollo, L., Inoue, M., Bachmanov, A. A., and Sullivan, S. L. (2010) Taste function in mice with a targeted mutation of the pkd1l3 gene, *Chem. Senses 35*, 565-577.

20. Yu Y.Ulbrich M.H., Li M.H., Buraei Z., Chen X.Z., Ong A.C., Tong L., Isacoff E.Y. andYang J.(2009) Structural and molecular basis of the assembly of the TRPP2/PKD1 complex. *Proc. Natl. Acad. Sci. U. S. A. 106*, 11558–11563.

21. Yu Y.Ulbrich M.H., Li M.H., Dobbins S., Zhang W.K., Tong L., Isacoff E.Y.andYang J.(2012) Molecular mechanism of the assembly of an acid-sensing receptor ion channel complex. *Nat. Commun. 3*, 1252.

22. Molland K. L., Narayanan A., Burgner J. W. and Yernool D. A. (2010)Identification of the structural motif responsible for trimeric assembly of the C-terminal regulatory domains of polycystin channels PKD2L1 and PKD2. *Biochem. J. 429*, 171–183.

23. Molland K. L., Paul L. N. and Yernool D. A.(2012)Crystal structure and characterization of coiled-coil domain of the transient receptor potential channel PKD2L1. *Biochim. Biophys. Acta. 1824*, 413–421.

24. Li Q., Liu Y., Zhao W. and Chen X. Z. (2002) The calcium-binding EF-hand in polycystin-L is not a domain for channel activation and ensuing inactivation. *FEBS Lett. 516*, 270–278.

25. Ishimaru, Y., Katano, Y., Yamamoto, K., Akiba, M., Misaka, T., Roberts, R. W., Asakura, T., Matsunami, H., and Abe, K. (2010) Interaction between PKD1L3 and PKD2L1 through their transmembrane domains is required for localization of PKD2L1 at taste pores in taste cells of circumvallate and foliate papillae, *FASEB J. 24*, 4058-4067.

26. Feng S., Okenka G.M., Bai C.X., Streets A.J., Newby L.J., DeChant B.T., Tsiokas L., Obara T.and Ong A.C.(2008) Identification and functional characterization of an N-terminal oligomerization domain for polycystin-2. *J. Biol. Chem. 283*, 28471–28479.

27. Feng S., Rodat-Despoix L., Delmas P. and Ong A. C.(2011) A single amino acid residue constitutes the third dimerization domain essential for the assembly and function of the tetrameric polycystin-2 (TRPP2) channel. *J. Biol. Chem. 286*, 18994–19000.

28. Giudici A. M. Molina M.L., Ayala J.L., Montoya E., Renart M.L., Fernández A.M., Encinar J.A., Ferrer-Montiel A.V., Poveda J.A.and González-Ros J.M.(2013) Detergent-labile, supramolecular assemblies of KcsA: relative abundance and interactions involved. *Biochim. Biophys. Acta. 1828*, 193–200.

29. Raja M. (2011) The potassium channel KcsA: a model protein in studying membrane protein oligomerization and stability of oligomeric assembly? *Arch. Biochem. Biophys. 510*, 1–10.

30. Milligan G.(2004) G protein-coupled receptor dimerization: function and ligand pharmacology. *Mol. Pharmacol. 66*, 1–7.

31. Thevenin D., Lazarova T., Roberts M. F. and Robinson C. R.(2005) Oligomerization of the fifth transmembrane domain from the adenosine A2A receptor. *Protein Sci. 14*, 2177–2186.

32. Faggiano S., Ronda L., Bruno S., Jankevics H. and Mozzarelli A.(2010) Polymerized and polyethylene glycol-conjugated hemoglobins: a globin-based calibration curve for dynamic light scattering analysis. *Anal. Biochem. 401*, 266–270.

33. Newby L. J., Streets A.J., Zhao Y., Harris P.C., Ward C.J. and Ong A.C.(2002) Identification, characterization, and localization of a novel kidney polycystin-1-polycystin-2 complex. *J. Biol. Chem. 277*, 20763–20773.

34. Latorre R., Zaelzer C. and Brauchi S.(2009) Structure-functional intimacies of transient receptor potential channels. *Q. Rev. Biophys. 42*, 201–246.

35. Liao M., Cao E., Julius D. and Cheng Y.(2013) Structure of the TRPV1 ion channel determined by electron cryo-microscopy. *Nature 504*, 107–112.

36. Kim J. Y., Kim M. K., Kang G. B., Park C. S. and Eom S. H.(2008) Crystal structure of the leucine zipper domain of small-conductance Ca^{2+}-activated K^{+} (SK(Ca)) channel from *Rattus norvegicus*. Proteins 70, 568–571.

37. MacKinnon R.(1991) Determination of the subunit stoichiometry of a voltage-activated potassium channel. *Nature 350*, 232–235.

38. Xu Q. and Minor D. L. Jr (2009) Crystal structure of a trimeric form of the K(V)7.1 (KCNQ1) A-domain tail coiled-coil reveals structural plasticity and context dependent changes in a putative coiled-coil trimerization motif. *Protein Sci. 18*, 2100–2114.

39. Matulef K. and Zagotta W. N.(2003) Cyclic nucleotide-gated ion channels. *Annu. Rev. Cell Dev. Biol. 19*, 23–44.

40. Zheng J., Trudeau M. C. and Zagotta W. N.(2002) Rod cyclic nucleotide-gated channels have a stoichiometry of three CNGA1 subunits and one CNGB1 subunit. *Neuron 36*, 891–896.

41. Zhong H., Molday L. L., Molday R. S. and Yau K. W.(2002) The heteromeric cyclic nucleotide-gated channel adopts a 3A:1B stoichiometry. *Nature 420*, 193–198.

42. Li, Q., Dai, X. Q., Shen, P. Y., Wu, Y., Long, W., Chen, C. X., Hussain, Z., Wang, S., and Chen, X. Z. (2007) Direct binding of alpha-actinin enhances TRPP3 channel activity, *J. Neurochem. 103*, 2391-2400.

43. Karey K. P. and Sirbasku D. A.(1989) Glutaraldehyde fixation increases retention of low molecular weight proteins (growth factors) transferred to nylon membranes for western blot analysis. *Anal. Biochem. 178*, 255–259.

44. Imam M., Singh S., Kaushik N. K. and Chauhan V. S.(2014) Plasmodium falciparum merozoite surface protein 3: oligomerization, self-assembly, and heme complex formation. *J. Biol. Chem. 289*, 3856–3868.

CHAPTER 4

4. RESULT #3 PKD2L1 is downstream of a phospholipase C pathway with a PKC-dependent inactivation mechanism

4.1 INTRODUCTION

The interest in studying the membrane lipid environment, downstream lipid messengers and their effect on ion channels regulation has emerged since late 1990s *(1-3)*. One major pathway that dynamically alters the membrane phospholipid composition and subsequently controls the function of many membrane ion channels and proteins is the phospholipase C (PLC) pathway. PLC enzymes have ubiquitous expression and a shared role in hydrolyzing the quantitatively minor membrane phospholipid phosphoinositide (4,5) biphosphate (PIP2) into the membrane bound DAG and the cytosolic inositol (1,4,5) triphosphate (IP3) *(4)*. Direct interaction between membrane phospholipids and ion channels has been reported to modulate channel functions, as the case for potassium channels *(5)*, and contribute to some channelopathies *(6)*. In addition to direct interactions, PLC activates downstream signalling kinases and triggers Ca^{2+} releases from the intracellular stores through IP3 receptors. Both the activation of kinases and increase in the intracellular Ca^{2+} level are important factors that further regulate ion channels *(7;8)*.

Transient receptor potential (TRP) superfamily is comprised of seven subfamilies of integral membrane ion channel proteins that are key determinants of many human senses and diseases *(9-13)*. TRP channels, akin to other ion channels, have been known for their interaction and regulation by phosphoinositides *(1-3;14-16)*. TRPC subfamily members represent nice examples of TRP channels modulated by diacylglycerols (DAGs) and subsequent protein kinase C (PKC) activation *(17-20)*. TRPC3, -5, -6 and -7 have been shown to be activated by PLC-mediated mechanisms *(18;20)* with the downstream activation of PKC inactivating TRPC3, -4 and -5 *(20)*.

Variations within the TRP superfamily, in regards to the effect of lipid messengers and kinase activation, are evident. Even among members of the same subfamily, different lipid messengers exert different effects. For example, while DAG activated TRPC3 in a PKC-independent manner, TRPC4 and -5 were inactivated by the elevation of DAG levels with the DAG associated activation of PKC *(20)*. Regulation of TRPV1 by lipids, especially its regulation by PIP2 and PI4P, is another controversial debate that has been reviewed recently. Some literature showed an inhibitory effect of PIP2 on TRPV1, while others showed it as a stimulatory factor. With a closer look, work using excised inside-out patches and lipid phosphatases determined that PIP2 and PI4P stimulatory effect has more support *(21)*.

One possible protein modification upon the activation of PLC pathway is phosphorylation. Phosphorylation is an important reversible posttranslational modification that regulates the function of the cellular protein repertoire. *Drosophila* eye specific PKC (ePKC) mutants were found to affect the photoreceptor deactivation *(22)*. Later, the *Drosophila* TRP (dTRP) was found to be phosphorylated by ePKC and such phosphorylation is part of the negative feedback mechanism that regulates Ca^{2+} influx *(23)*. However, dTRP phosphorylation mechanism is complicated and governed by several kinases and phosphatases *(8)*, and represents an example for complex regulation of TRP channels. Roles of phosphorylation in the regulation of TRPV1 channel was extensively studied and reviewed by Bevan *et al. (24)*. dTRP and TRPV1 phosphorylation studies indicated that there are multiple phosphorylation sites that control the channel function, but rather it is a coordinated simultaneous process that regulate the channel function, trafficking and sensitization/desensitization processes.

PKD2L1 is a TRP-type non-selective cation channel that is activated by Ca^{2+} and acid when expressed in *Xenopus* oocytes *(25;26)*, acquires an outwardly rectifying current in HEK and primary cilia *(27)*, and is activated by acid in the cerebrospinal fluid contacting neurons (CSF-cNs) and taste receptor cells *(28-30)*. PKD2L1 function is modulated by large cations *(31;32)*, amiloride and analogs *(33)*, and calmodulin agonists *(27)*. Besides, a number of PKD2L1 protein partners have been identified as important regulators of its function including, PKD1L3 *(26;29;34)*, PKD1L1 *(27)*, troponin I *(35)*, α-actinin *(36)* and receptor for activated C kinase 1 (RACK1) *(37)*. PKD2L1 has been shown to be modulated by pH, osmolarity, voltage and alkalization *(38;39)*. In addition, PKD2L1, in complex with PKD1L3, has been recently proposed as an alkali activated channel *(40)*. Moreover, we and others determined that PKD2L1 possesses a Ca^{2+}-dependent inactivation mechanism *(40)*.

From the above, PKD2L1 involvement in sour tasting and Ca^{2+} regulation is evident but the activation/inactivation mechanism remains largely unclear despite the known involvement of Ca^{2+} *(40)*, calmodulin *(27)* and the C-terminal domain *(41;42)*. Our previous work showed the involvement of RACK1 and intracellular Ca^{2+} in PKD2L1 functional regulation; these observations pointed to possible roles of PLC pathway and PKC in PKD2L1 channel sensitization and inactivation. Indeed, here we show that PKD2L1 activation/inactivation is downstream of the PLC activation pathway, with the involvement of a PKC-dependent inactivation mechanism.

4.2 MATERIALS AND METHODS

4.2.1 Materials

U73122 (PLC inhibitor), m-3M3FBS (PLC activator) and GF 109203x (PKC blocker) were obtained from Sigma (Sigma-Aldrich, Oakville, ON, Canada). Stock solutions were made in DMSO and stored at RT. Dilutions to the working concentrations were made fresh before each experiment. Phorbol 12-myristate 13-acetate (PMA, PKC activator) and 4α-Phorbol 12,13-didecanoate (4αPDD, PMA inactive analog) were purchased from Tocris Bioscience (Tocris Bioscience, Bristol, UK). Stock solutions of these compounds were made in DMSO, aliquoted, stored at -20 ºC, thawed and diluted to the working concentrations just before the experiment. Heparin sodium salt (Fisher Scientific, Toronto, ON, Canada) was dissolved in water (20 μg/ml) for injections.

4.2.2 Preparation of *PKD2L1* plasmid constructs

Human *PKD2L1* gene was cloned as previously described *(37)*. Mutations of threonine, serine and tyrosine residues to the neutral or negatively charged residues alanine or aspartic acid were performed using QuikChange Lightning site-directed mutagenesis kit (Agilent Technologies, La Jolla, CA, USA). Primer design and procedure was performed following the manufacturer's protocol.

4.2.3 mRNA preparation and micro-injection into *Xenopus laevis* oocytes

Plasmids pCHGF harbouring wild type (WT) or a mutant PKD2L1 cDNA were linearized with *Mlu I*, followed by phenol/chloroform purification and ethanol precipitation. Linearized plasmids were used to in vitro synthesize capped mRNAs

using the T7 mMessage mMachineTM kit (Ambion, Austin, TX, USA). Stage V-VI oocytes were isolated from *Xenopus laevis* under an approved institutional protocol. Defolliculation of oocytes was performed through incubation in Barth's solution *(37)* containing Type 2 collagenase (2 mg/mL) (Worthington, Lakewood, NJ, USA) at room temperature (RT) for 1.5 hours (hr). Oocytes were then incubated at 16-18 ºC in Barth's solution supplemented with 1% antibiotics (penicillin/streptomycin) (GIBCO™, Life Technologies, Burlington, ON, Canada) for at least 3 hr before injection of 50 nL H_2O containing 25-50 ng mRNAs or as stated in the experiment. An equal volume of H_2O was injected into control oocytes. Injected oocytes were incubated at 16-18 ºC in Barth's solution, for 2-4 days prior to experiments. For intracellular IP3 antagonist studies, oocytes were injected with 50 nL of 20 μg/ml to allow a final intracellular concentration of ~1 μg/ml prior to recordings.

4.2.4 Immunofluorescence

Xenopus oocytes were washed in PBS, fixed in 3% paraformaldehyde (PFA) for 15 min, and washed 3 times in PBS plus 50 mM NH_4Cl, and then permeabilized with 0.1% Triton X-100 for 4 min. Oocytes were then washed 3 times in PBS for 5 min each time, blocked in 3% skim milk in PBS for 30 min, and then incubated overnight with the PKD2L1 polyclonal antibody. This was followed by 3 times 10 min washes in PBS. The oocytes were then incubated with a secondary AlexaFluor 488-conjugated donkey anti-rabbit antibody (Jackson ImmunoResearch Laboratories, West Grove, PA, USA) for 30 min, followed by 3 times washes in PBS and mounting in Vectashield (Vector labs, Burlington, ON, Canada). The slides were examined on an AIVI spinning disc

confocal microscopy (Cell Imaging Facility, Faculty of Medicine and Dentistry, University of Alberta).

4.2.5 Electrophysiology

Current and voltage signals were measured with the conventional two microelectrode voltage clamp (TMVC) technique with a commercial amplifier (TEV-200A, Dagan, Minneapolis MN, USA). Electrodes were fabricated from borosilicate glass (Warner Instruments, Hamden CT, USA) by a micropipette puller (P-87, Sutter Instruments, Novato, CA, USA) and filled with 3 M KCl with typical tip resistance of 0.5-3 MΩ. Digidata 1320A converter and pClamp 9.2 (Axon Instruments, Union City, CA, USA) were used for data acquisition and analysis, respectively. In experiments using a ramp or gapfree protocol *(25)*, current/voltage signals were digitized at 200 ms/sample. Recorded tracings were then analyzed using pClamp 9.2 and plotted using SigmaPlot 12 (Systat Software, San Jose, CA, USA). Absolute amplitudes of channel activity were collected and normalized to the average activity of PKD2L1 wild-type obtained under the same day, condition and group. Normalized values were then expressed as a percentage value and plotted using SigmaPlot 12.

4.2.6 Statistical Analysis

Data were presented as mean ± standard error of the mean (SEM). All data were collected from at least two different experiments. Student's t-test was used to compare two groups of data for statistical significance indicated by a p value. P values of less than 0.05 and 0.01 were considered significant and very significant, respectively.

4.3 RESULTS

4.3.1 PKD2L1 is activated downstream of phospholipase C activation pathway

Our hypothesis was that the initiation of PKD2L1 channel activity is through the activation of PLC. Activation of PLC will result in the production of DAG and IP3, and at the same time will momentarily decrease the level of PIP2 in the plasma membrane. IP3 will bind to IP3R and releases Ca^{2+} from the intracellular stores. An initial increase in intracellular Ca^{2+} contributes either directly or indirectly (through an unknown protein) to channel activation. Subsequent activation of PKC will follow as free Ca^{2+} levels continue to rise in the cytosol besides the availability of DAG. PKC can activate some lipid kinases that help restore PIP2 levels. In addition, PKC will potentially phosphorylate PKD2L1 and contribute to channel desensitization process (Figure 4-1 A). To investigate whether this hypothesis is correct, we proposed a number of activators (with red arrows) and blockers (with the black arrows) for the proposed PKD2L1 activation/inactivation pathway (Figure 4-1 B).

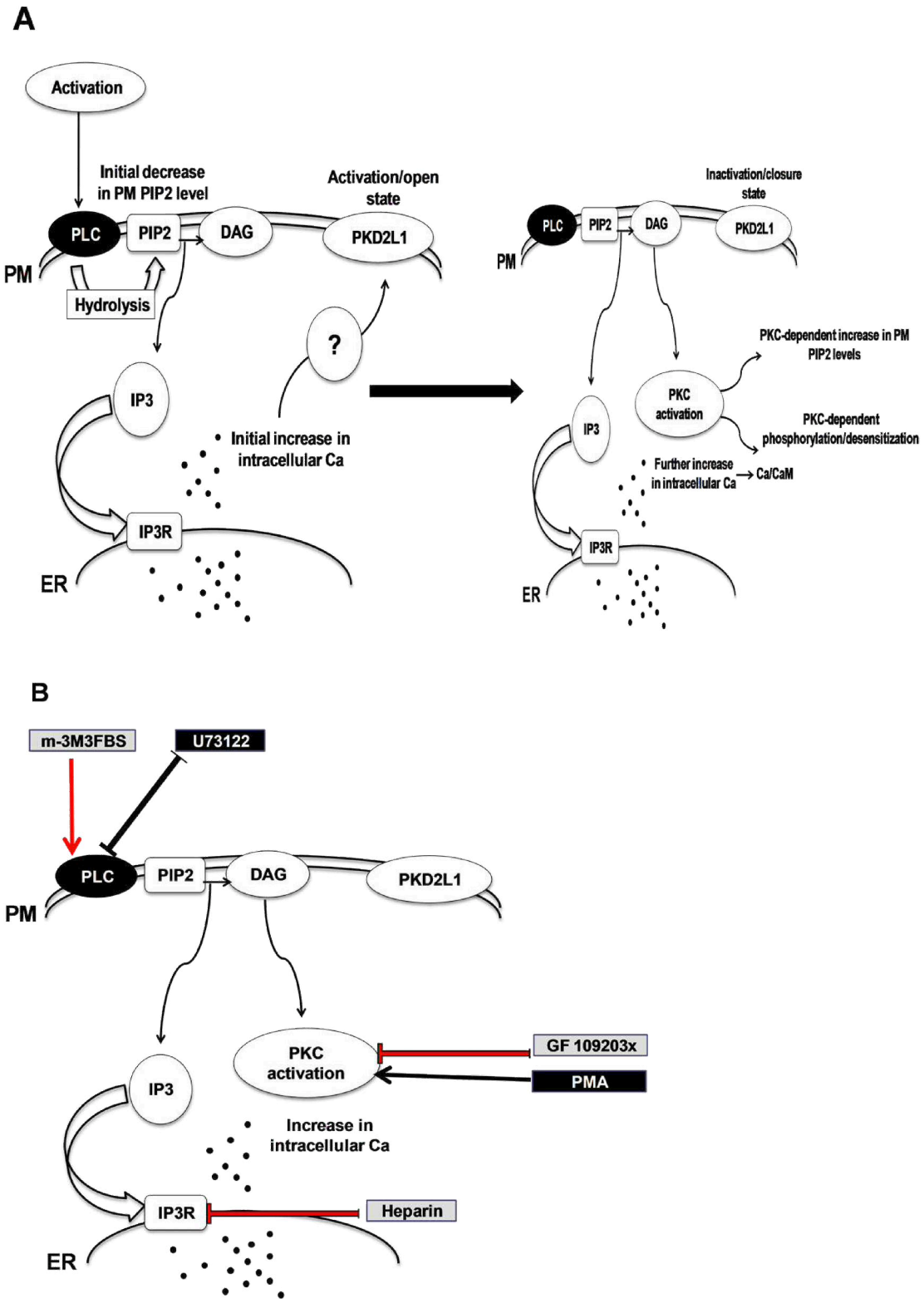

Figure 4-1 Proposed mechanism of PKD2L1 activation/inactivation process. (**A**) Schematic diagram to illustrate our hypothesis of the mechanism regulating PKD2L1. (**B**) Our

proposed PKD2L1 inhibitors (in black boxes and indicated by bold black lines) and PKD2L1 activators (in grey boxes and indicated by red bold lines) along the PLC signalling pathway and expected to be regulating PKD2L1 channel function.

Our first question was whether PKD2L1 is affected by the activation of PLC signalling pathway. To answer this question, we first tested the effect of the PLC activator m-3M3FBS on oocytes expressing PKD2L1. We found that the application of 10 μM m-3M3FBS in the perfusion solution stimulated channel activity in the presence of 1 mM Ca^{2+} but not in Ca^{2+} free environment (Figure 4-2 A and B). This was evident at different membrane potentials as indicated by the current-voltage relationship (Figure 4-2 C). The observed activity is specific to PKD2L1 and not to endogenous mediators as the H_2O-injected control oocytes did not show any response to the PLC activator either in the presence or absence of Ca^{2+} (Figure 4-2 D).

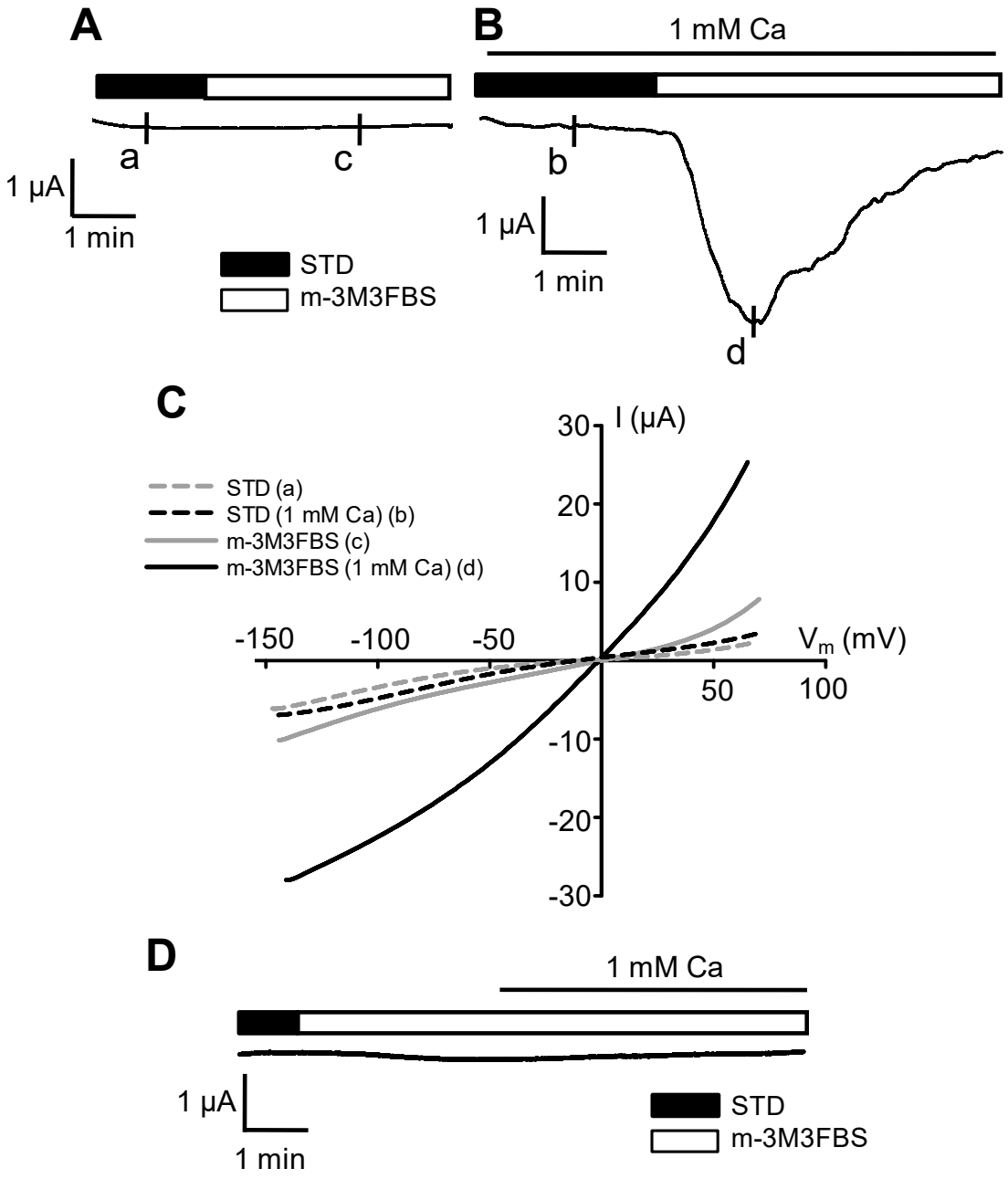

Figure 4-2 Effect of PLC activator m-3M3FBS on *Xenopus laevis* oocytes over-expressing human PKD2L1. (**A**), Representative currents recorded by TMVC at -50 mV from an oocyte expressing human PKD2L1 perfused with standard solution containing 10 µM m-3M3FBS PLC activator in the absence of Ca^{2+}. (**B**), Representative currents recorded by the TMVC at -50 mV from an oocyte expressing human PKD2L1 perfused with standard solution containing 10 µM m-3M3FBS PLC activator in the presence of 1 mM Ca^{2+}. (**C**), Representative current–voltage relationship curves obtained using a voltage ramp protocol generated at the time points

('a' - 'd') indicated in panels A and B. (**D**), Representative currents recorded by the TMVC at -50 mV from a H_2O-injected oocyte perfused with standard solution containing 10 μM m-3M3FBS PLC activator in both Ca^{2+} free and 1 mM Ca^{2+} conditions.

Next we wanted to provide further support for our hypothesis that PLC is involved in the mechanism regulating PKD2L1 channel function. We incubated PKD2L1-expressing oocytes in Barth's solution containing 10 μM of the PLC inhibitor U73122 for 30 min before testing the oocytes for the Ca^{2+}-induced on-responses. We found that PLC inhibition significantly reduced the Ca^{2+}-induced channel activity (Figure 4-3 A). PKD2L1 on-responses were reduced by an average 74.85 ± 23.24% compared to the on-response currents from non-treated oocytes ($p = 0.0002$, $N = 7\text{-}11$). In a paired experiment some of the oocytes showing high Ca^{2+} currents were allowed to recover after the Ca^{2+}-induced on response for 1 hr and 30 min then incubated with U73122 for 30 min. I-V curves collected from these oocytes confirmed the inhibitory effect of U73122 on PKD2L1 channel function (Figure 4-3 B).

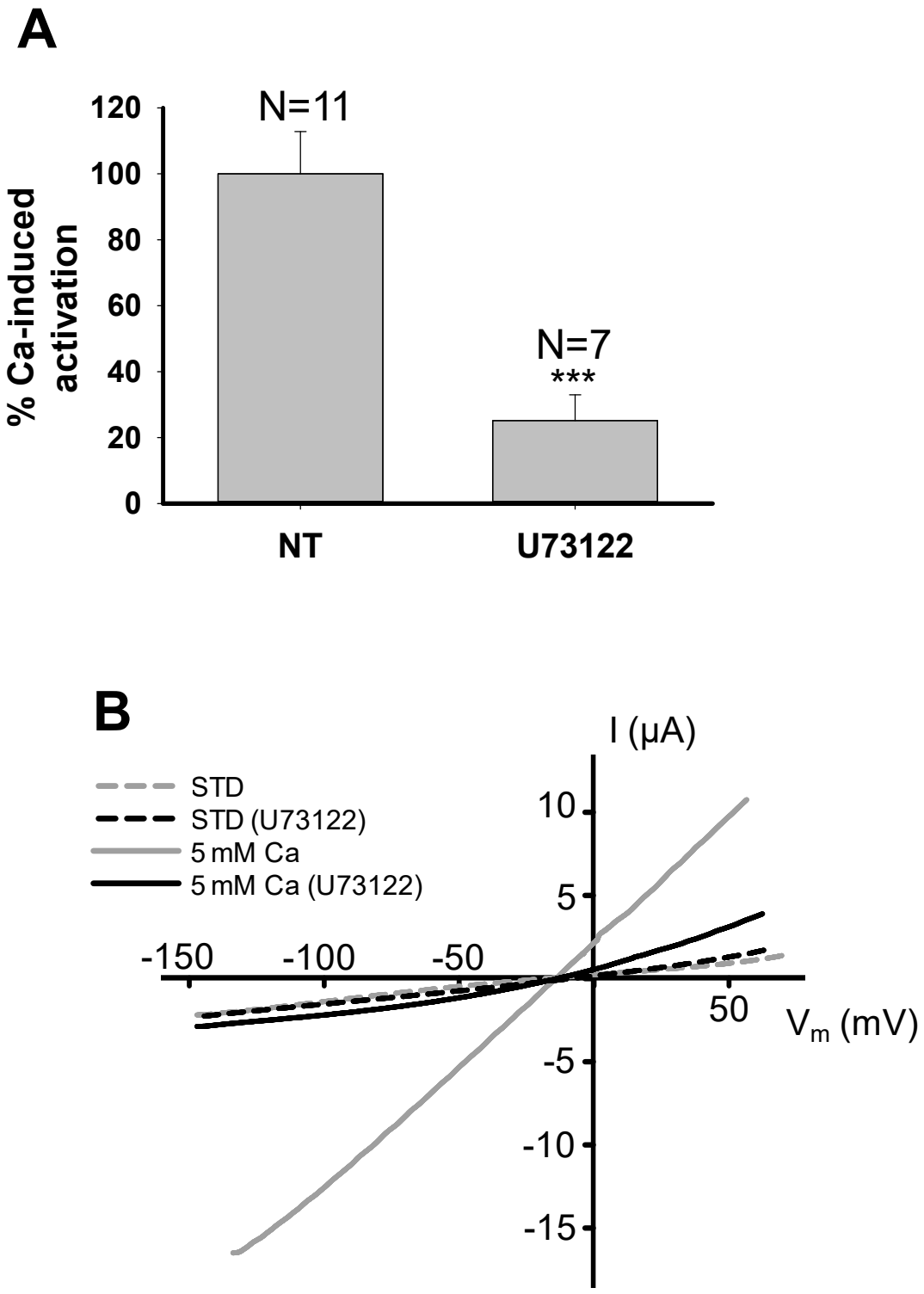

Figure 4-3 Effect of the PLC inhibitor U73122 on Ca^{2+}-induced current in PKD2L1-expressing oocytes. (**A**) Averaged and normalized PKD2L1 Ca^{2+}-induced currents elicited by extracellular 5 mM Ca^{2+} solution from oocytes non-treated (NT) and oocytes incubated with 10 μM U73122 for 30 min (U73122), voltage clamped at -50 mV. Shown Ca^{2+}-currents averaged

from different numbers of oocyte, as indicated. ***p = 0.0002, unpaired t-test. (**B**) Representative on-response I-V curves obtained using a ramp protocol under the same conditions as in panel **A**.

4.3.2 Phorbol esters inhibit PKD2L1 channel function through the activation of protein kinase C

As the activation of PLC pathway result in the formation of the key lipid messengers, DAG and IP3, we wanted to test whether both are involved in regulation of PKD2L1. The DAG analog, PMA had a significant inhibitory effect on PKD2L1 channel function ($p = 0.0006$, $N = 8$) when oocytes expressing the channel were incubated with 200 nM of this compound for 30 min before electrophysiological measurements (Figure 4-4 A). This inhibition was accompanied by a moderate decrease in PKD2L1 plasma membrane (PM) presence (Figure 4-4 B), however, this decrease cannot account for the 67.9 ± 9.7% decrease of the functional activity. Of note, the biologically inactive analog of PMA, 4αPDD, neither altered the channel function nor its PM density (Figure 4-4 A and B). We also tested the possible involvement of IP3 in PKD2L1 channel function by injecting the IP3R antagonist, heparin, which increased the channel function by 32.7 ± 3.2% ($p = 0.04$, $N = 16$) (Figure 4-4 C).

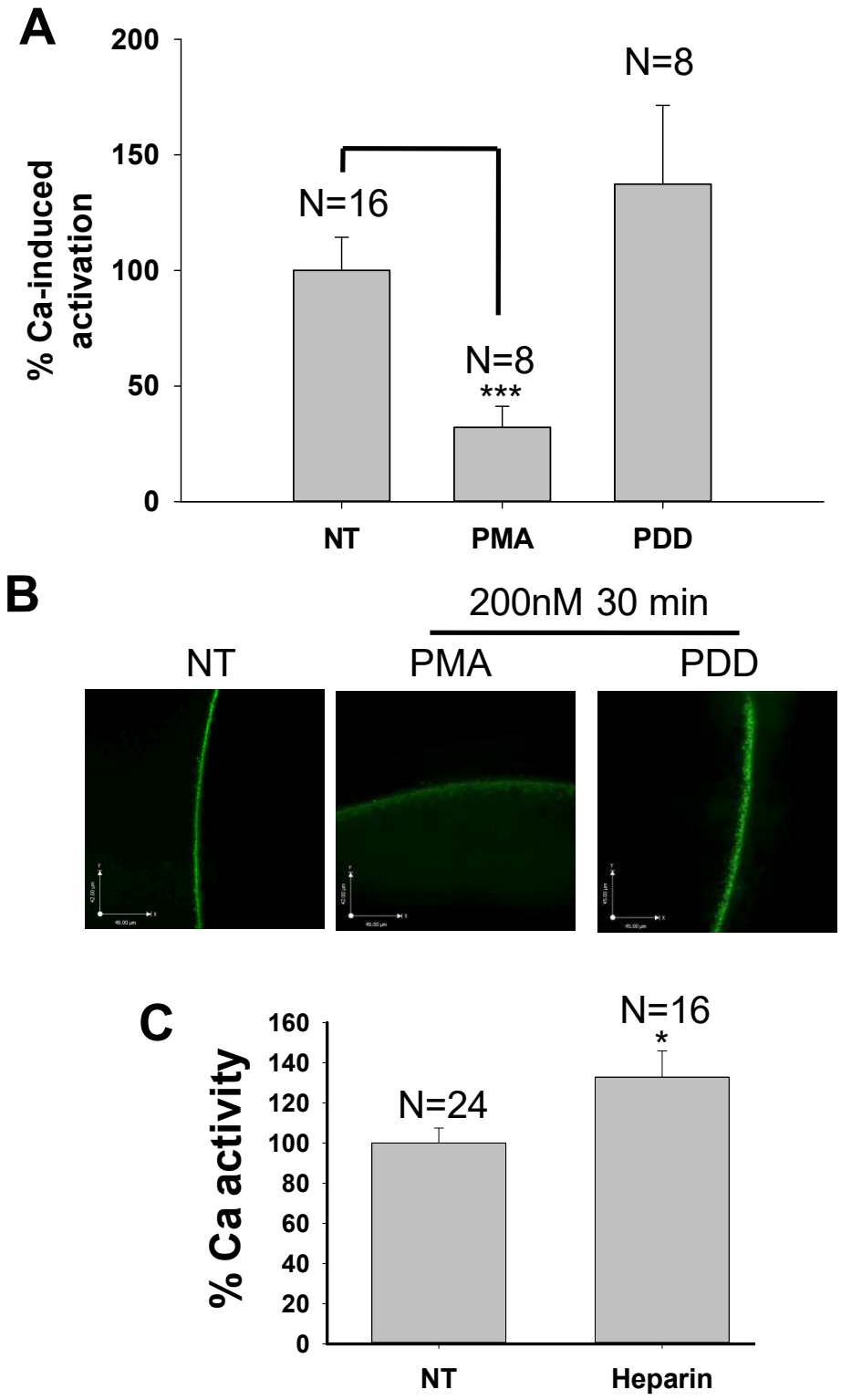

Figure 4-4 Effect of PMA on PKD2L1 Ca-induced channel function. (**A**)**,** Averaged and normalized PKD2L1 Ca^{2+}-induced currents elicited by extracellular 5 mM Ca^{2+} solution from

oocytes non-treated (NT) or oocytes incubated with 200 nM of either PMA or 4αPDD for 30 min, voltage clamped at -50 mV. Shown Ca^{2+}-currents averaged from different numbers of oocyte, as indicated. ***p = 0.0006, unpaired t-test. (**B**), Representative immunofluorescence data showing the PM intensity of PKD2L1 protein in oocytes under the same conditions as in panel **A**. (**C**), Averaged and normalized Ca^{2+}-induced on-response currents elicited by 5 mM Ca^{2+} in PKD2L1-expressing oocytes injected with the IP3 receptor antagonist, heparin, compared to PKD2L1-expressing H_2O-injected (NT) oocytes (*p = 0.04, unpaired t-test).

Whether or not the phorbol esters effect was mediated through the subsequent activation of PKC, this was our next question. To answer that question, we incubated PKD2L1 expressing oocytes with the PKC blocker, GF 109203x, either for 30 min at 500 nM or for 20 min at 1μM, and then we tested its Ca^{2+}-induced activity. Blocking PKC increased PKD2L1 Ca^{2+} currents as revealed by channel activity (Figure 4-5 A) as well as through I-V curves of the channel during Ca^{2+}-induced responses (Figure 4-5 B).

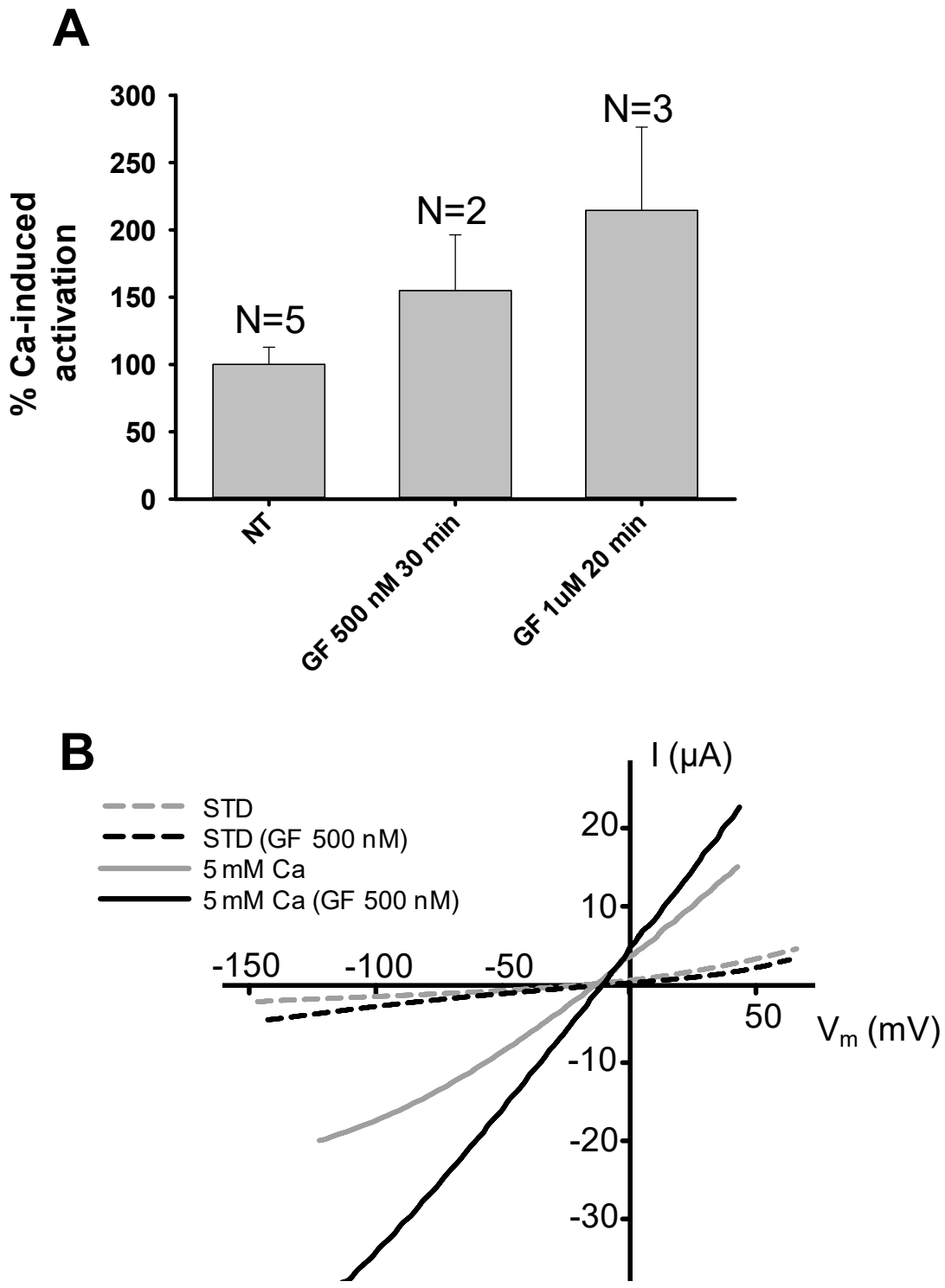

Figure 4-5 Effect of PKC blocker, GF 109203x incubation on PKD2L1 on-response. (**A**) Averaged and normalized PKD2L1 Ca^{2+}-induced currents elicited by extracellular 5 mM Ca^{2+} solution from oocytes non-treated (NT) and oocytes incubated with either 500 nM or 1 μM GF 109203x for 30 or 20 min, respectively. Oocytes were voltage clamped at -50 mV. Ca^{2+}-

currents averaged from different numbers of oocyte, as indicated. **B**, Representative on-response I-V curves obtained by a ramp protocol under the standard PKD2L1 Ca^{2+}-induced activation condition from a non-treated oocyte vs an oocyte incubated with 500 nM GF 109203x, PKC blocker, for 30 min.

We next scanned a number of potential phosphorylation sites as identified by KinasePhos 2.0 *(43)*. Interestingly, we found that threonine 338 when mutated to alanine the channel was no longer responsive to PMA-mediated inhibition (Figure 4-6 A) or PM reduced channel density (Figure 4-6 B). We also investigated the effect of mutating the other threonine and serine residues to alanine, including S333 and T591. These mutants were still responsive to PMA-mediated inhibition, with T591A mutation is characterized with surprisingly high Ca^{2+} current amplitude (data not shown).

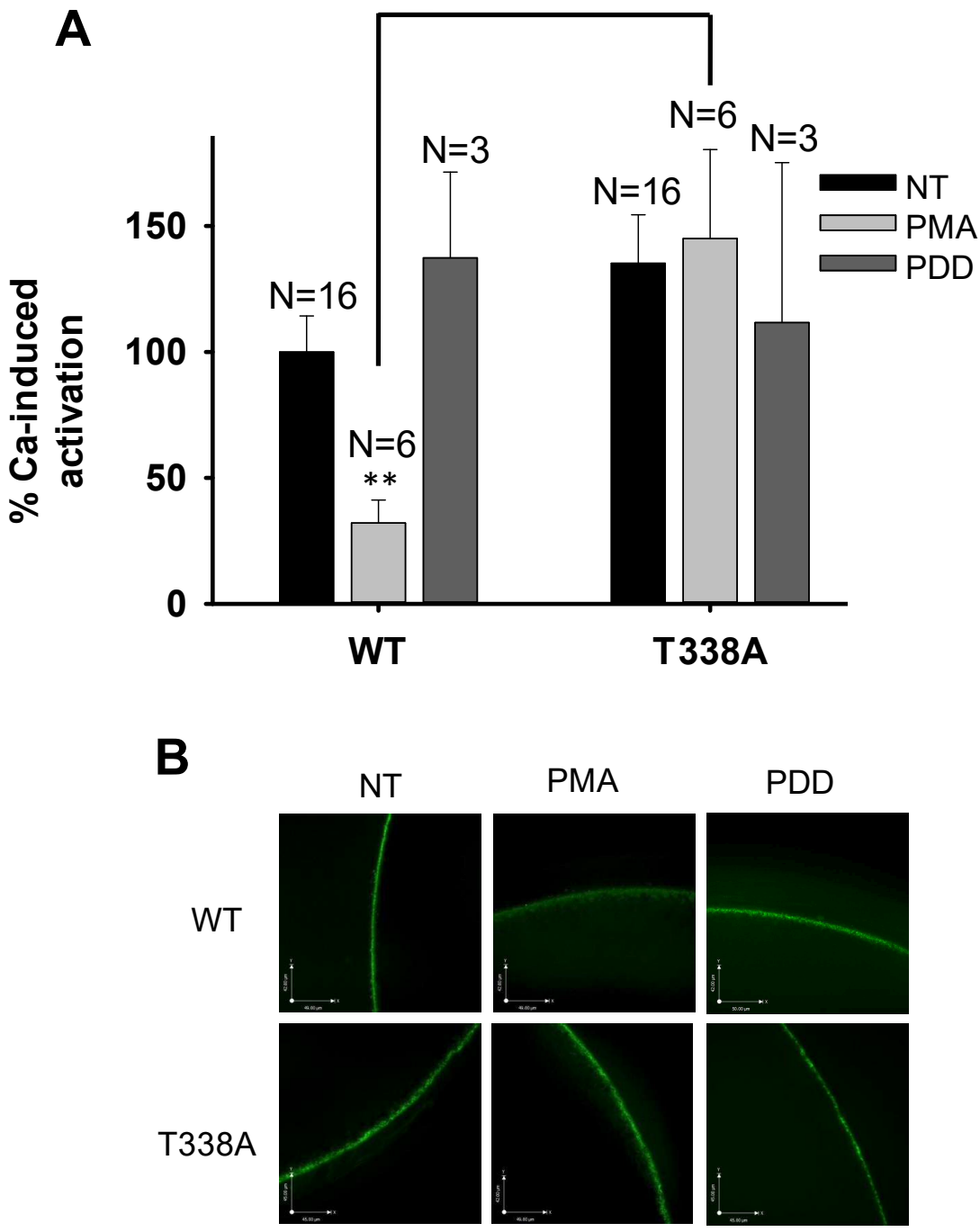

Figure 4-6 Effect of mutating PKD2L1 threonine 338 on PMA-mediated inhibiton of PKD2L1 Ca^{2+}-induced channel activation. (**A**), Averaged and normalized Ca^{2+}-induced currents elicited by extracellular 5 mM Ca^{2+} solution from oocytes expressing PKD2L1 or PKD2L1 T338A, non-treated (NT) or incubated with 200 nM of either PMA or 4αPDD for 30 min, voltage clamped at -50 mV. Shown Ca^{2+}-currents averaged from different numbers of oocyte, as indicated. **p = 0.01, unpaired t-test. (**B**), Representative immunofluorescence data

showing the PM intensity of PKD2L1 protein or its mutant PKD2L1 T338A in oocytes under the same conditions as in panel **A**.

4.4 DISCUSSION

Here we showed that PKD2L1 is activated downstream the activation of the PLC pathway. This regulation was accompanied by the involvement of DAG, PKC and IP3. We also identified one potential phosphorylation site, T338, within the first intracellular loop between the transmembrane domain 2 and 3, as a potential PKC regulatory sites. The involvement of IP3 and IP3 receptor is further supported by the work done by us *(25)* and others *(44;45)* highlighting the role of the increase in intracellular Ca^{2+} in regulating PKD2L1 channel function, both Ca^{2+}- and acid-induced.

PLC enzymes have a ubiquitous expression and their involvement in mediating the physiological effects of many extracellular stimuli is evident, including signalling in response to hormones, neurotransmitters and growth factors *(4)*. PLCβII is proved to mark type II taste receptor cells (TRCs) and regulate the taste responses in the bitter, sweet and umami tastes *(46;47)*. Although PKD2L1 is identified as the best sour taste receptor candidate responsible for 25% - 45% of tasting sour stimuli in mice *(48;49)*, the mechanism of its function and sour taste sensation is still poorly understood. PKD2L1 is expressed in murine type III TRCs *(47)* which possess a PLC-dependent Ca^{2+} signalling property *(50)*. Our results showing that PKD2L1 function is mediated through PLC pathway constitutes the first step towards understanding the mechanism underlying its function, including that related to the sense of tasting sour.

Of note, we previously showed that PKD2L1 channel on-response measured from *Xenopus* oocytes co-injected with 50 ng of Pkd2L1 and 25 ng of RACK1 is similar with that from the injection of 6.2 ng of Pkd2L1 alone *(37)*. This observation raised the possibility that PKD2L1 functional regulation by RACK1 might be mediated

by PKC. Other independent studies mentioned PKD2L1 T338 as a potential PKC phosphorylation site *(51)*. TRPV1 studies *(52)* showed a phosphorylation site at a similar position (S502) in the first cytoplasmic loop that is involved in the PMA-mediated channel sensitization to different stimuli, like enhancing TRPV1 capsaisin evoked currents. Another interesting effect of PMA is its modulation of the content of the phospholipid bilayer, by increasing the levels of PIP and PIP2 in oocytes membranes. This modulation of the phosphoinositide metabolism is through PKC activation that result in an increased phosphoinositide 4 kinase β (PI4Kβ) activity *(53)*. A cross talk between phosphoinositides levels and PKC is a key determinant in the regulation of many ion channels as reviewed recently *(2)*.

In summary, PKD2L1 is activated through phospholipase C and its inactivation/desensitization mechanism involves the activation of protein kinase C. This inactivation/desensitization may involve the threonine residue 338. As membrane phosphoinositide levels may be affected by the activation of PKC, it is yet-to-be determined the phosphoinositide species involved in PKD2L1 activation and/or inhibition mechanisms.

4.5 REFERENCES

1. Hardie, R. C. and Muallem, S. (2009) Lipids in Ca^{2+} signalling--an introduction, *Cell Calcium 45*, 517-520.

2. Hille, B., Dickson, E. J., Kruse, M., Vivas, O., and Suh, B. C. (2015) Phosphoinositides regulate ion channels, *Biochim. Biophys. Acta*. *1851*, 844-856.

3. Rohacs, T. (2014) Phosphoinositide regulation of TRP channels, *Handb. Exp. Pharmacol. 223*, 1143-1176.

4. Gresset, A., Sondek, J., and Harden, T. K. (2012) The phospholipase C isozymes and their regulation, *Subcell. Biochem. 58*, 61-94.

5. Hansen, S. B. (2015) Lipid agonism: The PIP paradigm of ligand-gated ion channels, *Biochim. Biophys. Acta 1851*, 620-628.

6. Logothetis, D. E., Petrou, V. I., Adney, S. K., and Mahajan, R. (2010) Channelopathies linked to plasma membrane phosphoinositides, *Pflugers Arch. 460*, 321-341.

7. Yang, J., Zheng, W., Wang, Q., Lara, C., Hussein, S., and Chen, X. Z. (2013) Translational up-regulation of polycystic kidney disease protein PKD2 by endoplasmic reticulum stress, *FASEB J. 27*, 4998-5009.

8. Voolstra, O., Bartels, J. P., Oberegelsbacher, C., Pfannstiel, J., and Huber, A. (2013) Phosphorylation of the Drosophila transient receptor potential ion channel is regulated by the phototransduction cascade and involves several protein kinases and phosphatases, *PLoS. One. 8*, e73787.

9. Clark, K., Middelbeek, J., and van Leeuwen, F. N. (2008) Interplay between TRP channels and the cytoskeleton in health and disease, *Eur. J. Cell Biol. 87*, 631-640.

10. Jordt, S. E. and Ehrlich, B. E. (2007) TRP channels in disease, *Subcell. Biochem. 45*, 253-271.

11. Kiselyov, K., Soyombo, A., and Muallem, S. (2007) TRPpathies, *J. Physiol 578*, 641-653.

12. Montell, C. (2001) Physiology, phylogeny, and functions of the TRP superfamily of cation channels, *Sci. STKE.2001*, re1.

13. Nilius, B. (2007) TRP channels in disease, *Biochim. Biophys. Acta 1772*, 805-812.

14. Hardie, R. C. (2007) TRP channels and lipids: from Drosophila to mammalian physiology, *J. Physiol 578*, 9-24.

15. Nilius, B., Owsianik, G., and Voets, T. (2008) Transient receptor potential channels meet phosphoinositides, *EMBO J. 27*, 2809-2816.

16. Rohacs, T. (2009) Phosphoinositide regulation of non-canonical transient receptor potential channels, *Cell Calcium 45*, 554-565.

17. Imai, Y., Itsuki, K., Okamura, Y., Inoue, R., and Mori, M. X. (2012) A self-limiting regulation of vasoconstrictor-activated TRPC3/C6/C7 channels coupled to PI(4,5)P(2)-diacylglycerol signalling, *J. Physiol 590*, 1101-1119.

18. Itsuki, K., Imai, Y., Hase, H., Okamura, Y., Inoue, R., and Mori, M. X. (2014) PLC-mediated PI(4,5)P2 hydrolysis regulates activation and inactivation of TRPC6/7 channels, *J. Gen. Physiol 143*, 183-201.

19. Ju, M., Shi, J., Saleh, S. N., Albert, A. P., and Large, W. A. (2010) Ins(1,4,5)P3 interacts with PIP2 to regulate activation of TRPC6/C7 channels by diacylglycerol in native vascular myocytes, *J. Physiol 588*, 1419-1433.

20. Venkatachalam, K., Zheng, F., and Gill, D. L. (2003) Regulation of canonical transient receptor potential (TRPC) channel function by diacylglycerol and protein kinase C, *J. Biol. Chem. 278*, 29031-29040.

21. Rohacs, T. (2015) Phosphoinositide regulation of TRPV1 revisited, *Pflugers Arch. 467,* 1851-1869.

22. Smith, D. P., Ranganathan, R., Hardy, R. W., Marx, J., Tsuchida, T., and Zuker, C. S. (1991) Photoreceptor deactivation and retinal degeneration mediated by a photoreceptor-specific protein kinase C, *Science 254*, 1478-1484.

23. Huber, A., Sander, P., Bahner, M., and Paulsen, R. (1998) The TRP Ca2+ channel assembled in a signaling complex by the PDZ domain protein INAD is phosphorylated through the interaction with protein kinase C (ePKC), *FEBS Lett. 425*, 317-322.

24. Bevan, S., Quallo, T., and Andersson, D. A. (2014) TRPV1, *Handb. Exp. Pharmacol. 222*, 207-245.

25. Chen, X. Z., Vassilev, P. M., Basora, N., Peng, J. B., Nomura, H., Segal, Y., Brown, E. M., Reeders, S. T., Hediger, M. A., and Zhou, J. (1999) Polycystin-L is a calcium-regulated cation channel permeable to calcium ions, *Nature 401*, 383-386.

26. Yu, Y., Ulbrich, M. H., Li, M. H., Dobbins, S., Zhang, W. K., Tong, L., Isacoff, E. Y., and Yang, J. (2012) Molecular mechanism of the assembly of an acid-sensing receptor ion channel complex, *Nat. Commun. 3*, 1252.

27. DeCaen, P. G., Delling, M., Vien, T. N., and Clapham, D. E. (2013) Direct recording and molecular identification of the calcium channel of primary cilia, *Nature 504*, 315-318.

28. Huang, A. L., Chen, X., Hoon, M. A., Chandrashekar, J., Guo, W., Trankner, D., Ryba, N. J., and Zuker, C. S. (2006) The cells and logic for mammalian sour taste detection, *Nature 442*, 934-938.

29. Ishimaru, Y., Inada, H., Kubota, M., Zhuang, H., Tominaga, M., and Matsunami, H. (2006) Transient receptor potential family members PKD1L3 and PKD2L1 form a candidate sour taste receptor, *Proc. Natl. Acad. Sci. U. S. A 103*, 12569-12574.

30. Lopezjimenez, N. D., Cavenagh, M. M., Sainz, E., Cruz-Ithier, M. A., Battey, J. F., and Sullivan, S. L. (2006) Two members of the TRPP family of ion channels, Pkd1l3 and Pkd2l1, are co-expressed in a subset of taste receptor cells, *J. Neurochem. 98*, 68-77.

31. Dai, X. Q., Karpinski, E., and Chen, X. Z. (2006) Permeation and inhibition of polycystin-L channel by monovalent organic cations, *Biochim. Biophys. Acta 1758*, 197-205.

32. Liu, Y., Li, Q., Tan, M., Zhang, Y. Y., Karpinski, E., Zhou, J., and Chen, X. Z. (2002) Modulation of the human polycystin-L channel by voltage and divalent cations, *FEBS Lett. 525*, 71-76.

33. Dai, X. Q., Ramji, A., Liu, Y., Li, Q., Karpinski, E., and Chen, X. Z. (2007) Inhibition of TRPP3 channel by amiloride and analogs, *Mol. Pharmacol. 72*, 1576-1585.

34. Ishimaru, Y., Katano, Y., Yamamoto, K., Akiba, M., Misaka, T., Roberts, R. W., Asakura, T., Matsunami, H., and Abe, K. (2010) Interaction between PKD1L3 and PKD2L1 through their transmembrane domains is required for localization of PKD2L1 at taste pores in taste cells of circumvallate and foliate papillae, *FASEB J. 24*, 4058-4067.

35. Li, Q., Liu, Y., Shen, P. Y., Dai, X. Q., Wang, S., Smillie, L. B., Sandford, R., and Chen, X. Z. (2003) Troponin I binds polycystin-L and inhibits its calcium-induced channel activation, *Biochemistry 42*, 7618-7625.

36. Li, Q., Dai, X. Q., Shen, P. Y., Wu, Y., Long, W., Chen, C. X., Hussain, Z., Wang, S., and Chen, X. Z. (2007) Direct binding of alpha-actinin enhances TRPP3 channel activity, *J. Neurochem. 103*, 2391-2400.

37. Yang, J., Wang, Q., Zheng, W., Tuli, J., Li, Q., Wu, Y., Hussein, S., Dai, X. Q., Shafiei, S., Li, X. G., Shen, P. Y., Tu, J. C., and Chen, X. Z. (2012) Receptor for activated C kinase 1 (RACK1) inhibits function of transient receptor

potential (TRP)-type channel Pkd2L1 through physical interaction, *J. Biol. Chem. 287*, 6551-6561.

38. Shimizu, T., Janssens, A., Voets, T., and Nilius, B. (2009) Regulation of the murine TRPP3 channel by voltage, pH, and changes in cell volume, *Pflugers Arch. 457*, 795-807.

39. Shimizu, T., Higuchi, T., Fujii, T., Nilius, B., and Sakai, H. (2011) Bimodal effect of alkalization on the polycystin transient receptor potential channel, PKD2L1, *Pflugers Arch. 461*, 507-513.

40. Chen, P., Wu, J. Z., Zhao, J., Wang, P., Luo, J., Yang, W., and Liu, X. D. (2015) PKD2L1/PKD1L3 channel complex with an alkali-activated mechanism and calcium-dependent inactivation, *Eur. Biophys. J. 44*, 483-492.

41. Li, Q., Liu, Y., Zhao, W., and Chen, X. Z. (2002) The calcium-binding EF-hand in polycystin-L is not a domain for channel activation and ensuing inactivation, *FEBS Lett. 516*, 270-278.

42. Molland, K. L., Narayanan, A., Burgner, J. W., and Yernool, D. A. (2010) Identification of the structural motif responsible for trimeric assembly of the C-terminal regulatory domains of polycystin channels PKD2L1 and PKD2, *Biochem. J. 429*, 171-183.

43. Wong, Y. H., Lee, T. Y., Liang, H. K., Huang, C. M., Wang, T. Y., Yang, Y. H., Chu, C. H., Huang, H. D., Ko, M. T., and Hwang, J. K. (2007) KinasePhos 2.0: a web server for identifying protein kinase-specific phosphorylation sites based on sequences and coupling patterns, *Nucleic Acids Res. 35*, W588-W594.

44. Kawaguchi, H., Yamanaka, A., Uchida, K., Shibasaki, K., Sokabe, T., Maruyama, Y., Yanagawa, Y., Murakami, S., and Tominaga, M. (2010) Activation of polycystic kidney disease-2-like 1 (PKD2L1)-PKD1L3 complex by acid in mouse taste cells, *J. Biol. Chem. 285*, 17277-17281.

45. Fujimoto, C., Ishimaru, Y., Katano, Y., Misaka, T., Yamasoba, T., Asakura, T., and Abe, K. (2011) The single pore residue Asp523 in PKD2L1 determines Ca^{2+} permeation of the PKD1L3/PKD2L1 complex, *Biochem. Biophys. Res. Commun. 404*, 946-951.

46. Rossler, P., Kroner, C., Freitag, J., Noe, J., and Breer, H. (1998) Identification of a phospholipase C beta subtype in rat taste cells, *Eur. J. Cell Biol. 77*, 253-261.

47. Kataoka, S., Yang, R., Ishimaru, Y., Matsunami, H., Sevigny, J., Kinnamon, J. C., and Finger, T. E. (2008) The candidate sour taste receptor, PKD2L1, is expressed by type III taste cells in the mouse, *Chem. Senses 33*, 243-254.

48. Horio, N., Yoshida, R., Yasumatsu, K., Yanagawa, Y., Ishimaru, Y., Matsunami, H., and Ninomiya, Y. (2011) Sour taste responses in mice lacking PKD channels, *PLoS. One. 6*, e20007.

49. Ishimaru, Y. (2015) Molecular mechanisms underlying the reception and transmission of sour taste information, *Biosci. Biotechnol. Biochem. 79*, 171-176.

50. Bystrova, M. F., Romanov, R. A., Rogachevskaja, O. A., Churbanov, G. D., and Kolesnikov, S. S. (2010) Functional expression of the extracellular-Ca^{2+}-sensing receptor in mouse taste cells, *J. Cell Sci. 123*, 972-982.

51. Nomura, H., Turco, A. E., Pei, Y., Kalaydjieva, L., Schiavello, T., Weremowicz, S., Ji, W., Morton, C. C., Meisler, M., Reeders, S. T., and Zhou, J. (1998) Identification of PKDL, a novel polycystic kidney disease 2-like gene whose murine homologue is deleted in mice with kidney and retinal defects, *J. Biol. Chem. 273*, 25967-25973.

52. Bhave, G., Hu, H. J., Glauner, K. S., Zhu, W., Wang, H., Brasier, D. J., Oxford, G. S., and Gereau, R. W. (2003) Protein kinase C phosphorylation sensitizes but does not activate the capsaicin receptor transient receptor potential vanilloid 1 (TRPV1), *Proc. Natl. Acad. Sci. U. S. A 100*, 12480-12485.

53. Chen, X., Zhang, X., Jia, C., Xu, J., Gao, H., Zhang, G., Du, X., and Zhang, H. (2011) Membrane depolarization increases membrane PtdIns(4,5)P2 levels through mechanisms involving PKC betaII and PI4 kinase, *J. Biol. Chem. 286*, 39760-39767.

CHAPTER 5

5. General discussion and future directions

5.1 INTRODUCTION

This PhD thesis investigated different aspects of the functional regulation of the TRP-type channel, PKD2L1. The work performed here provided new insights into the mechanism controlling the channel activation/inactivation with a special emphasis on the role of PKD2L1 protein in pH sensing with and without its protein partner, PKD1L3. In addition, we had identified different residues and domains mediating channel function and oligomerization. Moreover, our experiments highlighted the role of intracellular free Ca^{2+} concentration and PLC pathway as the major signalling mediators controlling PKD2L1 channel function.

5.2 PKD2L1 senses acids in the absence of PKD1L3

PKD2L1-expressing cells are identified for their ability to respond to acids in the tongue as well as the spinal cord. With a unique delayed response to acids, PKD2L1 responds to the acidic stimuli by a current evoked after washing the acid (*141*). Since 2008, this current was called the off-response but recently a new group has called it an alkali on-response (*145*). We tried this approach by applying alkali under our experimental conditions but we did not get similar results (data not shown). PKD2L1 expression is marking a specific population of TRCs, known to respond to sour stimuli, these are Type III TRCs (*134;156*). It marks as well a specific set of neurons lining the mouse central canal of spinal cord, known as CSF-cNs (*128-130*). This type of neurons responds to minute changes in extracellular pH. While pH sensing of PKD2L1 in complex with PKD1L3 protein has been studied in many expression systems as well as in animal models, it continued to be a point of debate. Although

mouse model did not show an effect for PKD1L3 deletion on sour taste in TRCs (*154*), heterologous expression systems continued to provide evidence for the necessity of PKD1L3 role in acid sensing (*45;134;141*). Even in *Xenopus* oocytes, previous report with slightly different experimental conditions showed the need for PKD1L3 in order to see PKD2L1 acid-induced off-response current (*42*).

Here we found that for PKD2L1 whole cell off-response current to be easily seen, the PM channel population needs to exceed a certain limit. In addition, off-response current was independent from endogenous PKD1L3. Moreover, the observed off-response was having the same previously reported current characteristics for PKD2L1/PKD1L3 complex (*130;141;143*); including 1) the channel response to acids is proportional to the H^+ concentration and to the degree of acid dissociation. 2) Having a threshold value for acid-induced activation which differs in accordance to the expression system. 3) Duration-independence is another characteristic, where the acid application time does not affect the off-response current.

5.3 Role of Ca^{2+} in channel activation/inactivation process

As a TRP-type channel has a preferred permeability and activity to Ca^{2+} ions, Ca^{2+} plays a pivotal role for PKD2L1 channel activity. First clue was from Chen and colleagues (*117*) when they identified the rise in intracellular Ca^{2+} as the main trigger for the Ca^{2+}-induced activation. Ca^{2+} imaging was used as well to detect the acid-induced channel function, for the rapid increase in Ca^{2+} levels upon triggering the off-response both in primary TRCs as well as *in vitro (120;142)*. Ca^{2+} is an important cofactor for the PLC enzymes to be activated (*157*); besides it may directly bind to one

or more of the residues causing conformational changes essential for channel opening. We continued to identify the roles of Ca^{2+} by determining the inhibitory role it has on PKD2L1 off-response. So from our perspective, the initial increase in intracellular Ca^{2+} initiates the channel activation, while further increase in intracellular free Ca^{2+} starts to activate the mediators of the inhibitory pathway. Ca^{2+} as a pivotal signalling molecule, it initiates the channel inhibition through more than one route. We determined that the K_i value for Ca^{2+} inhibition was as low as ≈ 170 μM. Ca^{2+} is an important factor for the activation of PKC and CaM. Both had been determined as inhibitory mediators of PKD2L1. CaM antagonists were having a stimulatory effect on PKD2L1-associated currents in a previous report (*23*). Moreover, our previous studies delineating the role of RACK1 in PKD2L1 regulation (*121*) as well as our current PKC experiments, all support PKC-mediated inhibition of PKD2L1.

5.4 Residues and domains critical for channel function

Our PKD2L1 structure/function studies were able to identify two negatively charged intramembrane residues that were critical for channel function. We assume that these residues are important and may potentially bind to the channel stimulators, Ca^{2+} and H^+ ions. The contribution of more than one residue to the proposed mechanism is evident. Previous studies identified the aspartic acid residues 523 and 525 as critical for channel Ca^{2+} permeability and selectivity filter (*42;120*).

Moreover, native PKD2L1 was found to form monomers, dimers, trimers and tetramers. Our lab was the first to identify that the EF hand and CCD is not important for PKD2L1 channel function (*18*), but rather they contribute to the inactivation

process. Later the CCD was identified to contain a trimerization domain (*47;48*), but surprisingly the absence of this domain did not affect the normal channel function, as confirmed by us and others (*18;45*). Further studies by our group revealed the existence of another conserved C-terminal domain that is critical for the channel oligomerization and function with its absence is detrimental to the channel function.

5.5 PLC pathway as a major regulatory signalling pathway controlling PKD2L1 channel

PLC enzyme isoforms are widely distributed and conserved throughout the animal kingdom. Their involvement in signalling throughout the body has been and is continued to be studied extensively (*157*). One of the interesting findings from a previous study is the presence of PLC-dependent Ca^{2+} activity in Type III TRCs downstream of the G protein, Ca^{2+} sensing receptor (*158*). As these are the TRCs that express PKD2L1, this raised the possibility that PKD2L1 is regulated by the same pathway. Our data is the first to provide the evidence that PKD2L1 is regulated by the PLC pathway and that this regulation is PKC-dependent.

5.6 Future directions

Sour tasting is one of the basic animal senses and a fundamental part of human and animal physiology. The signalling pathway underlying how sour tasting is transduced is still poorly understood. While PKD2L1 is a strong candidate for sour taste sensation (*159*), it would not be the sole receptor that senses acids. For this it is

critical to investigate the mechanism underlying PKD2L1 function and the necessity to identify more proteins that may contribute to sour taste sensation is urging.

Our PLC pathway work still needs further investigations. First, we need to identify the potential role of PIP2 in PKD2L1 channel function. To investigate PIP2 role on PKD2L1 expressed in oocytes, we are currently optimizing the conditions of using the polycation, neomycin, to chelate PIP2 and the activator of the 5-phosphatase, rapamycin, which depletes PIP2 by converting it to PI4P. We expect to observe increased sensitization and activation of the channel by decreasing the amount of PIP2 available for channel inhibition; however, as we are using whole cell recordings the optimizations become more challenging. For the same purpose we are optimizing the use of diC8, as a mimic of PIP2 to see whether it is going to decrease/inhibit PKD2l1 channel.

Second, further experiments are required with the PKC blocker, GF 109203x, to determine which isoform of PKC enzymes is responsible for the associated inhibition/desensitization of PKC activation. Our preliminary data indicate that the hypothesis we put forward is correct, but to get a statistically significant data we need to perform further experiments.

Third, from what is learned from TRPV1 and dTRP, more than one phosphorylation site is likely to be affected during the activation/inactivation pathway; so further scanning of potential phosphorylation sites might be of interest. We have already generated a number of potential phosphorylation site mutants that needs further characterization. This work will provide a better understanding of how PKC regulates the channel and contributes to the inactivation process.

Fourth, it is interesting to investigate the potential role of GPCR in the PKD2L1 channel function, and more specifically the role of Ca^{2+} sensing receptor. We think that different G proteins may distinctly regulate PKD2L1, which may explain differences in the biophysical and physiological properties of PKD2L1 channel observed in different tissues. A pilot experiment may include the use of different Ca^{2+} sensing receptor agonists and antagonists to check whether it is involved in PKD2L1 activation pathway.

With the availability of PKD2L1 knockout mice, a number of interesting experiments could be performed on them. Knowing that PKD2L1 interacts with TnI and is endougenously expressed in the heart, it will be interesting to challenge these mice with exercise and see whether their hearts are as healthy as the control mice. A number of heart function indicators could be measured in the plasma, including but not limited to, troponin, creatine kinase and collagen markers. The level of the latter indicates changes in either the myocardium or the extracellular matrix.

Understanding how PKD2L1 is regulated and deciphering the steps by which the channel is gate opened and closed will help proposing a signalling transduction mechanism for acid sensing.

6. REFERENCES

1. Clark, K., Middelbeek, J., and van Leeuwen, F. N. (2008) Interplay between TRP channels and the cytoskeleton in health and disease, *Eur. J. Cell Biol. 87*, 631-640.

2. Montell, C. (2011) The history of TRP channels, a commentary and reflection, *Pflugers Arch. 461*, 499-506.

3. Nilius, B. (2007) TRP channels in disease, *Biochim. Biophys. Acta 1772*, 805-812.

4. Woudenberg-Vrenken, T. E., Bindels, R. J., and Hoenderop, J. G. (2009) The role of transient receptor potential channels in kidney disease, *Nat. Rev. Nephrol. 5*, 441-449.

5. Nilius, B. and Owsianik, G. (2011) The transient receptor potential family of ion channels, *Genome Biol. 12*, 218.

6. Nilius, B., Owsianik, G., Voets, T., and Peters, J. A. (2007) Transient receptor potential cation channels in disease, *Physiol Rev. 87*, 165-217.

7. Owsianik, G., D'hoedt, D., Voets, T., and Nilius, B. (2006) Structure-function relationship of the TRP channel superfamily, *Rev. Physiol Biochem. Pharmacol. 156*, 61-90.

8. Gaudet, R. (2008) A primer on ankyrin repeat function in TRP channels and beyond, *Mol. Biosyst. 4*, 372-379.

9. Nagata, K., Duggan, A., Kumar, G., and Garcia-Anoveros, J. (2005) Nociceptor and hair cell transducer properties of TRPA1, a channel for pain and hearing, *J. Neurosci. 25*, 4052-4061.

10. Gaudet, R. (2007) Structural Insights into the Function of TRP Channels.

11. Rohacs, T., Lopes, C. M., Michailidis, I., and Logothetis, D. E. (2005) PI(4,5)P2 regulates the activation and desensitization of TRPM8 channels through the TRP domain, *Nat. Neurosci. 8*, 626-634.

12. Poblete, H., Oyarzun, I., Olivero, P., Comer, J., Zuniga, M., Sepulveda, R. V., Baez-Nieto, D., Gonzalez, L. C., Gonzalez-Nilo, F., and Latorre, R. (2015) Molecular determinants of phosphatidylinositol 4,5-bisphosphate (PI(4,5)P2) binding to transient receptor potential V1 (TRPV1) channels, *J. Biol. Chem. 290*, 2086-2098.

13. Teng, J., Loukin, S. H., Anishkin, A., and Kung, C. (2015) L596-W733 bond between the start of the S4-S5 linker and the TRP box stabilizes the closed state of TRPV4 channel, *Proc. Natl. Acad. Sci. U. S. A 112*, 3386-3391.

14. Valente, P., Garcia-Sanz, N., Gomis, A., Fernandez-Carvajal, A., Fernandez-Ballester, G., Viana, F., Belmonte, C., and Ferrer-Montiel, A. (2008) Identification of molecular determinants of channel gating in the transient receptor potential box of vanilloid receptor I, *FASEB J. 22*, 3298-3309.

15. Latorre, R., Zaelzer, C., and Brauchi, S. (2009) Structure-functional intimacies of transient receptor potential channels, *Q. Rev. Biophys. 42*, 201-246.

16. Zheng, W., Hussein, S., Yang, J., Huang, J., Zhang, F., Hernandez-Anzaldo, S., Fernandez-Patron, C., Cao, Y., Zeng, H., Tang, J., and Chen, X. Z. (2015) A novel PKD2L1 C-terminal domain critical for trimerization and channel function, *Sci. Rep. 5*, 9460.

17. Lee, K. P., Choi, S., Hong, J. H., Ahuja, M., Graham, S., Ma, R., So, I., Shin, D. M., Muallem, S., and Yuan, J. P. (2014) Molecular determinants mediating gating of Transient Receptor Potential Canonical (TRPC) channels by stromal interaction molecule 1 (STIM1), *J. Biol. Chem. 289*, 6372-6382.

18. Li, Q., Liu, Y., Zhao, W., and Chen, X. Z. (2002) The calcium-binding EF-hand in polycystin-L is not a domain for channel activation and ensuing inactivation, *FEBS Lett. 516*, 270-278.

19. Zurborg, S., Yurgionas, B., Jira, J. A., Caspani, O., and Heppenstall, P. A. (2007) Direct activation of the ion channel TRPA1 by Ca2+, *Nat. Neurosci. 10*, 277-279.

20. Numazaki, M., Tominaga, T., Takeuchi, K., Murayama, N., Toyooka, H., and Tominaga, M. (2003) Structural determinant of TRPV1 desensitization interacts with calmodulin, *Proc. Natl. Acad. Sci. U. S. A 100*, 8002-8006.

21. Lau, S. Y., Procko, E., and Gaudet, R. (2012) Distinct properties of Ca2+-calmodulin binding to N- and C-terminal regulatory regions of the TRPV1 channel, *J. Gen. Physiol 140*, 541-555.

22. Holakovska, B., Grycova, L., Bily, J., and Teisinger, J. (2011) Characterization of calmodulin binding domains in TRPV2 and TRPV5 C-tails, *Amino. Acids 40*, 741-748.

23. DeCaen, P. G., Delling, M., Vien, T. N., and Clapham, D. E. (2013) Direct recording and molecular identification of the calcium channel of primary cilia, *Nature 504*, 315-318.

24. Hardie, R. C. (2014) Photosensitive TRPs, *Handb. Exp. Pharmacol. 223*, 795-826.

25. Harteneck, C. (2003) Proteins modulating TRP channel function, *Cell Calcium 33*, 303-310.

26. Montell, C. (2005) TRP channels in Drosophila photoreceptor cells, *J. Physiol 567*, 45-51.

27. Clark, K., Middelbeek, J., Dorovkov, M. V., Figdor, C. G., Ryazanov, A. G., Lasonder, E., and van Leeuwen, F. N. (2008) The alpha-kinases TRPM6 and TRPM7, but not eEF-2 kinase, phosphorylate the assembly domain of myosin IIA, IIB and IIC, *FEBS Lett. 582*, 2993-2997.

28. Clark, K., Middelbeek, J., Morrice, N. A., Figdor, C. G., Lasonder, E., and van Leeuwen, F. N. (2008) Massive autophosphorylation of the Ser/Thr-rich domain controls protein kinase activity of TRPM6 and TRPM7, *PLoS. One. 3*, e1876.

29. Matsushita, M., Kozak, J. A., Shimizu, Y., McLachlin, D. T., Yamaguchi, H., Wei, F. Y., Tomizawa, K., Matsui, H., Chait, B. T., Cahalan, M. D., and Nairn, A. C. (2005) Channel function is dissociated from the intrinsic kinase activity and autophosphorylation of TRPM7/ChaK1, *J. Biol. Chem. 280*, 20793-20803.

30. Perraud, A. L., Fleig, A., Dunn, C. A., Bagley, L. A., Launay, P., Schmitz, C., Stokes, A. J., Zhu, Q., Bessman, M. J., Penner, R., Kinet, J. P., and Scharenberg, A. M. (2001) ADP-ribose gating of the calcium-permeable LTRPC2 channel revealed by Nudix motif homology, *Nature 411*, 595-599.

31. Voolstra, O. and Huber, A. (2014) Post-Translational Modifications of TRP Channels, *Cells 3*, 258-287.

32. Huber, A., Sander, P., Bahner, M., and Paulsen, R. (1998) The TRP Ca2+ channel assembled in a signaling complex by the PDZ domain protein INAD is phosphorylated through the interaction with protein kinase C (ePKC), *FEBS Lett. 425*, 317-322.

33. Streets, A. J., Wessely, O., Peters, D. J., and Ong, A. C. (2013) Hyperphosphorylation of polycystin-2 at a critical residue in disease reveals an essential role for polycystin-1-regulated dephosphorylation, *Hum. Mol. Genet. 22*, 1924-1939.

34. Wang, S., Joseph, J., Ro, J. Y., and Chung, M. K. (2015) Modality-specific mechanisms of protein kinase C-induced hypersensitivity of TRPV1: S800 is a polymodal sensitization site, *Pain 156*, 931-941.

35. Barrera, N. P., Shaifta, Y., McFadzean, I., Ward, J. P., Henderson, R. M., and Edwardson, J. M. (2007) AFM imaging reveals the tetrameric structure of the TRPC1 channel, *Biochem. Biophys. Res. Commun. 358*, 1086-1090.

36. Hanaoka, K., Qian, F., Boletta, A., Bhunia, A. K., Piontek, K., Tsiokas, L., Sukhatme, V. P., Guggino, W. B., and Germino, G. G. (2000) Co-assembly of

polycystin-1 and -2 produces unique cation-permeable currents, *Nature 408*, 990-994.

37. Lepage, P. K. and Boulay, G. (2007) Molecular determinants of TRP channel assembly, *Biochem. Soc. Trans. 35*, 81-83.

38. Kobori, T., Smith, G. D., Sandford, R., and Edwardson, J. M. (2009) The transient receptor potential channels TRPP2 and TRPC1 form a heterotetramer with a 2:2 stoichiometry and an alternating subunit arrangement, *J. Biol. Chem. 284*, 35507-35513.

39. Ferreira, F. M., Oliveira, L. C., Germino, G. G., Onuchic, J. N., and Onuchic, L. F. (2011) Macromolecular assembly of polycystin-2 intracytosolic C-terminal domain, *Proc. Natl. Acad. Sci. U. S. A 108*, 9833-9838.

40. Stewart, A. P., Smith, G. D., Sandford, R. N., and Edwardson, J. M. (2010) Atomic force microscopy reveals the alternating subunit arrangement of the TRPP2-TRPV4 heterotetramer, *Biophys. J. 99*, 790-797.

41. Hoenderop, J. G., Voets, T., Hoefs, S., Weidema, F., Prenen, J., Nilius, B., and Bindels, R. J. (2003) Homo- and heterotetrameric architecture of the epithelial Ca2+ channels TRPV5 and TRPV6, *EMBO J. 22*, 776-785.

42. Yu, Y., Ulbrich, M. H., Li, M. H., Dobbins, S., Zhang, W. K., Tong, L., Isacoff, E. Y., and Yang, J. (2012) Molecular mechanism of the assembly of an acid-sensing receptor ion channel complex, *Nat. Commun. 3*, 1252.

43. Feng, S., Rodat-Despoix, L., Delmas, P., and Ong, A. C. (2011) A single amino acid residue constitutes the third dimerization domain essential for the assembly and function of the tetrameric polycystin-2 (TRPP2) channel, *J. Biol. Chem. 286*, 18994-19000.

44. Garcia-Sanz, N., Fernandez-Carvajal, A., Morenilla-Palao, C., Planells-Cases, R., Fajardo-Sanchez, E., Fernandez-Ballester, G., and Ferrer-Montiel, A. (2004) Identification of a tetramerization domain in the C terminus of the vanilloid receptor, *J. Neurosci. 24*, 5307-5314.

45. Ishimaru, Y., Katano, Y., Yamamoto, K., Akiba, M., Misaka, T., Roberts, R. W., Asakura, T., Matsunami, H., and Abe, K. (2010) Interaction between PKD1L3 and PKD2L1 through their transmembrane domains is required for localization of PKD2L1 at taste pores in taste cells of circumvallate and foliate papillae, *FASEB J. 24*, 4058-4067.

46. Crawley, S. W. and Cote, G. P. (2009) Identification of dimer interactions required for the catalytic activity of the TRPM7 alpha-kinase domain, *Biochem. J. 420*, 115-122.

47. Molland, K. L., Narayanan, A., Burgner, J. W., and Yernool, D. A. (2010) Identification of the structural motif responsible for trimeric assembly of the C-terminal regulatory domains of polycystin channels PKD2L1 and PKD2, *Biochem. J. 429*, 171-183.

48. Molland, K. L., Paul, L. N., and Yernool, D. A. (2012) Crystal structure and characterization of coiled-coil domain of the transient receptor potential channel PKD2L1, *Biochim. Biophys. Acta 1824*, 413-421.

49. Balla, T. (2013) Phosphoinositides: tiny lipids with giant impact on cell regulation, *Physiol Rev. 93*, 1019-1137.

50. Hille, B., Dickson, E. J., Kruse, M., Vivas, O., and Suh, B. C. (2014) Phosphoinositides regulate ion channels, *Biochim. Biophys. Acta*.

51. Logothetis, D. E., Petrou, V. I., Adney, S. K., and Mahajan, R. (2010) Channelopathies linked to plasma membrane phosphoinositides, *Pflugers Arch. 460*, 321-341.

52. Nilius, B., Owsianik, G., and Voets, T. (2008) Transient receptor potential channels meet phosphoinositides, *EMBO J. 27*, 2809-2816.

53. Rohacs, T. (2014) Phosphoinositide regulation of TRP channels, *Handb. Exp. Pharmacol. 223*, 1143-1176.

54. Taberner, F. J., Fernandez-Ballester, G., Fernandez-Carvajal, A., and Ferrer-Montiel, A. (2015) TRP channels interaction with lipids and its implications in disease, *Biochim. Biophys. Acta 1848*, 1818-1827.

55. Falkenburger, B. H., Dickson, E. J., and Hille, B. (2013) Quantitative properties and receptor reserve of the DAG and PKC branch of G(q)-coupled receptor signaling, *J. Gen. Physiol 141*, 537-555.

56. Itsuki, K., Imai, Y., Hase, H., Okamura, Y., Inoue, R., and Mori, M. X. (2014) PLC-mediated PI(4,5)P2 hydrolysis regulates activation and inactivation of TRPC6/7 channels, *J. Gen. Physiol 143*, 183-201.

57. Venkatachalam, K., Zheng, F., and Gill, D. L. (2003) Regulation of canonical transient receptor potential (TRPC) channel function by diacylglycerol and protein kinase C, *J. Biol. Chem. 278*, 29031-29040.

58. Ma, R., Li, W. P., Rundle, D., Kong, J., Akbarali, H. I., and Tsiokas, L. (2005) PKD2 functions as an epidermal growth factor-activated plasma membrane channel, *Mol. Cell Biol. 25*, 8285-8298.

59. Rohacs, T. (2009) Phosphoinositide regulation of non-canonical transient receptor potential channels, *Cell Calcium 45*, 554-565.

60. Smani, T., Shapovalov, G., Skryma, R., Prevarskaya, N., and Rosado, J. A. (2015) Functional and physiopathological implications of TRP channels, *Biochim. Biophys. Acta 1853*, 1772-1782.

61. Minke, B. (2010) The history of the Drosophila TRP channel: the birth of a new channel superfamily, *J. Neurogenet. 24*, 216-233.

62. Niemeyer, B. A., Suzuki, E., Scott, K., Jalink, K., and Zuker, C. S. (1996) The Drosophila light-activated conductance is composed of the two channels TRP and TRPL, *Cell 85*, 651-659.

63. Wang, T. and Montell, C. (2007) Phototransduction and retinal degeneration in Drosophila, *Pflugers Arch. 454*, 821-847.

64. Wes, P. D., Chevesich, J., Jeromin, A., Rosenberg, C., Stetten, G., and Montell, C. (1995) TRPC1, a human homolog of a Drosophila store-operated channel, *Proc. Natl. Acad. Sci. U. S. A 92*, 9652-9656.

65. Nesin, V. and Tsiokas, L. (2014) TRPC1, *Handb. Exp. Pharmacol. 222*, 15-51.

66. Zhang, D., Freedman, B. I., Flekac, M., Santos, E., Hicks, P. J., Bowden, D. W., Efendic, S., Brismar, K., and Gu, H. F. (2009) Evaluation of genetic association and expression reduction of TRPC1 in the development of diabetic nephropathy, *Am. J. Nephrol. 29*, 244-251.

67. Chen, K., Jin, X., Li, Q., Wang, W., Wang, Y., and Zhang, J. (2013) Association of TRPC1 gene polymorphisms with type 2 diabetes and diabetic nephropathy in Han Chinese population, *Endocr. Res. 38*, 59-68.

68. Jiang, H. N., Zeng, B., Zhang, Y., Daskoulidou, N., Fan, H., Qu, J. M., and Xu, S. Z. (2013) Involvement of TRPC channels in lung cancer cell differentiation and the correlation analysis in human non-small cell lung cancer, *PLoS. One. 8*, e67637.

69. Zeng, B., Yuan, C., Yang, X., Atkin, S. L., and Xu, S. Z. (2013) TRPC channels and their splice variants are essential for promoting human ovarian cancer cell proliferation and tumorigenesis, *Curr. Cancer Drug Targets. 13*, 103-116.

70. Zeng, C., Tian, F., and Xiao, B. (2014) TRPC Channels: Prominent Candidates of Underlying Mechanism in Neuropsychiatric Diseases, *Mol. Neurobiol.*

71. Zhu, B., Chen, N., Wang, Z. H., Pan, X. X., Ren, H., Zhang, W., and Wang, W. M. (2009) Identification and functional analysis of a novel TRPC6 mutation associated with late onset familial focal segmental glomerulosclerosis in Chinese patients, *Mutat. Res. 664*, 84-90.

72. Winn, M. P., Conlon, P. J., Lynn, K. L., Farrington, M. K., Creazzo, T., Hawkins, A. F., Daskalakis, N., Kwan, S. Y., Ebersviller, S., Burchette, J. L.,

Pericak-Vance, M. A., Howell, D. N., Vance, J. M., and Rosenberg, P. B. (2005) A mutation in the TRPC6 cation channel causes familial focal segmental glomerulosclerosis, *Science 308*, 1801-1804.

73. Mukerji, N., Damodaran, T. V., and Winn, M. P. (2007) TRPC6 and FSGS: the latest TRP channelopathy, *Biochim. Biophys. Acta 1772*, 859-868.

74. Hofstra, J. M., Lainez, S., van Kuijk, W. H., Schoots, J., Baltissen, M. P., Hoefsloot, L. H., Knoers, N. V., Berden, J. H., Bindels, R. J., van, d., V, Hoenderop, J. G., Wetzels, J. F., and Nijenhuis, T. (2013) New TRPC6 gain-of-function mutation in a non-consanguineous Dutch family with late-onset focal segmental glomerulosclerosis, *Nephrol. Dial. Transplant. 28*, 1830-1838.

75. Heeringa, S. F., Moller, C. C., Du, J., Yue, L., Hinkes, B., Chernin, G., Vlangos, C. N., Hoyer, P. F., Reiser, J., and Hildebrandt, F. (2009) A novel TRPC6 mutation that causes childhood FSGS, *PLoS. One. 4*, e7771.

76. Obeidova, L., Reiterova, J., Lnenicka, P., Stekrova, J., Safrankova, H., Kohoutova, M., and Tesar, V. (2012) TRPC6 gene variants in Czech adult patients with focal segmental glomerulosclerosis and minimal change disease, *Folia Biol. (Praha) 58*, 173-176.

77. Kaneko, Y. and Szallasi, A. (2014) Transient receptor potential (TRP) channels: a clinical perspective, *Br. J. Pharmacol. 171*, 2474-2507.

78. Ma, X., Du, J., Zhang, P., Deng, J., Liu, J., Lam, F. F., Li, R. A., Huang, Y., Jin, J., and Yao, X. (2013) Functional role of TRPV4-KCa2.3 signaling in vascular endothelial cells in normal and streptozotocin-induced diabetic rats, *Hypertension 62*, 134-139.

79. Lee, E., Jung, D. Y., Kim, J. H., Patel, P. R., Hu, X., Lee, Y., Azuma, Y., Wang, H. F., Tsitsilianos, N., Shafiq, U., Kwon, J. Y., Lee, H. J., Lee, K. W., and Kim, J. K. (2015) Transient receptor potential vanilloid type-1 channel regulates diet-induced obesity, insulin resistance, and leptin resistance, *FASEB J.*

80. Tabur, S., Oztuzcu, S., Duzen, I. V., Eraydin, A., Eroglu, S., Ozkaya, M., and Demiryurek, A. T. (2015) Role of the transient receptor potential (TRP) channel gene expressions and TRP melastatin (TRPM) channel gene polymorphisms in obesity-related metabolic syndrome, *Eur. Rev. Med. Pharmacol. Sci. 19*, 1388-1397.

81. Eytan, O., Fuchs-Telem, D., Mevorach, B., Indelman, M., Bergman, R., Sarig, O., Goldberg, I., Adir, N., and Sprecher, E. (2014) Olmsted syndrome caused by a homozygous recessive mutation in TRPV3, *J. Invest Dermatol. 134*, 1752-1754.

82. Yang, P. and Zhu, M. X. (2014) TRPV3, *Handb. Exp. Pharmacol. 222*, 273-291.

83. Duncan, L. M., Deeds, J., Cronin, F. E., Donovan, M., Sober, A. J., Kauffman, M., and McCarthy, J. J. (2001) Melastatin expression and prognosis in cutaneous malignant melanoma, *J. Clin. Oncol. 19*, 568-576.

84. Mathar, I., Jacobs, G., Kecskes, M., Menigoz, A., Philippaert, K., and Vennekens, R. (2014) TRPM4, *Handb. Exp. Pharmacol. 222*, 461-487.

85. Ketterer, C., Mussig, K., Heni, M., Dudziak, K., Randrianarisoa, E., Wagner, R., Machicao, F., Stefan, N., Holst, J. J., Fritsche, A., Haring, H. U., and Staiger, H. (2011) Genetic variation within the TRPM5 locus associates with prediabetic phenotypes in subjects at increased risk for type 2 diabetes, *Metabolism 60*, 1325-1333.

86. Esteban-Oliva, D., Pintos-Morell, G., and Konrad, M. (2009) Long-term follow-up of a patient with primary hypomagnesaemia and secondary hypocalcaemia due to a novel TRPM6 mutation, *Eur. J. Pediatr. 168*, 439-442.

87. Guran, T., Akcay, T., Bereket, A., Atay, Z., Turan, S., Haisch, L., Konrad, M., and Schlingmann, K. P. (2012) Clinical and molecular characterization of Turkish patients with familial hypomagnesaemia: novel mutations in TRPM6 and CLDN16 genes, *Nephrol. Dial. Transplant. 27*, 667-673.

88. Katayama, K., Povalko, N., Yatsuga, S., Nishioka, J., Kakuma, T., Matsuishi, T., and Koga, Y. (2015) New TRPM6 mutation and management of hypomagnesaemia with secondary hypocalcaemia, *Brain Dev. 37*, 292-298.

89. Aarts, M., Iihara, K., Wei, W. L., Xiong, Z. G., Arundine, M., Cerwinski, W., MacDonald, J. F., and Tymianski, M. (2003) A key role for TRPM7 channels in anoxic neuronal death, *Cell 115*, 863-877.

90. Asrar, S. and Aarts, M. (2013) TRPM7, the cytoskeleton and neuronal death, *Channels (Austin.) 7*, 6-16.

91. Chen, W., Xu, B., Xiao, A., Liu, L., Fang, X., Liu, R., Turlova, E., Barszczyk, A., Zhong, X., Sun, C. L., Britto, L. R., Feng, Z. P., and Sun, H. S. (2015) TRPM7 inhibitor carvacrol protects brain from neonatal hypoxic-ischemic injury, *Mol. Brain 8*, 11.

92. Sun, H. S., Jackson, M. F., Martin, L. J., Jansen, K., Teves, L., Cui, H., Kiyonaka, S., Mori, Y., Jones, M., Forder, J. P., Golde, T. E., Orser, B. A., MacDonald, J. F., and Tymianski, M. (2009) Suppression of hippocampal TRPM7 protein prevents delayed neuronal death in brain ischemia, *Nat. Neurosci. 12*, 1300-1307.

93. Nicotera, P. and Bano, D. (2003) The enemy at the gates. Ca2+ entry through TRPM7 channels and anoxic neuronal death, *Cell 115*, 768-770.

94. Ong, A. C., Devuyst, O., Knebelmann, B., and Walz, G. (2015) Autosomal dominant polycystic kidney disease: the changing face of clinical management, *Lancet 385*, 1993-2002.

95. Vassilev, P. M., Guo, L., Chen, X. Z., Segal, Y., Peng, J. B., Basora, N., Babakhanlou, H., Cruger, G., Kanazirska, M., Ye, C., Brown, E. M., Hediger, M. A., and Zhou, J. (2001) Polycystin-2 is a novel cation channel implicated in defective intracellular Ca(2+) homeostasis in polycystic kidney disease, *Biochem. Biophys. Res. Commun. 282*, 341-350.

96. Li, Q., Montalbetti, N., Wu, Y., Ramos, A., Raychowdhury, M. K., Chen, X. Z., and Cantiello, H. F. (2006) Polycystin-2 cation channel function is under the control of microtubular structures in primary cilia of renal epithelial cells, *J. Biol. Chem. 281*, 37566-37575.

97. Liang, G., Li, Q., Tang, Y., Kokame, K., Kikuchi, T., Wu, G., and Chen, X. Z. (2008) Polycystin-2 is regulated by endoplasmic reticulum-associated degradation, *Hum. Mol. Genet. 17*, 1109-1119.

98. Liang, G., Yang, J., Wang, Z., Li, Q., Tang, Y., and Chen, X. Z. (2008) Polycystin-2 down-regulates cell proliferation via promoting PERK-dependent phosphorylation of eIF2alpha, *Hum. Mol. Genet. 17*, 3254-3262.

99. Wang, Q., Dai, X. Q., Li, Q., Wang, Z., Cantero, M. R., Li, S., Shen, J., Tu, J. C., Cantiello, H., and Chen, X. Z. (2012) Structural interaction and functional regulation of polycystin-2 by filamin, *PLoS. One. 7*, e40448.

100. Yang, J., Zheng, W., Wang, Q., Lara, C., Hussein, S., and Chen, X. Z. (2013) Translational up-regulation of polycystic kidney disease protein PKD2 by endoplasmic reticulum stress, *FASEB J. 27*, 4998-5009.

101. Garcia-Gonzalez, M. A., Outeda, P., Zhou, Q., Zhou, F., Menezes, L. F., Qian, F., Huso, D. L., Germino, G. G., Piontek, K. B., and Watnick, T. (2010) Pkd1 and Pkd2 are required for normal placental development, *PLoS. One. 5*.

102. Delling, M., DeCaen, P. G., Doerner, J. F., Febvay, S., and Clapham, D. E. (2013) Primary cilia are specialized calcium signalling organelles, *Nature 504*, 311-314.

103. Huque, T., Cowart, B. J., nkulich-Nagrudny, L., Pribitkin, E. A., Bayley, D. L., Spielman, A. I., Feldman, R. S., Mackler, S. A., and Brand, J. G. (2009) Sour ageusia in two individuals implicates ion channels of the ASIC and PKD families in human sour taste perception at the anterior tongue, *PLoS. One. 4*, e7347.

104. Delyfer, M. N., Raffelsberger, W., Mercier, D., Korobelnik, J. F., Gaudric, A., Charteris, D. G., Tadayoni, R., Metge, F., Caputo, G., Barale, P. O., Ripp, R., Muller, J. D., Poch, O., Sahel, J. A., and Leveillard, T. (2011) Transcriptomic analysis of human retinal detachment reveals both inflammatory response and photoreceptor death, *PLoS. One. 6*, e28791.

105. Demirkan, A., van Duijn, C. M., Ugocsai, P., Isaacs, A., Pramstaller, P. P., Liebisch, G., Wilson, J. F., Johansson, A., Rudan, I., Aulchenko, Y. S., Kirichenko, A. V., Janssens, A. C., Jansen, R. C., Gnewuch, C., Domingues, F. S., Pattaro, C., Wild, S. H., Jonasson, I., Polasek, O., Zorkoltseva, I. V., Hofman, A., Karssen, L. C., Struchalin, M., Floyd, J., Igl, W., Biloglav, Z., Broer, L., Pfeufer, A., Pichler, I., Campbell, S., Zaboli, G., Kolcic, I., Rivadeneira, F., Huffman, J., Hastie, N. D., Uitterlinden, A., Franke, L., Franklin, C. S., Vitart, V., Nelson, C. P., Preuss, M., Bis, J. C., O'Donnell, C. J., Franceschini, N., Witteman, J. C., Axenovich, T., Oostra, B. A., Meitinger, T., Hicks, A. A., Hayward, C., Wright, A. F., Gyllensten, U., Campbell, H., and Schmitz, G. (2012) Genome-wide association study identifies novel loci associated with circulating phospho- and sphingolipid concentrations, *PLoS. Genet. 8*, e1002490.

106. Wu, J. H., Lemaitre, R. N., Manichaikul, A., Guan, W., Tanaka, T., Foy, M., Kabagambe, E. K., Djousse, L., Siscovick, D., Fretts, A. M., Johnson, C., King, I. B., Psaty, B. M., McKnight, B., Rich, S. S., Chen, Y. D., Nettleton, J. A., Tang, W., Bandinelli, S., Jacobs, D. R., Jr., Browning, B. L., Laurie, C. C., Gu, X., Tsai, M. Y., Steffen, L. M., Ferrucci, L., Fornage, M., and Mozaffarian, D. (2013) Genome-wide association study identifies novel loci associated with concentrations of four plasma phospholipid fatty acids in the de novo lipogenesis pathway: results from the Cohorts for Heart and Aging Research in Genomic Epidemiology (CHARGE) consortium, *Circ. Cardiovasc. Genet. 6*, 171-183.

107. Dong, X. P., Wang, X., Shen, D., Chen, S., Liu, M., Wang, Y., Mills, E., Cheng, X., Delling, M., and Xu, H. (2009) Activating mutations of the TRPML1 channel revealed by proline-scanning mutagenesis, *J. Biol. Chem. 284*, 32040-32052.

108. Kiselyov, K., Colletti, G. A., Terwilliger, A., Ketchum, K., Lyons, C. W., Quinn, J., and Muallem, S. (2011) TRPML: transporters of metals in lysosomes essential for cell survival?, *Cell Calcium 50*, 288-294.

109. Wakabayashi, K., Gustafson, A. M., Sidransky, E., and Goldin, E. (2011) Mucolipidosis type IV: an update, *Mol. Genet. Metab 104*, 206-213.

110. Shen, D., Wang, X., Li, X., Zhang, X., Yao, Z., Dibble, S., Dong, X. P., Yu, T., Lieberman, A. P., Showalter, H. D., and Xu, H. (2012) Lipid storage disorders block lysosomal trafficking by inhibiting a TRP channel and lysosomal calcium release, *Nat. Commun. 3*, 731.

111. Meotti, F. C., Lemos de, A. E., and Calixto, J. B. (2014) TRP modulation by natural compounds, *Handb. Exp. Pharmacol. 223*, 1177-1238.

112. Nilius, B., Appendino, G., and Owsianik, G. (2012) The transient receptor potential channel TRPA1: from gene to pathophysiology, *Pflugers Arch. 464*, 425-458.

113. Preti, D., Saponaro, G., and Szallasi, A. (2015) Transient receptor potential ankyrin 1 (TRPA1) antagonists, *Pharm. Pat Anal. 4*, 75-94.

114. Walker, R. G., Willingham, A. T., and Zuker, C. S. (2000) A Drosophila mechanosensory transduction channel, *Science 287*, 2229-2234.

115. Nagarajan, A., Ning, Y., Reisner, K., Buraei, Z., Larsen, J. P., Hobert, O., and Doitsidou, M. (2014) Progressive degeneration of dopaminergic neurons through TRP channel-induced cell death, *J. Neurosci. 34*, 5738-5746.

116. Nomura, H., Turco, A. E., Pei, Y., Kalaydjieva, L., Schiavello, T., Weremowicz, S., Ji, W., Morton, C. C., Meisler, M., Reeders, S. T., and Zhou, J. (1998) Identification of PKDL, a novel polycystic kidney disease 2-like gene whose murine homologue is deleted in mice with kidney and retinal defects, *J. Biol. Chem. 273*, 25967-25973.

117. Chen, X. Z., Vassilev, P. M., Basora, N., Peng, J. B., Nomura, H., Segal, Y., Brown, E. M., Reeders, S. T., Hediger, M. A., and Zhou, J. (1999) Polycystin-L is a calcium-regulated cation channel permeable to calcium ions, *Nature 401*, 383-386.

118. Elliott, D. J., Neale, E. J., Munsey, T. S., Bannister, J. P., and Sivaprasadarao, A. (2012) Role of hydrophobic and ionic forces in the movement of S4 of the Shaker potassium channel, *Mol. Membr. Biol. 29*, 321-332.

119. Grimm, C., Barthmes, M., and Wahl-Schott, C. (2014) TRPML3, *Handb. Exp. Pharmacol. 222*, 659-674.

120. Fujimoto, C., Ishimaru, Y., Katano, Y., Misaka, T., Yamasoba, T., Asakura, T., and Abe, K. (2011) The single pore residue Asp523 in PKD2L1 determines Ca2+ permeation of the PKD1L3/PKD2L1 complex, *Biochem. Biophys. Res. Commun. 404*, 946-951.

121. Yang, J., Wang, Q., Zheng, W., Tuli, J., Li, Q., Wu, Y., Hussein, S., Dai, X. Q., Shafiei, S., Li, X. G., Shen, P. Y., Tu, J. C., and Chen, X. Z. (2012) Receptor for activated C kinase 1 (RACK1) inhibits function of transient receptor potential (TRP)-type channel Pkd2L1 through physical interaction, *J. Biol. Chem. 287*, 6551-6561.

122. Murakami, M., Ohba, T., Xu, F., Shida, S., Satoh, E., Ono, K., Miyoshi, I., Watanabe, H., Ito, H., and Iijima, T. (2005) Genomic organization and functional analysis of murine PKD2L1, *J. Biol. Chem. 280*, 5626-5635.

123. Dai, X. Q., Karpinski, E., and Chen, X. Z. (2006) Permeation and inhibition of polycystin-L channel by monovalent organic cations, *Biochim. Biophys. Acta 1758*, 197-205.

124. Liu, Y., Li, Q., Tan, M., Zhang, Y. Y., Karpinski, E., Zhou, J., and Chen, X. Z. (2002) Modulation of the human polycystin-L channel by voltage and divalent cations, *FEBS Lett. 525*, 71-76.

125. Clapham, D. E., Runnels, L. W., and Strubing, C. (2001) The TRP ion channel family, *Nat. Rev. Neurosci. 2*, 387-396.

126. Feng, P., Zheng, J., Rossiter, S. J., Wang, D., and Zhao, H. (2014) Massive losses of taste receptor genes in toothed and baleen whales, *Genome Biol. Evol. 6*, 1254-1265.

127. Djenoune, L., Khabou, H., Joubert, F., Quan, F. B., Nunes, F. S., Bodineau, L., Del, B. F., Burckle, C., Tostivint, H., and Wyart, C. (2014) Investigation of spinal cerebrospinal fluid-contacting neurons expressing PKD2L1: evidence for a conserved system from fish to primates, *Front Neuroanat. 8*, 26.

128. Orts-Del'immagine, A., Wanaverbecq, N., Tardivel, C., Tillement, V., Dallaporta, M., and Trouslard, J. (2012) Properties of subependymal cerebrospinal fluid contacting neurones in the dorsal vagal complex of the mouse brainstem, *J. Physiol 590*, 3719-3741.

129. Orts-Del'immagine, A., Kastner, A., Tillement, V., Tardivel, C., Trouslard, J., and Wanaverbecq, N. (2014) Morphology, Distribution and Phenotype of Polycystin Kidney Disease 2-like 1-Positive Cerebrospinal Fluid Contacting Neurons in The Brainstem of Adult Mice, *PLoS. One. 9*, e87748.

130. Huang, A. L., Chen, X., Hoon, M. A., Chandrashekar, J., Guo, W., Trankner, D., Ryba, N. J., and Zuker, C. S. (2006) The cells and logic for mammalian sour taste detection, *Nature 442*, 934-938.

131. Basora, N., Nomura, H., Berger, U. V., Stayner, C., Guo, L., Shen, X., and Zhou, J. (2002) Tissue and cellular localization of a novel polycystic kidney disease-like gene product, polycystin-L, *J. Am. Soc. Nephrol. 13*, 293-301.

132. Li, Q., Dai, X. Q., Shen, P. Y., Wu, Y., Long, W., Chen, C. X., Hussain, Z., Wang, S., and Chen, X. Z. (2007) Direct binding of alpha-actinin enhances TRPP3 channel activity, *J. Neurochem. 103*, 2391-2400.

133. Takumida, M. and Anniko, M. (2010) Expression of transient receptor potential channel mucolipin (TRPML) and polycystine (TRPP) in the mouse inner ear, *Acta Otolaryngol. 130*, 196-203.

134. Ishimaru, Y., Inada, H., Kubota, M., Zhuang, H., Tominaga, M., and Matsunami, H. (2006) Transient receptor potential family members PKD1L3 and PKD2L1 form a candidate sour taste receptor, *Proc. Natl. Acad. Sci. U. S. A 103*, 12569-12574.

135. Lopezjimenez, N. D., Cavenagh, M. M., Sainz, E., Cruz-Ithier, M. A., Battey, J. F., and Sullivan, S. L. (2006) Two members of the TRPP family of ion channels, Pkd1l3 and Pkd2l1, are co-expressed in a subset of taste receptor cells, *J. Neurochem. 98*, 68-77.

136. Liman, E. R., Zhang, Y. V., and Montell, C. (2014) Peripheral coding of taste, *Neuron 81*, 984-1000.

137. Zhang, Y., Hoon, M. A., Chandrashekar, J., Mueller, K. L., Cook, B., Wu, D., Zuker, C. S., and Ryba, N. J. (2003) Coding of sweet, bitter, and umami tastes: different receptor cells sharing similar signaling pathways, *Cell 112*, 293-301.

138. Bui-Xuan, E. F., Li, Q., Chen, X. Z., Boucher, C. A., Sandford, R., Zhou, J., and Basora, N. (2006) More than colocalizing with polycystin-1, polycystin-L is in the centrosome, *Am. J. Physiol Renal Physiol 291*, F395-F406.

139. Li, Q., Liu, Y., Shen, P. Y., Dai, X. Q., Wang, S., Smillie, L. B., Sandford, R., and Chen, X. Z. (2003) Troponin I binds polycystin-L and inhibits its calcium-induced channel activation, *Biochemistry 42*, 7618-7625.

140. Shimizu, T., Janssens, A., Voets, T., and Nilius, B. (2009) Regulation of the murine TRPP3 channel by voltage, pH, and changes in cell volume, *Pflugers Arch. 457*, 795-807.

141. Inada, H., Kawabata, F., Ishimaru, Y., Fushiki, T., Matsunami, H., and Tominaga, M. (2008) Off-response property of an acid-activated cation channel complex PKD1L3-PKD2L1, *EMBO Rep. 9*, 690-697.

142. Kawaguchi, H., Yamanaka, A., Uchida, K., Shibasaki, K., Sokabe, T., Maruyama, Y., Yanagawa, Y., Murakami, S., and Tominaga, M. (2010) Activation of polycystic kidney disease-2-like 1 (PKD2L1)-PKD1L3 complex by acid in mouse taste cells, *J. Biol. Chem. 285*, 17277-17281.

143. Ishii, S., Misaka, T., Kishi, M., Kaga, T., Ishimaru, Y., and Abe, K. (2009) Acetic acid activates PKD1L3-PKD2L1 channel--a candidate sour taste receptor, *Biochem. Biophys. Res. Commun. 385*, 346-350.

144. Shimizu, T., Higuchi, T., Fujii, T., Nilius, B., and Sakai, H. (2011) Bimodal effect of alkalization on the polycystin transient receptor potential channel, PKD2L1, *Pflugers Arch. 461*, 507-513.

145. Chen, P., Wu, J. Z., Zhao, J., Wang, P., Luo, J., Yang, W., and Liu, X. D. (2015) PKD2L1/PKD1L3 channel complex with an alkali-activated mechanism and calcium-dependent inactivation, *Eur. Biophys. J.*

146. Dai, X. Q., Ramji, A., Liu, Y., Li, Q., Karpinski, E., and Chen, X. Z. (2007) Inhibition of TRPP3 channel by amiloride and analogs, *Mol. Pharmacol. 72*, 1576-1585.

147. Li, F., Dai, X. Q., Li, Q., Wu, Y., and Chen, X. Z. (2006) Inhibition of polycystin-L channel by the Chinese herb Sparganum stoloniferum Buch.-Ham, *Can. J. Physiol Pharmacol. 84*, 923-927.

148. Pei, Y. (2003) Molecular genetics of autosomal dominant polycystic kidney disease, *Clin. Invest Med. 26*, 252-258.

149. Ramsey, I. S., Delling, M., and Clapham, D. E. (2006) An introduction to TRP channels, *Annu. Rev. Physiol 68*, 619-647.

150. Gallagher, A. R., Germino, G. G., and Somlo, S. (2010) Molecular advances in autosomal dominant polycystic kidney disease, *Adv. Chronic. Kidney Dis. 17*, 118-130.

151. Ishimaru, Y. and Matsunami, H. (2009) Transient receptor potential (TRP) channels and taste sensation, *J. Dent. Res. 88*, 212-218.

152. Ishii, S., Kurokawa, A., Kishi, M., Yamagami, K., Okada, S., Ishimaru, Y., and Misaka, T. (2012) The response of PKD1L3/PKD2L1 to acid stimuli is inhibited by capsaicin and its pungent analogs, *FEBS J. 279*, 1857-1870.

153. Adams, D. R., Ron, D., and Kiely, P. A. (2011) RACK1, A multifaceted scaffolding protein: Structure and function, *Cell Commun. Signal. 9*, 22.

154. Horio, N., Yoshida, R., Yasumatsu, K., Yanagawa, Y., Ishimaru, Y., Matsunami, H., and Ninomiya, Y. (2011) Sour taste responses in mice lacking PKD channels, *PLoS. One. 6*, e20007.

155. Gilliam, J. C. and Wensel, T. G. (2011) TRP channel gene expression in the mouse retina, *Vision Res. 51*, 2440-2452.

156. Kataoka, S., Yang, R., Ishimaru, Y., Matsunami, H., Sevigny, J., Kinnamon, J. C., and Finger, T. E. (2008) The candidate sour taste receptor, PKD2L1, is expressed by type III taste cells in the mouse, *Chem. Senses 33*, 243-254.

157. Gresset, A., Sondek, J., and Harden, T. K. (2012) The phospholipase C isozymes and their regulation, *Subcell. Biochem. 58*, 61-94.

158. Bystrova, M. F., Romanov, R. A., Rogachevskaja, O. A., Churbanov, G. D., and Kolesnikov, S. S. (2010) Functional expression of the extracellular-Ca2+-sensing receptor in mouse taste cells, *J. Cell Sci. 123*, 972-982.

159. Ishimaru, Y. (2015) Molecular mechanisms underlying the reception and transmission of sour taste information, *Biosci. Biotechnol. Biochem. 79*, 171-176.